ISSN 1732-9353 (suspended)
eISSN 2543-7496

Scientific Review

Engineering and Environmental Sciences

Przegląd Naukowy

Inżynieria i Kształtowanie Środowiska

Vol. 34 (2) 2025 Issue 108
Quarterly

SCIENTIFIC REVIEW
ENGINEERING AND ENVIRONMENTAL SCIENCES
Quarterly

EDITORIAL OFFICE ADDRESS
Wydział Budownictwa i Inżynierii Środowiska SGGW, ul. Nowoursynowska 159, 02-776 Warsaw, Poland
tel. (+48 22) 59 35 363, 59 35 210, 59 35 302
e-mail: srees@sggw.edu.pl
https://srees.sggw.edu.pl

Electronic version of the Scientific Review Engineering and Environmental Sciences is primary version

All papers are indexed in the data bases as follows: AGRO(Poznań), BazTech, Biblioteka Nauki, **CrossRef**, **DOAJ**, **Google Scholar**, **Index Copernicus**, INFONA, POL-Index, **SCOPUS**, SIGŻ(CBR)

Scientific Review

Engineering and Environmental Sciences

Przegląd Naukowy

Inżynieria i Kształtowanie Środowiska

Vol. 34 (2) **2025** **Issue 108**

Contents

Wydawnictwo SGGW, Warsaw 2025

Wydawnictwo SGGW wydawnictwosggw

Editorial work – Anna Dołomisiewicz, Tomasz Ruchniewicz

ISSN 1732-9353 (suspended) eISSN 2543-7496

Scientific Review Engineering and Environmental Sciences (2025), 34 (2), 109–127

Sci. Rev. Eng. Env. Sci. (2025), 34 (2) https://srees.sggw.edu.pl

ISSN 1732-9353 (suspended) eISSN 2543-7496 DOI 10.22630/srees.10299

Received: 05.02.2025
Accepted: 10.04.2025

Kharisma Wira NINDHITA[1]

Ahmad ZAKI[1, 2]✉

Muhammad ZAINI[2]

Arfa Maulana KUSUMAWIJAYA[2]

[1] Universitas Muhammadiyah Yogyakarta, Master Program in Civil Engineering, Bantul, Special Region of Yogyakarta, Indonesia
[2] Universitas Muhammadiyah Yogyakarta, Department of Civil Engineering, Bantul, Special Region of Yogyakarta, Indonesia

Corrosion analysis of concrete based on industrial waste and bacteria by non-destructive test methods

Keywords: fly ash, bacteria, NDT, corrosion, mechanical properties

Introduction

Concrete is a primary construction material widely utilized in the building industry. Its extensive application in residential and commercial infrastructure stems not only from its exceptional properties, such as structural performance, sustainability, affordability, and versatility, but also from its adaptability in achieving complex geometric shapes (Li et al., 2022). However, steel corrosion within concrete structures significantly compromises durability and is frequently identified as a major cause of premature failure and damage in reinforced concrete construction. The global economic impact of corrosion is substantial,

✉ahmad.zaki@umy.ac.id

with associated costs estimated at approximately USD 2.5 trillion (Rahita & Zaki, 2023). This issue underscores the necessity of innovative strategies to enhance the resilience and longevity of concrete structures in corrosive environments. One of the primary limitations of concrete is its susceptibility to steel reinforcement corrosion, an electrochemical process involving iron anode dissolution and oxygen cathode reduction, with the concrete's pore solution acting as an electrolyte. This phenomenon is exacerbated by aggressive agents, such as CO^{2+} and Cl^{-}, which penetrate the concrete matrix to reach the reinforcement. The degradation of the protective layer formed on the steel surface in dense concrete accelerates the corrosion process, progressively undermining the performance of reinforced concrete structures. The resulting corrosion products deposit and generate tensile stress, leading to the formation of cracks (Rodrigues et al., 2021). Addressing this challenge requires the development of methods to inhibit the natural corrosion rate by advancing more durable and long-lasting concrete mixtures capable of withstanding such deterioration over time. Fly ash (FA) is a byproduct of coal-fired power plants and is widely utilized as a mineral additive in cement and concrete. Incorporating FA in concrete is cost-effective and enhances its properties in both fresh and hardened states, including improved workability, strength, and reduced drying shrinkage. Furthermore, the use of FA addresses issues related to the storage and disposal of this industrial byproduct (Nayak et al., 2022). Similarly, silica fume (SF) is an ultrafine, non-crystalline byproduct of the silicon production process. It is a highly reactive pozzolanic material composed primarily of amorphous silicon dioxide, with a specific surface area ranging from 15 to 25 $m^2 \cdot g^{-1}$ (Adil et al., 2020). The inclusion of SF in concrete significantly enhances its corrosion resistance, as evidenced by studies showing that reinforcement corrosion does not initiate even after 300 days of exposure to a five-percent solution of NaCl (Ahmad et al., 2022). The combination of FA and SF has demonstrated superior performance compared to their individual use, particularly in improving the durability of concrete in corrosive environments (Anwar et al., 2022).

Thermal power plants generate large quantities of coal ash, approximately one-fifth of which is bottom ash (BA), with the remainder being FA. Bottom ash exhibits a granular structure, making it a subject of ongoing research as a substitute for sand and cement in concrete (Monika et al., 2022). However, due to its porous structure and higher water absorption capacity compared to natural sand, the inclusion of BA in concrete mixtures increases water demand, consequently reducing workability (Nanda & Rout, 2021). In addition to mineral additives, the use of bacteria offers a novel approach to enhancing concrete performance. Certain bacteria can convert chemical precursors into calcium carbonate, commonly known as limestone.

Bacillus subtilis, a rod-shaped bacterium found in soil and the human gastrointestinal tract, has been identified as an effective self-healing agent for concrete. Concrete incorporating *Bacillus subtilis* exhibits higher compressive strength than conventional concrete and demonstrates self-healing properties (Premalatha et al., 2023). Studies have shown that *Bacillus subtilis* enhances both the compressive and flexural strength of concrete, making it a promising agent for improving durability and extending the lifespan of concrete structures (Nindhita et al., 2024).

Early detection of the corrosion process can significantly minimize the extent of repairs or replacements required, thereby reducing rehabilitation costs. Non-destructive testing (NDT) methods have proven valuable for in-situ evaluation of steel corrosion in reinforced concrete, allowing for effective assessment of corrosion effects and structural integrity (Zaki et al., 2015). Among these methods, electrical resistivity (ER) testing has been employed to evaluate the extent of concrete damage caused by steel reinforcement corrosion. Studies indicate a significant correlation between ER values and the degree of corrosion--induced damage, making resistivity measurements a reliable, non-destructive approach for estimating potential corrosion damage in concrete structures (Robles et al., 2024). Ultrasonic pulse velocity (UPV) testing is another widely used NDT method for assessing concrete quality and detecting damage, including that caused by corrosion. When combined with other techniques, such as electrical resistivity measurements, UPV provides more accurate results for identifying corrosion and evaluating the condition of concrete structures (Almashakbeh & Saleh, 2022). These methods highlight the importance of integrating advanced testing techniques to enhance the durability and maintenance of reinforced concrete systems.

Various studies have explored various aspects of the use of *Bacillus subtilis* in improving the mechanical properties of concrete (Ganesh et al., 2020; Jena et al., 2020; Nindhita et al., 2024), as well as the use of fly ash, bottom ash, and silica fume materials in increasing the resistance of concrete to corrosion and chloride attack (Mh et al., 2020; Morla et al., 2021; Anwar et al., 2022; Meena et al., 2023; Malaiškienė & Vaičienė, 2024; Panda et al., 2024), However, these studies have not been correlated with the evaluation of concrete using NDT. Meanwhile, studies of NDT evaluation methods such as ER and UPV in detecting concrete degradation due to corrosion (Almashakbeh & Saleh, 2022; Robles et al., 2024) are still focused on research on ordinary concrete and have not yet explored concrete mixtures based on *Bacillus subtilis* bacteria and mining waste as a substitute for cement. In addition, there is still a gap in research that comprehensively links the synergistic effects of the combination of *Bacillus subtilis* with fly ash, bottom ash, and silica fume on concrete resistance to corrosion while validating the results through destructive testing (DT) and NDT to obtain a more accurate correlation between the physical condition of the concrete and the results of NDT measurements. Therefore, this study aims to bridge the existing research gaps while analyzing the impact of fly ash and silica fume compositions, combined with the addition of bottom ash, superplasticizer, and *Bacillus subtilis* bacteria, on the performance of corroded concrete. In addition, this study aims to offer a comparative analysis of the performance of normal concrete versus pozzolan-based concrete incorporating *Bacillus subtilis* in overcoming corrosion phenomena. This study is expected to provide valuable references for research related to corrosion detection in reinforced concrete using ER and UPV methods.

Material and methods

Materials

The materials used in this study include sand with a particle size range of 0.15–4.75 mm and gravel with a maximum size of 20 mm. Sieve analysis of the sand, conducted in accordance with ASTM C33/33M (ASTM International [ASTM], 2018), indicates a size distribution consistent with gradation classification number 3, as shown in Figure 1. The cement utilized in this research is Portland composite cement (PCC) branded as Semen Merdeka Indonesia. The fly ash and bottom ash used are sourced from power plant waste in Indonesia. The *Bacillus subtilis* bacteria were cultured in the laboratory to a concentration of 10^5 cfu·ml^{-1}. Silica fume was supplied by PT. Sika Indonesia was under the SikaFume brand, while the superplasticizer (SP) used was ViscoCrete-1003, also produced by PT. Sika Indonesia.

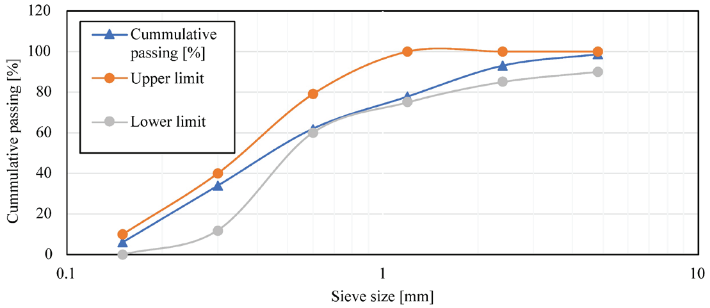

FIGURE 1. Sand sieve analysis
Source: own work.

The material testing process is carried out before the mix design process, which includes testing the specific gravity, gradation, wear, and mud content of the material. Testing of specific gravity and absorption of coarse aggregate is based on SNI 1969:2016 (Badan Standardisasi Nasional [BSN], 2016) and SNI 1970:2016 (BSN, 2016) for fine aggregate. Gradation testing refers to SNI ASTM C136:2012 (ASTM, 2012). Wear testing refers to SNI 2417:2008 (BSN, 2008). Mud content testing refers to SNI ASTM C117:2012 (ASTM, 2012). The aggregate properties are presented in Table 1.

TABLE 1. Properties of aggregates

Property	Gravel	Sand
Bulk specific gravity [kg·m^{-3}]	2.65	1.78
Apparent specific gravity [kg·m^{-3}]	2.71	2.97
Saturated surface-dry specific gravity [kg·m^{-3}]	2.67	2.18
Water absorption [%]	0.75	22.62
Fineness modulus [-]	–	2.435
Mud content [%]	–	2.0
Aggregate wear [%]	15.0	–

Source: own work.

Mix properties

The concrete mix design was prepared following the ACI 211.1 standard (Dixon et al., 1991), targeting a compressive strength of 25 MPa with a water-to-cement ratio (w/c) of 0.61 for all specimens. The material proportions for preparing the specimens are detailed in Table 2.

TABLE 2. Specimen mixture proportion

Material content [kg·m^{-3}]	Specimen			
	Vn	V1	V2	V3
Water	313.59	313.59	313.59	313.59
Cement	336.07	235.25	235.25	235.25
Sand	805.87	684.99	684.99	684.99
Gravel	1 064.55	1 064.55	1 064.55	1 064.55
Fly ash (FA)	–	50.41	67.21	84.02
Silica fume (SF)	–	50.41	33.61	16.80
Bottom ash (BA)	–	120.88	120.88	120.88
Superplasticizer	–	8.40	8.40	8.40

Source: own work.

Nindhita, K. W., Zaki, A., Zaini, M., Kusumawijaya, A. M. (2025). Corrosion analysis of concrete based on industrial waste and bacteria by non-destructive test methods. *Sci. Rev. Eng. Env. Sci.*, *34* (2), 109–127. DOI 10.22630/srees.10299

The specimens included one control mix (Vn) and three pozzolan concrete variations: V1 (15% FA + 15% SF), V2 (20% FA + 10% SF), and V3 (25% FA + + 5% SF). In the pozzolan variations, 15% of the sand was replaced with BA, and SP was added at 2.5% of the cement weight. Additionally, *Bacillus subtilis* was incorporated directly into the mixture at 1% of the specimen's volume. This mix design ensures consistency across specimens while evaluating the effects of pozzolan variations and bacterial addition on the performance of the concrete.

Testing specimen

Rectangular beam specimens with dimensions of 50 × 10 × 10 cm were used. Each beam was reinforced with a 12-millimeter diameter steel bar, embedded with a concrete cover thickness of 2 cm (Fig. 2). A cable was connected to the reinforcement to facilitate the corrosion acceleration process using a DC power supply.

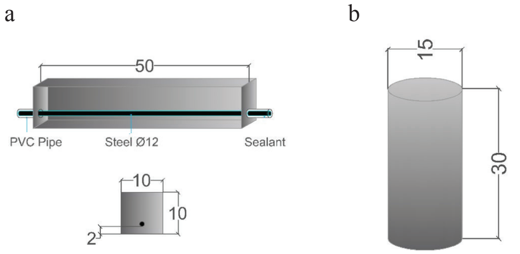

FIGURE 2. Testing specimen: a – beam, b – cylinder
Source: own work.

These specimens were used to evaluate both corrosion testing and flexural strength. Cylindrical specimens with dimensions of 15 × 30 cm were prepared for compressive strength testing. All test specimens were cured in water for 28 days to ensure proper hydration and strength development.

Corrosion testing

Corrosion testing was conducted using an accelerated corrosion method. In this setup, the positive cable terminal was connected to the reinforcement within the concrete specimen, while the negative terminal was attached to a steel bar submerged in a 5% five-percent solution of NaCl (Su et al., 2022). The test employed a constant voltage of 25 V, with the current fluctuating throughout the 72-hour testing period. The corrosion test was performed on beam specimens after the curing process. The degree of corrosion was determined by calculating the percentage mass loss of the reinforcement, utilizing Faraday's law (El Maaddawy & Soudki, 2003), as follows:

$$\Delta m = \frac{\mathrm{M} \cdot I \cdot t}{z \cdot \mathrm{F}},$$

Δm – mass loss of the reinforcement [g],
M – atomic weight of the metal (M = 56) [$\mathrm{g \cdot mol^{-1}}$],
I – electric current [A],
t – duration of corrosion [s],
z – electron charge (z = 2) [C],
F – Faraday's constant (F = 96,500) [$\mathrm{A \cdot s^{-1}}$].

The crack width resulting from corrosion was subsequently measured on three distinct sections: the right side, closest to the connection cable; the middle section; and the left side, furthest from the cable. These measurements were conducted using a crack gauge with a precision of 0.05 mm.

Mechanical testing

The mechanical properties of concrete were evaluated through compressive and flexural strength tests after a curing period of 28 days. The compressive strength test was conducted on cylindrical specimens (15 × 30 cm) following the guidelines of ASTM C39/C39M (ASTM, 2021), while the flexural strength test was performed on beam specimens (50 × 10 × 10 cm) in accordance with ASTM C293/C293M (ASTM, 2016). These tests aimed to determine the compressive strength of the concrete cylinders and the flexural strength of the concrete beams. Additionally, the study sought to compare the performance of control concrete with that of pozzolan concrete variations.

Non-destructive testing methods

The tests (NDT) were conducted using the ER method to measure the electrical resistance of concrete, as well as the UPV method, both before and after the corrosion acceleration process. The results were then compared with the previous data. The resistivity test was performed using the Wenner four-point method (probe technique). Data were collected three times at each measurement point, and the average values were computed and categorized according to the corrosion classification by Robles et al., 2022. The sides of the concrete specimen were divided into four areas: the left side, which is directly connected to the cable, and the right, top, and bottom sides. This division of points aimed to ensure accurate and uniform results, thereby providing a precise average. The distribution of the points is illustrated in Figure 3.

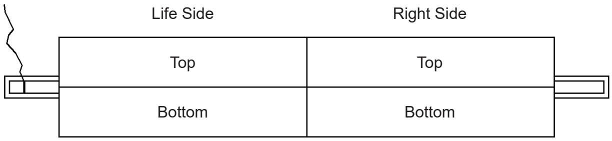

FIGURE 3. Illustration of the ER testing point

Source: own work.

The UPV testing was conducted using a 54 kHz longitudinal wave transducer. The UPV measurements were performed by positioning the two transducers on opposite sides of the specimen (direct method), as shown in Figure 4; on adjacent sides (semi-direct method), as shown in Figure 5; and on the same side (indirect method) (Almasaeid et al., 2022), as shown in Figure 6.

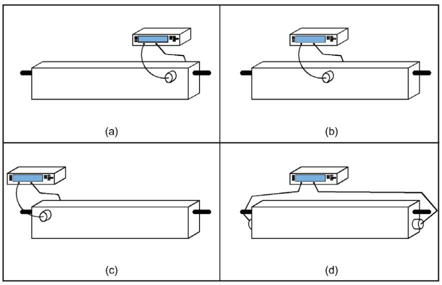

FIGURE 4. Direct method: a – left, b – center, c – right, d – edge-to-end

Source: own work.

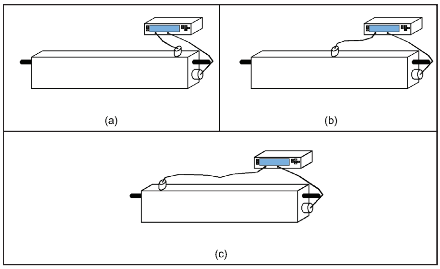

FIGURE 5. Semi-direct method: a – 5 cm, b – 25 cm, c – 45 cm

Source: own work.

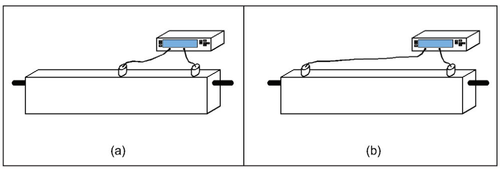

FIGURE 6. Indirect method: a – 20 cm, b – 40 cm

Source: own work.

Results and discussion

Corrosion testing

Results of corrosion acceleration over 72 h (Fig. 7) indicate a continuous increase in current until the final duration, with variations in the mix. In the control concrete, a decrease in current occurred after 55 h due to the reinforcement connected to the wire no longer being able to effectively conduct the current. Concrete with mixed variations exhibited both lower initial and average current compared to normal concrete. Concrete with the V1-B code, containing 15% of FA and 15% of SF, demonstrated the best corrosion resistance, with an average current of 0.075 A. Using Faraday's law, the corrosion level and mass loss of the corroded reinforcement can be estimated, as shown in Table 3. Then, the corrosion level values were averaged, as shown in Figure 8.

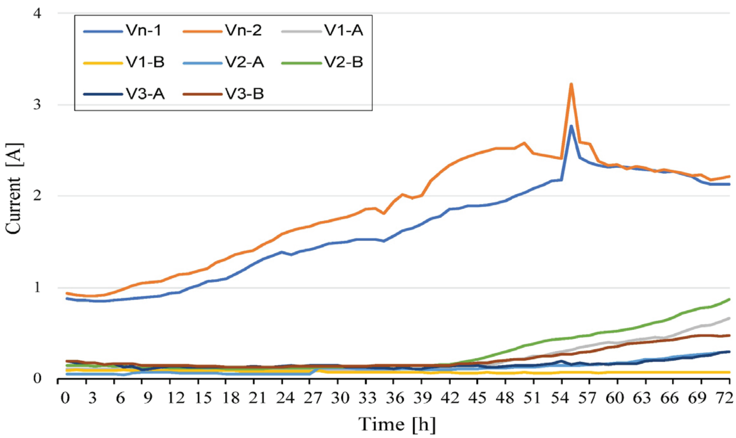

FIGURE 7. Corrosion acceleration current monitoring results
Source: own work.

TABLE 3. Concrete corrosion level

Specimen	Current [A]	Corrosion duration [h]	Estimated corrosion level [%]	Estimated mass loss [g]	Actual corrosion level [%]	Actual mass loss [g]	Derivation [%]
Vn-1	1.636	72	23.893	123.049	15.73	81	8.16
Vn-2	1.861	72	27.181	139.981	20.58	106	6.60
V1-A	0.209	72	3.082	15.721	2.94	15	0.14
V1-B	0.075	72	1.110	5.662	1.96	10	0.85

TABLE 3 (cont.)

Specimen	Current [A]	Corrosion duration [h]	Estimated corrosion level [%]	Estimated mass loss [g]	Actual corrosion level [%]	Actual mass loss [g]	Derivation [%]
V2-A	0.118	72	1.728	8.900	2.52	13	0.80
V2-B	0.286	72	4.213	21.487	3.73	19	0.49
V3-A	0.157	72	2.316	11.814	2.55	13	0.23
V3-B	0.221	72	3.255	16.598	3.33	17	0.08

Source: own work.

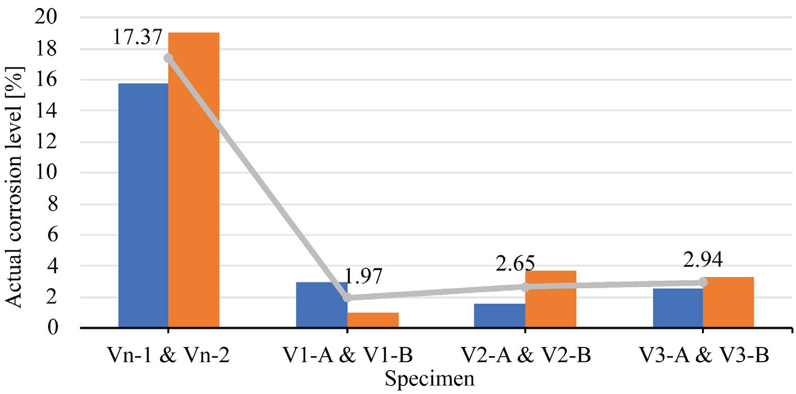

FIGURE 8. Average actual corrosion level

Source: own work.

Table 3 demonstrates that higher average current values correspond to an increased actual corrosion rate with higher percentages. Figure 8 indicates that normal concrete exhibits a higher corrosion rate compared to concrete incorporating industrial waste and *Bacillus subtilis* bacteria. Additionally, an increase in average corrosion levels is observed from Variation 1 to Variation 3. Concrete with Variation 1, containing 15% of FA and 15% of SF, showed good performance in resisting chloride ion penetration, though its performance was not significantly different from other pozzolan variations. The use of FA and SF effectively reduces concrete porosity and permeability by enhancing its microstructural quality. The formation of calcium silicate hydrate (CSH) as a product of the pozzolanic reaction plays a crucial role in impeding chloride ion ingress into the concrete (Zhang & Zhang, 2020). Fly ash and silica fume reduce the number of pores and optimize pore size distribution within the concrete. Silica fume contributes to the formation of uniform micro-sized pores, while FA fills larger voids, thereby increasing concrete density (Wang et al., 2021).

Moreover, the replacement of sand with bottom ash up to 20% limits chloride ion ingress, enhancing the corrosion resistance of reinforced concrete. However, using more than 20% bottom ash increases porosity and reduces concrete durability, making it unsuitable for aggressive environments (Mh et al., 2020). Measurements of cracks in V1-B concrete revealed the smallest crack width among the specimens, which corresponded to lower current readings during corrosion acceleration. This can be attributed to the 15% SF substitution for cement, which reduces concrete pore volume. The crack widths after corrosion are shown in Table 4.

TABLE 4. Crack width measurement

Specimen	Duration of corrosion [h]	Crack width [mm]			AVG	Actual corrosion level [%]
		left	middle	right		
Vn-1	72	0.65	2.50	0.75	1.30	15.73
Vn-2	72	0.15	5.00	0.60	1.92	19.01
V1-A	72	0.75	0.25	0.10	0.37	2.94
V1-B	72	0.10	0	0	0.03	0.99
V2-A	72	0.20	0.20	0.15	0.18	1.57
V2-B	72	0	0.80	1.00	0.60	3.73
V3-A	72	0.1	0.25	0.15	0.17	2.55
V3-B	72	0.9	0.20	0.15	0.42	3.33

Source: own work.

Corrosion products generate tensile stress, leading to crack formation (Rodrigues et al., 2021). Concrete containing supplementary materials exhibited smaller crack widths compared to normal concrete. Figure 9 confirms that crack width correlates with the corrosion rate – higher corrosion levels result in more visible damage, including cracking.

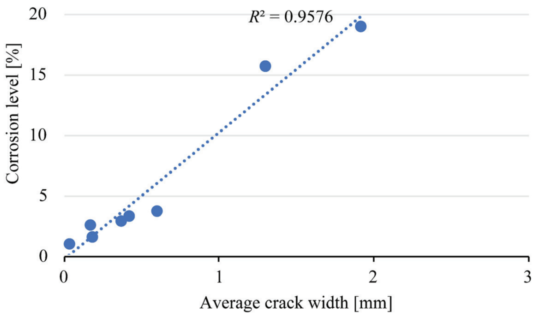

FIGURE 9. Correlation of corrosion level with crack width

Source: own work.

Biocalcification (microbially induced calcium carbonate precipitation – MICP), facilitated through bacterial biofilm formation, has been shown to enhance mechanical strength and repair concrete cracks by precipitating calcium carbonate. The bacterial biofilm also acts as an effective protective layer, inhibiting steel reinforcement corrosion in corrosive environments (Kanwal et al., 2023).

Non-destructive testing

Figure 10 illustrates the results of ER testing before and after corrosion. The resistivity measurements prior to corrosion categorized the specimens with pozzolan-based admixtures as ranging from negligible to low levels of corrosion risk, with resistivity values between 14.11 kΩ·cm and 20.5 kΩ·cm. In contrast, the control concrete fell into the low-risk category with resistivity values below 20 kΩ·cm. After corrosion, the resistivity values decreased across all specimens. Concrete with pozzolan admixtures shifted to categories ranging from low to moderate, while normal concrete reached the high-risk category (Robles et al., 2022).

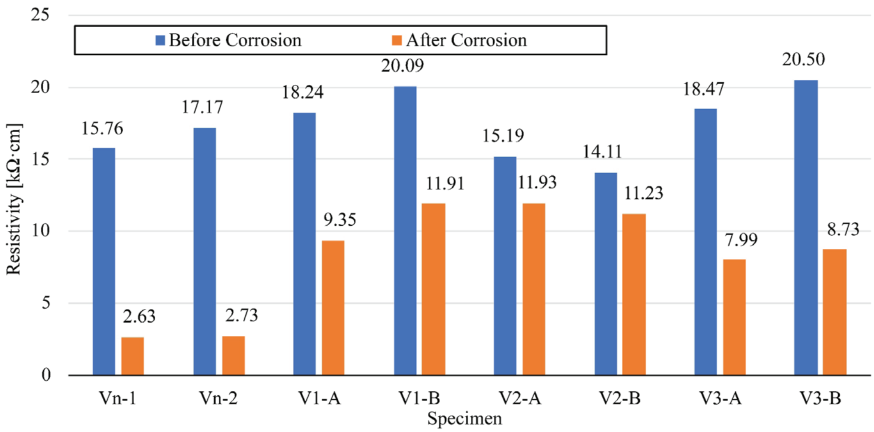

FIGURE 10. Electrical resistivity result
Source: own work.

Figure 11 shows the differences in wave velocity measured by transducers before and after corrosion. Specimens prior to corrosion demonstrated average wave velocities exceeding 4,500 m·s^{-1}, classified as *excellent*, while specimens after corrosion exhibited average velocities below 4,500 m·s^{-1}, classified as *good*

(Solís-Carcaño & Moreno, 2008). Specimens containing pozzolan admixtures maintained better structural integrity after corrosion compared to the control concrete. Furthermore, the direct method yielded higher wave velocity values than the semi-direct method, which, in turn, was higher than the indirect method. These findings align with the results reported by Almasaeid et al. (2022). Corrosion-induced microstructural changes in concrete impact wave propagation, with the direct method penetrating deeper into the material and better detecting these changes. This results in higher velocity readings, reflecting a more intact structure compared to the semi-direct and indirect methods, which are more influenced by surface-level damage.

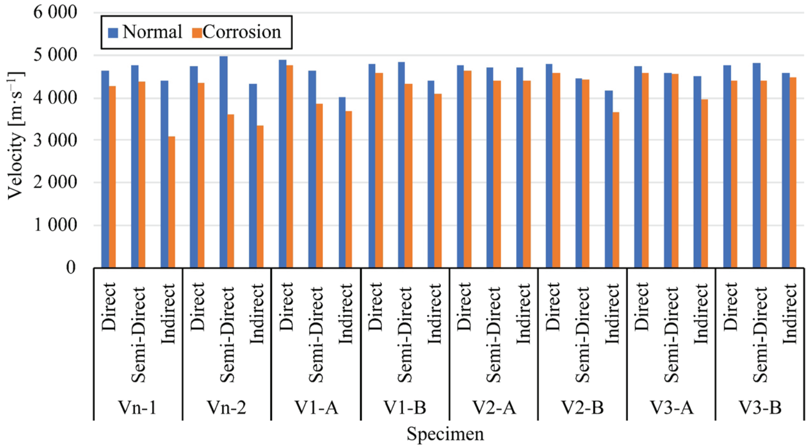

FIGURE 11. Ultrasonic pulse velocity test results before and after corrosion
Source: own work.

Among all specimens tested using NDT, those with pozzolan-based admixtures exhibited the best corrosion resistance, as evidenced by both ER and UPV results. Although varying degrees of decline were observed in pozzolan specimens, the final ER and UPV readings indicated lower corrosion risks compared to control concrete, aligning with actual corrosion monitoring. This performance is attributed to the positive effects of FA and SF as cement replacements (Anwar et al., 2022) and BA as a sand substitute (Ali et al., 2022), which significantly enhanced corrosion resistance. The test results confirmed that pozzolan-based admixture variations effectively reduced both the risk and rate of corrosion. Figure 12 presents the correlation between UPV testing results (output velocity) and ER testing.

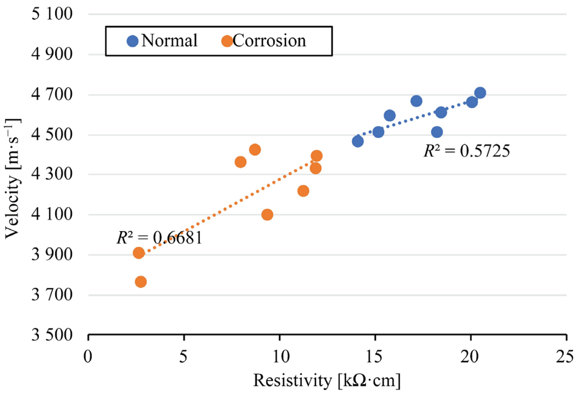

FIGURE 12. Velocity and resistivity correlation

Source: own work.

The analysis yielded a correlation coefficient of 0.5725 for pre-corrosion testing and 0.6681 for post-corrosion testing. These results indicate that both methods provide comparable parameters for evaluating concrete corrosion.

Mechanical testing

Compressive strength and flexural strength tests were conducted on specimens aged 28 days. Concrete with a mixture of 25% of FA and 5% of SF achieved the highest average compressive strength, as shown in Figure 13. Similarly, in the flexural strength tests conducted after corrosion acceleration, the same mixture (25% FA and 5% SF) exhibited the highest average flexural strength, as depicted in Figure 14.

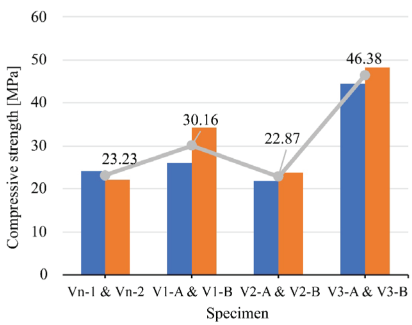

FIGURE 13. Compressive strength result

Source: own work.

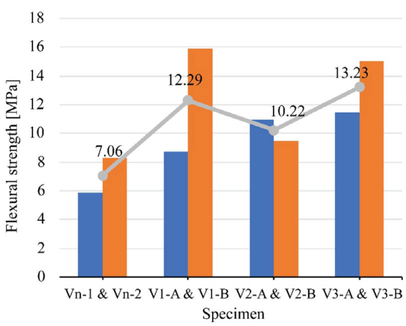

FIGURE 14. Flexural strength result

Source: own work.

The test results demonstrated that increasing the substitution of FA for cement improves the quality of concrete. SF plays a critical role in enhancing the mechanical properties of concrete through the pozzolanic reaction, while FA minimizes the number of pores and increases concrete density (Falmata et al., 2020). Additionally, the inclusion of *Bacillus subtilis* bacteria in the concrete mix improved compressive strength and crack resistance. This improvement is attributed to the formation of calcium carbonate, which fills voids and small cracks in the concrete, thereby strengthening the structure (Priyom et al., 2021). Self-compacting concrete (SCC) incorporating up to 20% bottom ash exhibited compressive strength equal to or greater than that of normal concrete. This is due to the fine particles of bottom ash enhancing the density of the concrete (Mh et al., 2020).

Conclusions

Based on the testing results and analysis, the following conclusions can be drawn:

- The corrosion acceleration tests demonstrated that specimens incorporating fly ash, bottom ash, silica fume, and *Bacillus subtilis* bacteria effectively inhibited the rate of corrosion.
- Crack dimensions were found to be directly proportional to the current during corrosion acceleration. Control concrete exhibited higher current values compared to concrete with pozzolan admixtures, which corresponded to larger crack sizes.
- The resistivity and UPV tests revealed a correlation in estimating the risk of corrosion.
- The addition of 15% fly ash, 15% silica fume, 15% bottom ash, 2.5% superplasticizer, and 1% *Bacillus subtilis* bacteria improved the mechanical properties of the concrete while significantly reducing the rate of corrosion.

Acknowledgments

The researchers would like to thank the Ministry of Education, Culture, Research, and Technology (Indonesia), and the Directorate General of Higher Education, Research, and Technology with Penelitian Tesis Magister (PTM) (Grant year 2024 with number 107/E5/PG.02.00.PL/2024) for funding the study.

References

Adil, G., Kevern, J. T., & Mann, D. (2020). Influence of silica fume on mechanical and durability of pervious concrete. *Construction and Building Materials*, *247*, 118453. https://doi.org/10.1016/j.conbuildmat.2020.118453

Ahmad, S., Al-Amoudi, O. S. B., Khan, S. M., & Maslehuddin, M. (2022). Effect of silica fume inclusion on the strength, shrinkage and durability characteristics of natural pozzolan--based cement concrete. *Case Studies in Construction Materials*, *17*, e01255. https://doi.org/10.1016/j.cscm.2022.e01255

Ali, T., Buller, A. S., Abro, F. u. R., Ahmed, Z., Shabbir, S., Lashari, A. R., & Hussain, G. (2022). Investigation on mechanical and durability properties of concrete mixed with silica fume as cementitious material and coal bottom ash as fine aggregate replacement material. *Buildings*, *12* (1), 44. https://doi.org/10.3390/buildings12010044

Almasaeid, H. H., Suleiman, A., & Alawneh, R. (2022). Assessment of high-temperature damaged concrete using non-destructive tests and artificial neural network modelling. *Case Studies in Construction Materials*, *16*, e01080. https://doi.org/10.1016/j.cscm.2022.e01080

Almashakbeh, Y., & Saleh, E. (2022). Evaluation of ultrasonic pulse velocity (UPV) for reinforced concrete corrosion. *Journal of Applied Engineering Science*, *20* (4), 1226–1233. https://doi.org/10.5937/jaes0-38140

Anwar, M., Gad, A. I., & Sayed Khalil, M. (2022). Influence of Using Fly ash and Silica Fume on the Concrete Performance against Chloride Attack. JES. *Journal of Engineering Sciences*, *50* (6), 325–334. https://doi.org/10.21608/jesaun.2022.140662.1141

ASTM International [ASTM]. (2016). *Standard test method for flexural strength of concrete (using simple beam with center-point loading)* (ASTM C293/C293M-16).

ASTM International [ASTM]. (2018). *Standard specification for concrete aggregates* (ASTM C33/C33M-18).

ASTM International [ASTM]. (2021). *Standard test method for compressive strength of cylindrical concrete specimens* (ASTM C39/C39M-21).

Badan Standardisasi Nasional [BSN]. (2008). *Cara uji keausan agregat dengan mesin abrasi los angeles* (SNI 2417:2008).

Badan Standardisasi Nasional [BSN]. (2012a). *Metode uji bahan yang lebih halus dari saringan 75 µm (No. 200) dalam agregat mineral dengan pencucian* (SNI ASTM C117:2012).

Badan Standardisasi Nasional [BSN]. (2012b). *Metode uji untuk analisis saringan agregat halus dan agregat kasar* (SNI ASTM C136:2012).

Badan Standardisasi Nasional [BSN]. (2016a). *Cara uji berat jenis dan penyerapan air agregat kasar* (SNI 1969:2016).

Badan Standardisasi Nasional [BSN]. (2016b). *Cara uji berat jenis dan penyerapan air agregat halus* (SNI 1970:2016).

Dixon, D. E., Prestrera, J. R., Burg, G. R., Chairman, S. A., Abdun-Nur, E. A., Barton, S. G., Bell, L. W., Blas Jr, S. J., Carraquillo, R. L., & Carraquillo, P. M. (1991). *Standard practice for selecting proportions for normal heavyweight, and mass concrete* (ACI 211.1-91) reapproved 1997. ACI Committee.

El Maaddawy, T. A., & Soudki, K. A. (2003). Effectiveness of impressed current technique to simulate corrosion of steel reinforcement in concrete. *Journal of Materials in Civil Engineering*, *15* (1), 41–47. https://doi.org/10.1061/(ASCE)0899-1561(2003)15:1(41)

Falmata, A., Sulaiman, A., Mohamed, R., & Shettima, A. (2020). Mechanical properties of self-compacting high-performance concrete with fly ash and silica fume. *SN Applied Sciences*, *2*, 1–11. https://doi.org/10.1007/s42452-019-1746-z

Ganesh, S., Danish, P., Anita Jessie, J., Ganie, M., & Raina, C. (2020). Experimental study on self-healing concrete with the effect of bacillus subtilis bacteria to improve the strength and sustainability of the concrete. *Journal of Green Engineering*, *10* (4), 1909–1923.

Jena, S., Basa, B., Panda, K. C., & Sahoo, N. K. (2020). Impact of Bacillus subtilis bacterium on the properties of concrete. *Materials Today: Proceedings*, *32*, 651–656. https://doi.org/10.1016/j.matpr.2020.03.129

Kanwal, M., Khushnood, R. A., Adnan, F., Wattoo, A. G., & Jalil, A. (2023). Assessment of the MICP potential and corrosion inhibition of steel bars by biofilm forming bacteria in corrosive environment. *Cement and Concrete Composites*, *137*, 104937. https://doi.org/10.1016/j.cemconcomp.2023.104937

Li, W., Lin, X., Bao, D. W., & Xie, Y. M. (2022). A review of formwork systems for modern concrete construction. *Structures*, *38*, 52–63. https://doi.org/10.1016/j.istruc.2022.01.089

Malaiškienė, J., & Vaičienė, M. (2024). The Influence of silica fly ash and wood bottom ash on cement hydration and durability of concrete. *Materials*, *17* (16), 4031. https://doi.org/10.3390/ma17164031

Meena, A., Singh, N., & Singh, S. (2023). Sustainable development of high-volume fly ash self-compacting concrete incorporating bottom ash and recycled concrete aggregates. *Journal of Materials and Engineering Structures – JMES*, *10* (4), 615–630. https://revue.ummto.dz/index.php/JMES/article/view/3426

Mh, W., Hamzah, A., Jamaluddin, N., Mangi, S., & Ramadhansyah, P. (2020). Influence of bottom ash as a sand replacement material on durability of self-compacting concrete exposed to seawater. *Journal of Engineering Science and Technology*, *15* (1), 555–571. https://jestec.taylors.edu.my/Vol%2015%20issue%201%20February%202020/15_1_40.pdf

Monika, F., Prayuda, H., Cahyati, M. D., Augustin, E. N., Rahman, H. A., & Prasintasari, A. D. (2022). Engineering properties of concrete made with coal bottom ash as sustainable construction materials. *Civil Engineering Journal*, *8* (1), 181–194. http://doi.org/10.28991/CEJ-2022-08-01-014

Morla, P., Gupta, R., Azarsa, P., & Sharma, A. (2021). Corrosion evaluation of geopolymer concrete made with fly ash and bottom ash. *Sustainability*, *13* (1), 398. https://doi.org/10.3390/su13010398

Nanda, B., & Rout, S. (2021). Properties of concrete containing fly ash and bottom ash mixture as fine aggregate. *International Journal of Sustainable Engineering*, *14* (4), 809–819. https://doi.org/10.1080/19397038.2021.1920641

Nayak, D. K., Abhilash, P., Singh, R., Kumar, R., & Kumar, V. (2022). Fly ash for sustainable construction: A review of fly ash concrete and its beneficial use case studies. *Cleaner Materials*, *6*, 100143. https://doi.org/10.1016/j.clema.2022.100143

Nindhita, K. W., Zaki, A., & Zeyad, A. M. (2024). Effect of *Bacillus subtilis* Bacteria on the mechanical properties of corroded self-healing concrete. *Fracture & Structural Integrity/ /Frattura ed Integrità Strutturale*, *18* (68), 140–158. https://doi.org/10.3221/IGF-ESIS.68.09

Panda, S., Pradhan, M., & Panigrahi, S. K. (2024). Comparative study of OPC and PPC-based concrete properties containing bottom ash and fly ash as fine aggregate. *Indian Concrete Journal*, *98* (7), 7–19.

Premalatha, P., Geethanjali, M., Sundararaman, S., & Murali, C. (2023). An experimental investigation on self-healing concrete using "Bacillus subtilis". *Materials Today: Proceedings*, *2023*, 1–5. https://doi.org/10.1016/j.matpr.2023.08.118

Priyom, S. N., Islam, M. M., & Shumi, W. (2021). The utilization of Bacillus Subtilis Bacteria to improve the mechanical properties of concrete. *Journal of the Civil Engineering Forum*, *7* (1), 97–108. https://doi.org/10.1016/j.matpr.2023.08.118

Rahita, A. C., & Zaki, A. (2023, 9–10 August). *Corrosion analysis on reinforcing steel in concrete using the eddy current method*. 2023 3rd International Conference on Electronic and Electrical Engineering and Intelligent System (ICE3IS), Yogyakarta, Indonesia. https://doi.org/10.1109/ICE3IS59323.2023.10335487

Robles, K. P. V., Gucunski, N., & Kee, S.-H. (2024). Evaluation of steel corrosion-induced concrete damage using electrical resistivity measurements. *Construction and Building Materials*, *411*, 134512. https://doi.org/10.1016/j.conbuildmat.2023.134512

Robles, K. P. V., Yee, J. J., & Kee, S. H. (2022). Electrical resistivity measurements for nondestructive evaluation of chloride-induced deterioration of reinforced concrete – a review. *Materials*, *15* (8), 2725. https://doi.org/10.3390/ma15082725

Rodrigues, R., Gaboreau, S., Gance, J., Ignatiadis, I., & Betelu, S. (2021). Reinforced concrete structures: A review of corrosion mechanisms and advances in electrical methods for corrosion monitoring. *Construction and Building Materials*, *269*, 121240. https://doi.org/10.1016/j.conbuildmat.2020.121240

Solís-Carcaño, R., & Moreno, E. I. (2008). Evaluation of concrete made with crushed limestone aggregate based on ultrasonic pulse velocity. *Construction and Building Materials*, *22* (6), 1225–1231. https://doi.org/10.1016/j.conbuildmat.2007.01.014

Su, T., Wu, J., Zou, Z., Wang, Z., Yuan, J., & Yang, G. (2022). Influence of environmental factors on resistivity of concrete with corroded steel bar. *European Journal of Environmental and Civil Engineering*, *26* (4), 1229–1242. https://doi.org/10.1080/19648189.2019.1670265

Wang, L., Jin, M., Guo, F., Wang, Y., & Tang, S. (2021). Pore structural and fractal analysis of the influence of fly ash and silica fume on the mechanical property and abrasion resistance of concrete. *Fractals*, *29* (02), 2140003. https://doi.org/10.1142/S0218348X2140003X

Zaki, A., Chai, H. K., Aggelis, D. G., & Alver, N. (2015). Non-destructive evaluation for corrosion monitoring in concrete: A review and capability of acoustic emission technique. *Sensors*, *15* (8), 19069–19101. https://doi.org/10.3390/s150819069

Zhang, C., & Zhang, F. (2020). Incorporation of silicon fume and fly ash as partial replacement of Portland cement in reinforced concrete: Electrochemical study on corrosion behavior of 316LN stainless steel rebar. *International Journal of Electrochemical Science*, *15* (5), 3740–3749. https://doi.org/10.20964/2020.05.77

Summary

Corrosion analysis of concrete based on industrial waste and bacteria by non--destructive test methods. Corrosion of concrete can lead to cracking and a decline in serviceability, necessitating effective methods to minimize the risk of corrosion. This study investigates the use of pozzolanic materials, specifically fly ash, bottom ash, and silica fume, combined with *Bacillus subtilis* bacteria as fillers to enhance the concrete structure's resistance to corrosion. The research involves substituting fly ash (15–25%) and silica fume (5–15%) for cement by weight, alongside replacing sand with bottom ash at 15%. Additionally, *Bacillus subtilis* is incorporated into all pozzolanic concrete specimens. The study evaluates the mechanical properties of the concrete and employs non-destructive testing to correlate the physical condition with test results while preserving the structural integrity. The findings demonstrate that the inclusion of fly ash, bottom ash, silica fume, and *Bacillus subtilis* bacteria improves the mechanical properties of the concrete and effectively reduces the rate of corrosion, highlighting the potential for these materials to enhance the durability of concrete structures.

Scientific Review Engineering and Environmental Sciences (2025), 34 (2), 128–143

Sci. Rev. Eng. Env. Sci. (2025), 34 (2) https://srees.sggw.edu.pl

ISSN 1732-9353 (suspended) eISSN 2543-7496 DOI 10.22630/srees.10183

Received: 20.12.2024
Accepted: 17.02.2025

Loubna ENKAIKI[1]✉

Oussama JARACHI[1]

Petru MIHAI[2]

Hanane MOULAY ABDELALI[1]

Om El Khaiat MOUSTACHI[1]

[1] Mohammed V University in Rabat, Mohammadia School of Engineers, Civil Engineering Laboratory, Rabat, Morocco

[2] Technical University "Gheorghe Asachi", Faculty of Civil Engineering and Building Services, Department of Concrete Structures, Building Materials, Technology and Management, Iasi, Romania

Flexural and tensile behavior of rubberized concrete: experimental analysis

Keywords: rubberized concrete, density, splitting tensile strength, flexural testing

Introduction

Due to the rising presence of rubber in the environment, the incorporation of crumb rubber into concrete mixtures has garnered significant research interest. While benefiting the environment, this innovative approach also tries to enhance some of the concrete properties. Numerous studies have explored the influence of rubber additives on concrete properties such as strength, durability, and environmental impact.

Replacing coarse aggregate with crumb rubber in concrete results in a reduction in concrete mechanical properties such as compressive and tensile strength

✉enkaiki.loubna@gmail.com

and modulus of elasticity (Deshpande et al., 2014; Girskas & Nagrockienė, 2017; Karunarathna et al., 2021; Fauzan et al., 2023). However, rubberized concrete beams showed reduced displacements compared to reference beams when subjected to similar impact (Pham et al., 2020). Furthermore, rubberized concrete beams experience a lower maximum impact force in a collision and have greater crack resistance compared to the control mixes. Meanwhile, workability does not significantly decrease with the addition of crumb rubber (Fauzan et al., 2023).

In the case of Portland pozzolana cement concrete, Bisht and Ramana (2017) concluded that 4% of fine aggregates might be substituted by weight with crumb rubber to produce a suitable concrete mix for non-structural elements.

In a static and dynamic evaluation, Atahan and Yücel (2012) propose rubberized concrete produced with 20–40% crumb rubber to substitute natural aggregates in concrete safety barriers that necessitate strength, energy dissipation, and fracture resistance. For substitution percentages greater than 60%, rubberized concrete would be beneficial for concrete impact attenuators where low impact severity is important, and some fracture or fragmentation upon impact is acceptable.

In another study, Walid et al. (2022) replaced fine aggregate with crumb rubber at 0%, 10%, 15%, and 20% by volume and found that compressive strength was acceptable with up to 20% replacement. Rubberized concrete has shown more ductile behavior than reference concrete. The evaluation of the failure modes revealed that crumb rubber can enhance the deformability of the mixture. Moreover, impact resistance under flexural loading increased as the rubber content increased (Abdelmonem et al., 2019).

A study by Mendis et al. (2017) investigating the flexural behavior of reinforced rubberized concrete beams compared to reference concrete showed that reinforced concrete beams using rubberized concrete of similar strength perform similarly under flexural loads.

The incorporation of rubber fibers into natural aggregate concrete showed an enhancement in ductility, compressive strength, tensile strength, and deflection behavior compared to reference concrete (Ismail & Hassan, 2017a, 2017b; Al-Azzawi et al., 2018; Eisa et al., 2020).

Hybrid reinforced rubberized concrete beams outperformed reinforced rubberized concrete beams (Alasmari et al., 2019) in terms of failure patterns, first cracking load, deflection load, and flexural strength, even though reinforced rubberized concrete beams seem to have better ultimate deflection, ductility index, and stress-strain curve.

A synergistic effect was observed between rubber and corrugated round steel fibers (Mohammed & Ali, 2023; Ghoniem & Aboul Nour, 2024), leading to better fresh and hardened concrete properties (workability, density, compressive strength, indirect tensile strength, and flexural strength) when used together. The addition of fiber reinforcement mitigated the negative influence of rubber and vice versa.

The impact of the ratio of crumb rubber and welded wire mesh layers (WWM) on the flexural behavior of reinforced concrete beams was investigated by Ismail et al. (2020) and showed a decrease in compressive strength while increasing the content of crumb rubber, while the addition of WWM improved the beam performance against shear failure. Beams cast with rubberized concrete exhibited a slight reduction in load capacity compared to those without rubber. Furthermore, all beams incorporating crumb rubber exhibited a notable increase in ductility index.

By strengthening the reinforced concrete beams with high-performance rubberized engineered cementitious composite (RECC), AbdelAleem and Hassan (2022) showed an enhancement in flexural strength, ductility cracking behavior, deformability, and bond strength.

In conclusion, based on existing literature, rubberized concrete shows a decrease in compressive and tensile strength, but at the same time, it significantly enhances ductility, energy absorption, and crack resistance. In addition, rubber, in combination with steel or synthetic fibers, can further enhance some of its mechanical properties and durability.

Existing research studies have generally focused on standardized small-scale samples and utilized very low percentages of rubber. Furthermore, rubber incorporation into a concrete mixture reinforced with rebar is yet to be investigated. In this context, our study tries to explore the effect of higher crumb rubber content incorporation on the density, tensile strength, and flexural behavior of steel-reinforced beams. This approach seeks to provide a more comprehensive understanding of the material's potential for practical applications.

Research significance

This study aims to contribute to the understanding of using rubberized concrete in structural applications, particularly in the case of reinforced beams, which is an area that is still underexplored despite the extensive research carried out on rubberized concrete behavior. Reinforced beams are structural elements that play a critical role in load-bearing systems; thus, understanding the effect of rubber on their performance is essential for its practical use in construction.

The study aims to analyze the flexural performance of reinforced concrete beams incorporating crumb rubber up to 30% by volume. We provide essential insights into the feasibility of using rubberized concrete in structural applications by evaluating key mechanical properties such as bending capacity, deflection, and failure modes.

Furthermore, with the increasing environmental concerns about waste tire disposal, this research contributes to the development of an eco-friendly construction material. By providing experimental validation and discussing the feasibility of incorporating rubberized concrete in reinforced beams, this study paves the way for future research and practical implementation in sustainable construction projects.

Experimental investigation

Materials

To ensure the quality of our mixture, the material selection process for concrete production was conducted carefully. The cement utilized is CEM II/B-M (S-LL) 42.5R, according to SR EN 197-1 standard (Asociatia de Standardizare din România [ASRO], 2011) type Structo Plus® from HOLCIM (Holcin, 2023). Natural aggregates with rounded edges, sourced from rivers, were selected based on their quality and size distribution and were classified into three groups (0–4 mm, 4–8 mm, 8–16 mm).

Crumb rubber was obtained from a local supplier by cutting end-of-life tires. They underwent a cleaning process aiming to eliminate any foreign elements. Tap water meeting standard quality requirements was used as the mixing water.

Specimen preparation

In this research, Group 1 is defined as the reference group and has 0% of crumb rubber. Fine and coarse aggregates have been replaced with crumb rubber for Groups 2, 3, and 4 at 10%, 20%, and 30% by volume, respectively.

The concrete used is class C30/37 (Toma et al., 2021), commonly used in standard applications. The water-cement ratio remained constant (W/C = 0.43) for the four mixtures, eliminating the influence of this parameter on the results and isolating the effect of the other variables studied (the addition of crumb rubber).

Preparation of the concrete mixture. The mix was prepared according to the proportions in Table 1 using a concrete mixer. Dry natural and crumb rubber aggregates were initially combined and mixed; afterward, dry cement was added, and the mixture was thoroughly mixed for an additional minute. Water and additives were included gradually. The entire mixture was continuously mixed until it was a homogenous mixture.

TABLE 1. Mix proportions

Specification	Group			
	1 (0%)	2 (10%)	3 (20%)	4 (30%)
Cement [kg·m^{-3}]	489			
Water [kg·m^{-3}]	210			
W/C [-]	0.43			
Regular aggregates [kg·m^{-3}]				
0–4 mm	582	523.80	465.60	407.40
4–8 mm	388	310.40	232.80	155.20
8–16 mm	646.70	646.70	646.70	646.70
Rubber aggregates [kg·m^{-3}]				
0–4 mm	0	10.95	21.90	32.85
4–8 mm	0	14.60	29.20	43.80
8–16 mm	0	0	0	0
Additives [kg·m^{-3}]	4.89			

Source: own work.

Mold preparation. A formwork oil application was performed on the internal surfaces of all molds before concrete casting. Afterward, the molds were filled, gradually compacted, and vibrated. A trowel was utilized to make a smooth surface. The samples were left to dry until the age of 28 days in standard laboratory conditions.

Preparation of specimens for tensile testing. To evaluate the tensile strength of each mix, cylinders of identical dimensions (diameter 100 mm × height 200 mm) were cast. It was performed according to SR EN 12390-1 standard (ASRO, 2000). A minimum of four cylinders from each group were prepared.

Stripping. The stripping age was 24 h. All the elements were identified based on their group, number, and casting date.

Preparation of beams for flexural testing. A total of 16 beams (four from each group) of identical dimensions (length 1,500 mm, height 120 mm, width 90 mm) were cast to evaluate the bending behavior of rubberized concrete beams.

Longitudinal reinforcement. It was made using two high-adhesion steel bars of 10 mm spaced 5 cm apart. Transversal reinforcement was made using 6 mm diameter pins with 10-centimeter spacing. To prevent confusion during the tests, a rectangle was marked on the beam to indicate the area devoid of reinforcements. A three-centimeter concrete cover was maintained. The stripping age was 48 h. All the elements were identified according to their group, number, and casting date.

Density measurement

At 28 days of age, the dimensions of concrete cylinders (diameter and height) were measured using calibrated instruments. The elements were weighed using a calibrated precision scale, and all the data were recorded. The density was calculated using Equation 1, according to the BS EN 12390-7 standard (British Standards Institution [BSI], 2009). Three measurements were conducted on each prepared sample, and the average value was calculated, thereby accounting for measurement errors:

$$\rho = \frac{m}{V}, \tag{1}$$

where: ρ represents the apparent density of the sample [kg·m^{-3}], m is the dry mass [kg], and V denotes the apparent volume of the sample [m^3].

Tensile testing procedure

The tensile test (Fig. 1) was carried out in the form of a splitting test on the rubberized concrete cylinders at the age of 28 days using a universal testing machine WAW-600E with a capacity of 600 kN. The procedure was executed according to SR EN 12390-6 (ASRO, 2019b).

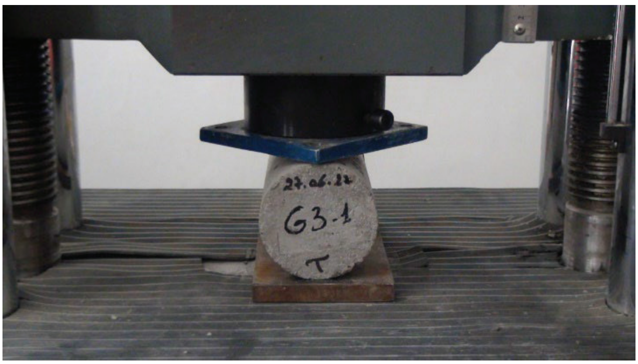

FIGURE 1. Splitting test
Source: own photo.

Enkaiki, L., Jarachi, O., Mihai, P., Moulay Abdelali, H., Moustachi, O. E. K. (2025). Flexural and tensile behavior of rubberized concrete: experimental analysis. *Sci. Rev. Eng. Env. Sci.*, *34* (2), 128–143. DOI 10.22630/srees.10183

During the whole test, the loading speed was maintained constant and equal to $v = 2\ \text{kN}\cdot\text{s}^{-1}$. A load distribution plate was placed on the top surface of the specimen to ensure uniform load distribution. The results (maximum load applied) were obtained using a measurement acquisition system.

The splitting tensile strength f_{ctm} [MPa] is then calculated using the following formula:

$$f_{\text{ctm}} = \frac{2F}{\pi\, d\, h}, \tag{2}$$

where: F is the maximum applied load [kN], d is the cylinder diameter [mm] and h is the cylinder height [mm].

Flexural testing procedure

Four-point flexural tests were conducted on beams at the age of 28 days employing a universal testing machine WAW-600E with a capacity of 600 kN (Fig. 2). The procedure was executed according to SR EN 12390-5 (ASRO, 2019a). The beams were positioned horizontally on two support rollers, and a steel spreader beam was used to distribute the load onto two points.

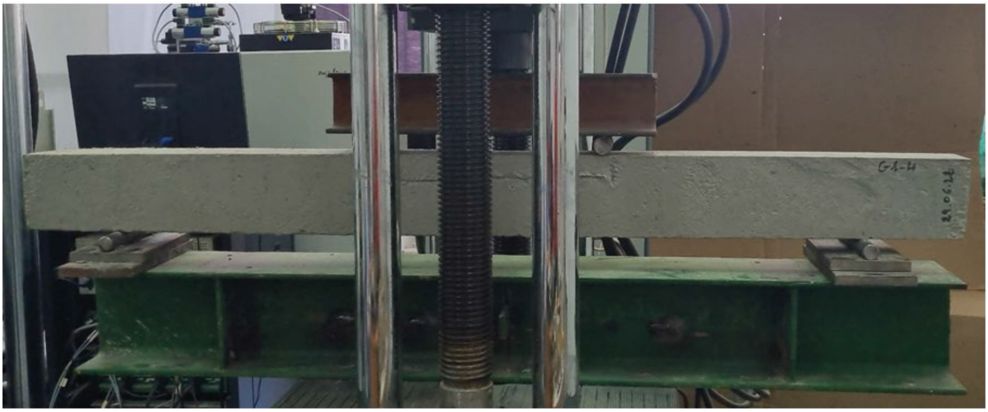

FIGURE 2. Test configuration of beams
Source: own photo.

During the whole test, the loading speed was maintained constant and equal to $v = 0.1\ \text{kN}\cdot\text{s}^{-1}$. The results of the flexural breaking strength and deflection at mid-span were obtained using a measurement acquisition system.

Results and discussions

Density

The variation in density across the four groups is presented in Table 2 and Figure 3.

TABLE 2. Density (ρ) variation

Specification	Group			
	1 (0%)	2 (10%)	3 (20%)	4 (30%)
ρ [kg·m^{-3}]	2 238.09	2 181.66	2 170.22	2 113.16
StDev	6.45	10.46	6.20	5.21
Average + 1StDev	2 244.54	2 192.12	2 176.42	2 118.37
Average − 1StDev	2 231.64	2 171.19	2 164.02	2 107.95

StDev – the standard deviation.

Source: own work.

The density results reveal a clear decreasing trend with an increasing percentage of crumb rubber. Group 1 has the highest density at 2,238.09 kg·m^{-3}. For Group 2, with 10% of crumb rubber, the density decreases to 2,181.66 kg·m^{-3}, representing a 2.5% reduction. A further decrease in density was observed in Group 3 at 20% to 2,170.22 kg·m^{-3}, indicating a 3% reduction compared to the reference group. Finally, the lowest density at 2,113.16 kg·m^{-3} was recorded for Group 4 at 30%, indicating a 5.6% reduction from the reference group (Fig. 4).

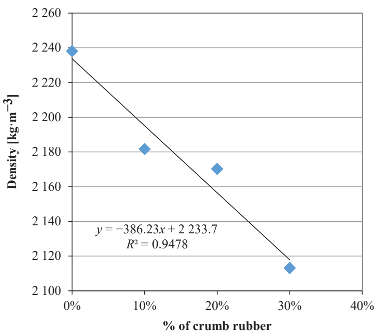

FIGURE 3. Density curve as a function of crumb rubber content

Source: own work.

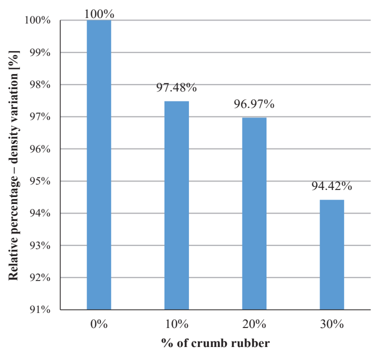

FIGURE 4. Variations in density normalized to the reference group

Source: own work.

The decreasing trend reflects the lower density of crumb rubber in comparison to natural aggregates leading to a progressively lighter concrete as the percentage of crumb rubber increased.

Splitting tensile strength

The variation in splitting tensile strength across the four groups is presented in Table 3 and Figure 5.

TABLE 3. Splitting tensile strength (f_{ctm}) variation

Specification	Group			
	1 (0%)	2 (10%)	3 (20%)	4 (30%)
f_{ctm} [MPa]	2.66	2.26	1.89	1.46
StDev	0.15	0.25	0.08	0.11
Average + 1StDev	2.82	2.50	1.97	1.57
Average − 1StDev	2.51	2.01	1.80	1.35

StDev – the standard deviation.

Source: own work.

The test results show a clear decreasing trend as the percentage of crumb rubber substituting natural fine and coarse aggregates increased. Group 1 (reference concrete) exhibits the maximum value of tensile strength at 2.66 MPa, serving as the reference group. Group 2, with 10% of crumb rubber, shows a decrease in tensile strength to 2.26 MPa, representing a 15% reduction. This reduction was more pronounced for Group 3 at 20% of crumb rubber to 1.89 MPa, indicating a 29% reduction compared to the reference group. The minimum value of 1.46 MPa was recorded for Group 4 at 30% of crumb rubber, making a 45% reduction from the reference group (Fig. 6).

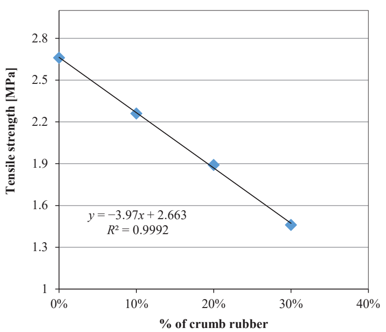

FIGURE 5. Tensile strength curve as a function of crumb rubber content

Source: own work.

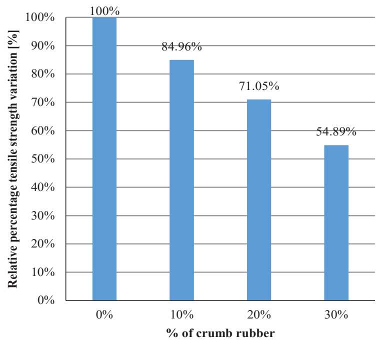

FIGURE 6. Variations in tensile strength normalized to the reference group

Source: own work.

The tensile strength reduction may be explained by the weak bonding between crumb rubber and the cement paste, which may lead to early crack propagation, as well as the lower density of rubberized concrete, which may lead to a less compact and uniform microstructure and a higher porosity which makes it more prone to crack formation.

Flexural testing

Flexural breaking strength

The variation in flexural breaking strength across the four groups is presented in Table 4 and Figure 7.

TABLE 4. Variation in flexural breaking strength (F)

Specification	Group			
	1 (0%)	2 (10%)	3 (20%)	4 (30%)
F [kN]	31.68	28.97	30.68	28.79
StDev	1.22	0.80	0.88	1.69
Average + 1StDev	32.90	29.77	31.56	30.48
Average − 1StDev	30.46	28.17	29.80	27.09

StDev – the standard deviation.

Source: own work.

The maximum value of the flexural breaking strength was observed for the reference group at 31.68 kN. For Group 2, with 10% of crumb rubber, a decrease to 28.97 kN was noticed, indicating an 8.6% reduction, which may be explained by the lower stiffness and weaker bonding properties of rubber. Group 3 showed a flexural breaking strength of 30.68 kN, which is slightly lower by only 3% than the reference group; the 20% replacement might be an optimal balance between flexibility and structural integrity. Group 4, with 30% of crumb rubber, showed a further reduction in flexural breaking strength up to 28.79 kN, a 9% drop from the reference group (Fig. 8).

A decrease in flexural breaking strength may be attributed to the soft nature of crumb rubber, which can reduce the stiffness of concrete. In addition, the weak bonding between crumb rubber and cement and the increased air voids may also contribute to the premature failure of concrete.

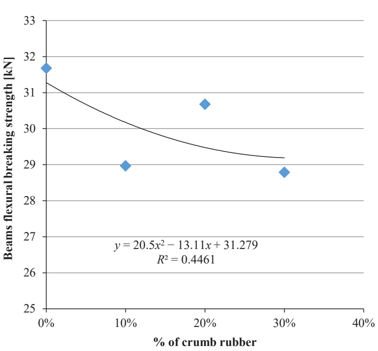

FIGURE 7. Flexural breaking strength variation curve as a function of crumb rubber content

Source: own work.

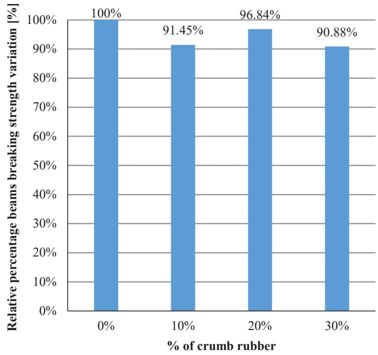

FIGURE 8. Variations in breaking strength normalized to the reference group

Source: own work.

Deflection at mid-span

The variation of the deflection at mid-span across the four groups is presented in Table 5 and Figure 9.

TABLE 5. Deflection variation at mid-span

Specification	Group			
	1 (0%)	2 (10%)	3 (20%)	4 (30%)
Deflection [mm]	17.23	14.84	13.36	14.96
StDev	3.28	1.89	0.59	1.54
Average + 1StDev	20.51	16.73	13.95	16.50
Average − 1StDev	13.95	12.95	12.76	13.42

StDev – the standard deviation.

Source: own work.

The peak deflection value of 17.23 mm at the mid-span was observed for the reference group, which serves as the baseline for the comparison. Group 2 showed a drop to 14.84 mm, indicating a 14% reduction in deflection. Group 3, with 20% crumb rubber replacement, shows a more remarkable reduction in deflection up to 13.36 mm, representing a 22.5% decrease from the reference group, which might be explained by an optimal balance in stiffness and flexibility. Group 4 exhibits a deflection of 14.96 mm, which represents a 13% drop from Group 1. The results show that at an optimal rubber content, deflection is reduced by enhancing energy absorption, while above a specific percentage, crumb rubber substitution may start to negatively affect the stiffness of concrete (Fig. 10).

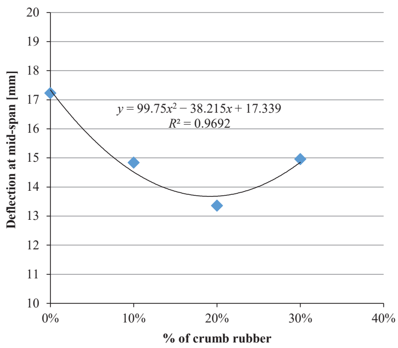

FIGURE 9. The curve of mid-span deflection as a function of crumb rubber content

Source: own work.

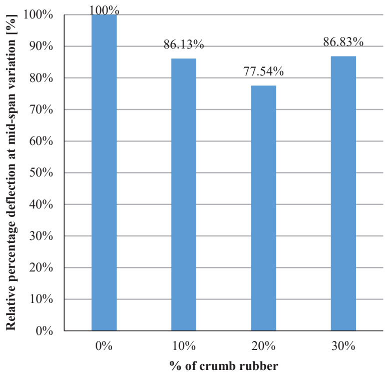

FIGURE 10. Variations of mid-span deflection normalized to the reference group

Source: own work.

Failure mode

The results of the failure modes across the four groups are presented in Figure 11. The addition of crumb rubber as a replacement for natural aggregates results in distinct variations in the failure mode of beams across the four different groups.

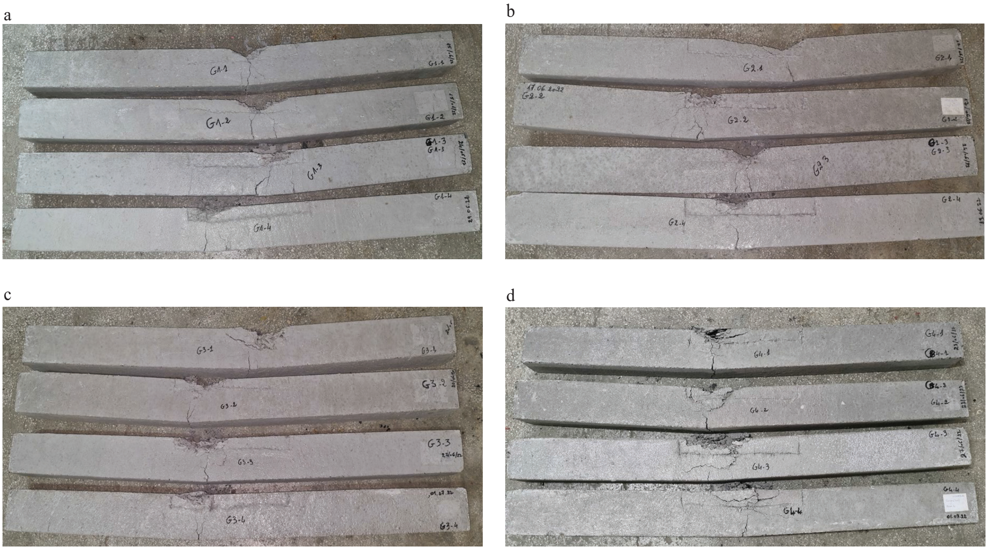

FIGURE 11. Failure modes of Group 1 (a), Group 2 (b), Group 3 (c) and Group 4 (d)

Source: own work.

For Group 1, a brittle failure mode was observed, which might be explained by the low ductility and high rigidity of reinforced concrete. Group 2 beams tend to show a more ductile failure mode compared to the reference group, which might be attributed to the energy-absorbing properties of rubber. Group 3, with 20% of crumb rubber, shows a further enhancement in ductility as demonstrated by the breaking flexural strength of 30.68 kN and the reduced deflection at mid-span of 13.36 mm. Group 3 beams indicate an optimal balance between flexibility and structural integrity. Finally, for Group 4, at 30% of crumb rubber, beams exhibit a highly ductile failure mode. This behavior might be explained by the flexible nature of crumb rubber, which enhances energy absorption and toughness.

Conclusion

The study investigates the impact of introducing crumb rubber into concrete at varying percentages (10%, 20%, and 30%) and evaluates its effect on concrete properties. The key findings are summarized as follows:

– Density tends to decrease slightly as the percentage of crumb rubber increases, which can be beneficial for lightweight construction applications.
– Splitting tensile strength was observed to decrease linearly as the percentage of crumb rubber increased, reaching 45%. This can be attributed to the soft nature of rubber compared to natural aggregates, as well as the weak adherence between rubber and cement.
– The addition of crumb rubber led to a slight decrease in the flexural breaking strength of the beams. The loss in strength was smaller compared to the reduction in tensile strength, suggesting that the addition of crumb rubber up to 30% of the volume can maintain sufficient structural integrity.
– Deflection at mid-span decreases as crumb rubber content increases, which indicates that rubberized concrete beams are less prone to excessive deformation under load, potentially improving their overall serviceability.
– Beam failure mode evolves from a brittle failure mode for the reference group to a more ductile failure for rubberized concrete beams with 10%, 20%, and 30% of crumb rubber content. A ductility enhancement was noticed with higher rubber content, which could improve the safety and energy-absorption capacity of structures under dynamic loads as for anti-seismic constructions.

The addition of crumb rubber as a replacement of naturally fine and coarse aggregates at 10%, 20%, and 30% by volume resulted in a significant reduction in splitting tensile strength, while the reduction in flexural breaking strength of the beams was lower. This suggests that rubberized concrete may not be an ideal option for high-load-bearing structural elements but can still be used for some specific applications, such as for non-load-bearing walls and pavement blocks. However, ductility was significantly improved, which could be a desirable characteristic in impact-resistance structures, such as protective barriers. Furthermore, the gradual failure mode makes rubberized concrete a promising material for applications that demand higher deformation capacity, such as shock-absorbing panels.

Based on these findings, it can be noted that rubberized concrete may require careful mix design adjustments to control strength losses. However, its improved ductility, lightweight properties, and improved failure behavior make it a promising material for sustainable and specific construction applications.

References

AbdelAleem, B. H., & Hassan, A. A. A. (2022). Use of rubberized engineered cementitious composite in strengthening flexural concrete beams. *Engineering Structures*, *262*, 114304. https://doi.org/10.1016/j.engstruct.2022.114304

Abdelmonem, A., El-Feky, M. S., Nasr, E. S. A., & Kohail, M. (2019). Performance of high strength concrete containing recycled rubber. *Construction and Building Materials*, *227*, 116660. https://doi.org/10.1016/j.conbuildmat.2019.08.041

Alasmari, H. A., Bakar, B. A., & Noaman, A. T. (2019). A comparative study on the flexural behaviour of rubberized and hybrid rubberized reinforced concrete beams. *Civil Engineering Journal*, *5* (5), 1052–1067. http://dx.doi.org/10.28991/cej-2019-03091311

Al-Azzawi, A. A., Shakir, D., & Saad, N. (2018). Flexural behavior of rubberized reinforced concrete beams. *International Journal of Engineering & Technology*, *7* (4.20), 316–320. https://doi.org/10.14419/ijet.v7i4.20.25946

Asociatia de Standardizare din România [ASRO] (2019a). *Încercare pe beton întărit. Partea 5: Rezistenţa la încovoiere a epruvetelor* (SR EN 12390-5).

Asociatia de Standardizare din România [ASRO] (2019b). *Încercare pe beton întărit. Partea 6: Rezistenţa la întindere prin despicare a epruvetelor* (SR EN 12390-6).

Asociatia de Standardizare din România [ASRO] (2000). *Încercare pe beton întărit. Partea 1: Forma, dimensiuni şi alte condiţii pentru epruvete şi tipare* (SR EN 12390-1).

Atahan, A. O., & Yücel, A. Ö. (2012). Crumb rubber in concrete: Static and dynamic evaluation. *Construction and Building Materials*, *36*, 617–622. https://doi.org/10.1016/j.conbuildmat.2012.04.068

Bisht, K., & Ramana, P. V. (2017). Evaluation of mechanical and durability properties of crumb rubber concrete. *Construction and Building Materials*, *155*, 811–817. https://doi.org/10.1016/j.conbuildmat.2017.08.131

British Standards Institution [BSI] (2009). *Testing hardened concrete. Part 7: Density of hardened concrete* (BS EN 12390-7).

Deshpande, N., Kulkarni, S. S., Pawar, T., & Gunde, V. (2014). Experimental investigation on strength characteristics of concrete using tyre rubber as aggregates in concrete. *International Journal of Applied Engineering Research and Development (IJAERD)*, *4* (2), 97–108.

Eisa, A. S., Elshazli, M. T., & Nawar, M. T. (2020). Experimental investigation on the effect of using crumb rubber and steel fibers on the structural behavior of reinforced concrete beams. *Construction and Building Materials*, *252*, 119078. https://doi.org/10.1016/j.conbuildmat.2020.119078

Holcim (2023). *Declaration of performance No. CPR-049-CP*. Holcim. https://www.holcim.ro/sites/romania/files/2023-03/49-dop-cem-ii-bm_s-ll-42.5r-structo-plus-campulung-v4_15.03.2023.pdf

Fauzan, Putri, E. E., Evir, H. P., Agista, G. A., & Juliafad, E. (2023). Experimental investigation on the use of crumb rubber as partial replacement of coarse aggregate in concrete incorporating cement replacement materials. *GEOMATE Journal*, *25* (111), 246–253. https://doi.org/10.21660/2023.111.gxi399

Ghoniem, A., & Aboul Nour, L. (2024). Experimental investigation into the properties of crumb rubberized concrete incorporating corrugated round steel fibers. *Archives of Civil and Mechanical Engineering*, *24* (2), 100. https://doi.org/10.1007/s43452-024-00883-z

Girskas, G., & Nagrockienė, D. (2017). Crushed rubber waste impact of concrete basic properties. *Construction and Building Materials*, *140*, 36–42. https://doi.org/10.1016/j.conbuildmat.2017.02.107

Ismail, M. K., & Hassan, A. A. (2017a). An experimental study on flexural behaviour of large--scale concrete beams incorporating crumb rubber and steel fibres. *Engineering Structures*, *145*, 97–108. https://doi.org/10.1016/j.engstruct.2017.05.018

Ismail, M. K., & Hassan, A. A. A. (2017b). Shear behaviour of large-scale rubberized concrete beams reinforced with steel fibres. *Construction and Building Materials*, *140*, 43–57. https://doi.org/10.1016/j.conbuildmat.2017.02.109

Karunarathna, S., Linforth, S., Kashani, A., Liu, X., & Ngo, T. (2021). Effect of recycled rubber aggregate size on fracture and other mechanical properties of structural concrete. *Journal of Cleaner Production*, *314*, 128230. https://doi.org/10.1016/j.jclepro.2021.128230

Mendis, A. S. M., Al-Deen, S., & Ashraf, M. (2017). Effect of rubber particles on the flexural behaviour of reinforced crumbed rubber concrete beams. *Construction and Building Materials*, *154*, 644–657. https://doi.org/10.1016/j.conbuildmat.2017.07.220

Mohammed, H. H., & Ali, A. S. (2023). Flexural Behavior of Reinforced Rubberized Reactive Powder Concrete Beams under Repeated Loads. *Journal of Engineering*, *29* (08), 27–46. https://doi.org/10.31026/j.eng.2023.08.03

Pham, T. M., Chen, W., Elchalakani, M., Karrech, A., & Hao, H. (2020). Experimental investigation on lightweight rubberized concrete beams strengthened with BFRP sheets subjected to impact loads. *Engineering Structures*, *205*, 110095. https://doi.org/10.1016/j.engstruct.2019.110095

Sharaky, I. A., Mohamed, H. A., Torres, L., & Emara, M. (2020). Flexural behavior of rubberized concrete beams strengthened in shear using welded wire mesh. *Composite Structures*, *247*, 112485. https://doi.org/10.1016/j.compstruct.2020.112485

Toma, I. O., Alexa-Stratulat, S. M., Mihai, P., Toma, A. M., & Taranu, G. (2021). Experimental investigations on the long term material properties of rubberized portland cement concrete. *Applied Sciences*, *11* (22), 10868. https://doi.org/10.3390/app112210868

Walid, M., Abdelrahman, A., Kohail, M., & Moustafa, A. (2022). Stress–Strain behavior of rubberized concrete under compressive and flexural stresses. *Journal of Building Engineering*, *59*, 105026. https://doi.org/10.1016/j.jobe.2022.105026

Summary

Flexural and tensile behavior of rubberized concrete: experimental analysis. The escalating accumulation of rubber waste, especially from end-of-life tires, represents a very significant and pressing environmental challenge that requires particular attention from environmental organizations worldwide, as well as industries, to minimize its negative effects on ecosystems, human well-being, and the planet's long-term sustainability as much as possible. The goal of this study is to explore a sustainable solution by introducing crumb rubber into a concrete mixture and evaluate its feasibility for structural applications. Thus, crumb rubber was introduced at different percentages by volume (0%, 10%, 20%, and 30%) to examine its effect on density, splitting tensile strength, and flexural behavior. The results shed light on the potential of rubberized concrete as an eco-friendly substitute while addressing its challenges. In fact, at 30% of crumb rubber content, density decreased by 5.6%, while splitting tensile strength decreased by 45%. However, beam flexural breaking strength marginally decreased by 9%, and deflection at mid-span decreased by around 13% for 30% of crumb rubber content. The failure mode evolved from brittle in concrete to slightly ductile with increased rubber content. The cracks observed in both reference concrete and rubberized concrete were similar, implying that the introduction of rubber did not result in a significant change in the overall behavior of the concrete at ultimate strength.

Scientific Review Engineering and Environmental Sciences (2025), 34 (2), 144–169

Sci. Rev. Eng. Env. Sci. (2025), 34 (2) https://srees.sggw.edu.pl

ISSN 1732-9353 (suspended) eISSN 2543-7496 DOI 10.22630/srees.10055

Received: 05.11.2024
Accepted: 14.04.2025

Libor ANSORGE✉

Dagmar VOLOŠINOVÁ

Robert KOŘÍNEK

Výzkumný ústav vodohospodářský T.G. Masaryka, Praha

Life cycle assessment in the Visegrad Group: a bibliometric analysis

Keywords: life cycle assessment, LCA, bibliometric analysis, Visegrad Group

Introduction

Life cycle assessment (LCA) is one of the frequently used tools for environmental impact assessment. It provides an analytical tool for evaluating a wide range of environmental aspects of the life cycle of a product or service (Hauschild et al., 2018). Although the idea of LCA dates back to the 1970s and was termed resource and environmental profile analysis (Klöpffer & Grahl, 2014), the LCA methodology saw great methodological development in the 1980s and 1990s, when many methodological procedures were developed and are still being developed today (Bjørn et al., 2018a). Like many other methodologies for environmental impact assessment, LCA has its shortcomings and limitations (Bjørn et al., 2018b). The complexity of environmental assessment using LCA is made possible by a number of simplifications and uncertainties (Hellweg et al., 2014). There is also a need to develop LCA based on current knowledge and technological progress (Karuppiah et al., 2023). The task of the LCA scientific community

✉libor.ansorge@vuv.cz

is to find ways to solve the outstanding problems of LCA (Reap et al., 2008). The Society of Environmental Toxicology and Chemistry (SETAC) has played a key role in the development and advancement of LCA through workshops, publications, and support for standardization (Fava et al., 2014). The three most active countries in LCA research are the USA, China, and Italy (Gaurav et al., 2021, 2023).

Four post-communist countries in Central Europe: Poland, Czechia, Hungary, and Slovakia, created an informal association called the Visegrad Group (Visegrad Four, V4) in 1991 with the aim of deepening mutual cooperation and harmonizing the development of these countries. The state of research and mutual cooperation of scientific teams dealing with LCA in the V4 has not yet been investigated. The purpose of this review is to map LCA research in the V4 using bibliometric methods. Bibliometrics is a research methodology that uses statistical methods to extract, aggregate, and analyze quantitative aspects of bibliographic information (Moed, 2005). Bibliometric analysis uses methods such as statistical analysis, citation analysis, and bibliometric mapping for a description of the intellectual structure in individual fields of study by analyzing the social and structural relationships between authors, countries, institutions, topics, etc. (Donthu et al., 2021). Therefore, this methodology was selected for mapping of LCA research in the V4.

For the purpose of mapping LCA research in the V4, the study seeks to answer the following research questions:

- RQ1 – What literature is relevant to LCA research in the V4 countries in terms of major publications and key authors?
- RQ2 – What specific areas of research are related to LCA in the V4 countries?
- RQ3 – How do the V4 countries cooperate in LCA research with each other and with other countries?
- RQ4 – What is the development of the production of scientific literature on LCA in the V4 countries?

Material and methods

Data collection

The Scopus database was used for bibliometric data collection, which is a source--neutral abstract and citation database indexing peer-reviewed scientific works such as articles, contributions at conferences, or books. Scopus was chosen because it covers more journals published in Europe than the Web of Science database (Asubiaro et al., 2024) and ensures high accuracy of metadata records

(Baas et al., 2020). Moutik et al. (2023) showed that Scopus indexes more articles focusing on LCA than Web of Science. Also, unlike new databases such as Dimension.AI, Crossref, or Lens.org, which rely primarily on Crossref data, i.e., on articles with an assigned DOI, Scopus is not limited to scientific articles with a DOI, but indexes all articles in selected journals.

Previous bibliometric analyses focused on LCA were analyzed to determine suitable search terms. Especially in the last few years, a large number of such studies focusing on individual countries have been published such as Brazil (Bodunrin et al., 2018), China (Nie, 2013), South Korea (Odey et al., 2021), Mexico (Güereca et al., 2015), New Zealand (Engelbrecht et al., 2018), Portugal (Burman et al., 2018), Sweden (Croft et al., 2019), groups of countries (Maepa et al., 2017) or parts of/entire continents such as Africa (Brent et al., 2002; Harding et al., 2021; Isah et al., 2024) or globally (Hou et al., 2015; He & Yu, 2020; Gaurav et al., 2021, 2023). On the other hand, other studies focus on particular areas such as construction (Yılmaz & Seyis, 2021; Aparna & Baskar, 2024), agriculture, and the food industry (Koblianska et al., 2024; Matos et al., 2024; Villagrán et al., 2024). Another area is the application of LCA to natural resources, such as bibliometric analysis of LCA studies evaluating groundwater (Carrión-Mero et al., 2022; Herrera-Franco et al., 2022). Dunmade (2019) analyzed a review of LCA teaching in Nigeria using bibliometric approaches. Other studies are focused on subfields of LCA, such as life cycle cost analysis (Martinho, 2023) or social life cycle assessment (Ghosh, 2023).

Based on the keywords used in previously published bibliometric studies of LCA, a list of keywords and their variants describing the field of LCA was created and used in this study. The following query was used to search for publications by authors from the V4 countries:

> TITLE-ABS-KEY (“life cycle assessment” OR “life-cycle assessment” OR “lifecycle assessment” OR “environmental LCA” OR “social LCA” OR “life cycle sustainability assessment” OR “lifecycle sustainability assessment” OR “life-cycle sustainability assessment” OR “economic LCA” OR “conceptual LCA” OR “life cycle management” OR “life-cycle management” OR “lifecycle management” OR “life cycle cost*” OR “life-cycle cost*” OR “lifecycle cost*” OR “life cycle impact” OR “life-cycle impact” OR “lifecycle impact”) AND (AFFILCOUNTRY (Czech OR Slovakia OR Hungary OR Poland)) AND PUBYEAR < 2024

Data collection was performed on 2 July 2024, and data was exported in CSV format. Due to the date of data collection and the limitation to the year 2023 and older (including information on the number of citations), it is unlikely that there will be a significant expansion of the indexed works or the number of citations during this period. Of course, this can happen due to additional inclusion of conference proceedings or corrections to import mechanisms, when some works are omitted. Diacritics were removed as part of pre-processing, as names with diacritics are not always listed correctly in the Scopus database.

Method selection

Every scientific article includes some kind of literature review, which demonstrates that the author has placed their study in the context of current knowledge. However, the usual descriptive (narrative) literature reviews can be biased by the researcher's criteria, which threatens scientific objectivity (Tranfield et al., 2003). Therefore, several robust methods have been developed in recent years to eliminate possible biases in literature reviews. To obtain the latest picture of the development of the scientific field and the current state of knowledge, bibliometrics, systematic reviews, and meta-analyses were used. All three methods use statistical analysis of large amounts of data. Bibliometrics focuses on the analysis of descriptive information of scientific publications (keywords, data on authors, etc.) and is therefore suitable for analyses of large sets of publications ranging from hundreds to thousands of publications (Donthu et al., 2021). Bibliometric methods introduce objectivity into the evaluation of scientific literature and have the potential to increase rigor and mitigate researcher bias in scientific literature searches (Zupic & Čater, 2015). Similarly, systematic reviews and meta-analyses make it possible to bring new knowledge about the development in a specific scientific field in a methodologically robust and verifiable way. However, these methods are based on examining the content of published studies (Hodgkinson & Ford, 2014). Meta-analyses are more narrowly focused than systematic reviews. Meta-analysis aims to analyze the variability of the value of some quantity in the examined set of documents. These three methods are often combined depending on the goals of the analysis. Based on the size of the obtained data set and the set of research questions, bibliometrics was chosen as the main research method.

Data analysis

In order to find answers to the research questions, several types of bibliometric data analysis were performed using different tools. Using the Scopus web interface, basic analyses of the number and types of publications, number of citations, number of authors, and cooperation between countries were performed. These analyses were performed by enlarging or narrowing the basic query, and the data was transferred to a spreadsheet to generate graphs and tables. Bibliometric network analysis was used to express links between publications. Links between countries and between keywords were analyzed to answer the research questions. The bibliometric software VOSviewer (van Eck & Waltman, 2010) version 1.6.20, which uses a mapping technique called similarity visualization (van Eck & Waltman, 2007), was used to analyze the bibliometric networks. In the case of countries, a co-authorship analysis was used. Researchers, research institutions, or countries are linked in co-authorship networks based on the number of publications they have co-authored. In the case of keywords, co-occurrence analysis was used. Keyword co-occurrence networks were limited to keywords that achieved at least 10 co-occurrences. The number of co-occurrences of two keywords is the number of publications in which both appear together in the title, abstract, or keywords (van Eck & Waltman, 2014). Weights by number were not considered either for countries or for keywords.

Results and discussion

Structure and number of publications on life cycle assessment in V4 countries

A total of 1,665 records meeting the criteria listed in the data collection were searched. The dominant type of output is the research article ($n = 961$), followed by contributions in proceedings ($n = 549$) and review articles ($n = 82$). The chapters in a book also reach a significant number ($n = 53$). A total of nine books on LCA were published by authors from V4 countries. Minority outputs were letters to editors ($n = 4$), editorials ($n = 4$), notes ($n = 2$), and errata ($n = 1$). Figure 1 shows the share of individual types of publications. Figure 2 shows the development in the number of publications and citations. Before 2005, publications on LCA written by authors from V4 countries were rather rare. After 2005, there is a clear trend of an increasing number of these publications. It can be assumed that the increase in the number of articles is associated with the standardization of the entire methodology in the ISO 14000 series of standards (International Organization for Standardization [ISO], 2015), and the resolution of a number of methodological shortcomings, which culminated in 2006 with the adoption of a number of revised ISO standards (Pryshlakivsky & Searcy, 2013). The increasing impact of LCA

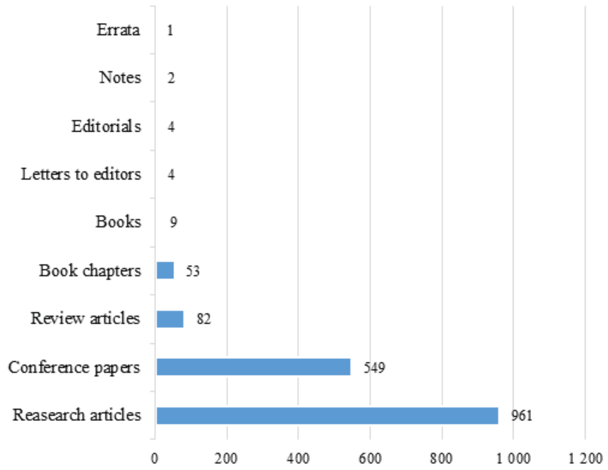

FIGURE 1. Structure of publications on LCA written by authors from V4 countries
Source: own work based on Scopus data.

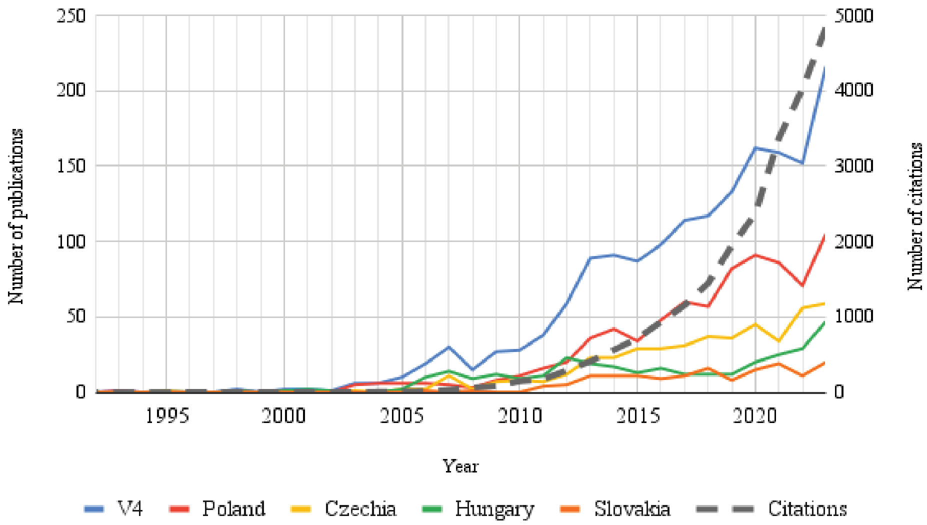

FIGURE 2. Number of publications on LCA written by authors from V4 countries over time
Source: own work based on Scopus data.

research in the V4 countries is evidenced not only by the number of publications but also by the number of citations, which is growing every year (Fig. 2 – grey dashed line), even though recent publications have not yet had enough time to gain many citations.

In total, publications written by authors from V4 countries received 22,613 citations. Authors from Poland participated in the most publications; they authored a total of 801 publications, and these publications received 11,573 citations. Czech authors participated in 455 publications that received 5,317 citations, Hungarian authors participated in 317 publications that received 5,401, and Slovak authors participated in 153 publications that received 1,187 citations.

TABLE 1. Number of publications by language used

Language	Number of publications	Share of the total number of publications [%]
English	1,626	97.66
Polish	37	2.22
Czech	7	0.42
German	2	0.12
Serbian	1	0.06
Lithuanian	1	0.06
Hungarian	1	0.06
Chinese	1	0.06

Source: own work.

Even in the case of authors from V4 countries, it is evident that the dominant language of contemporary science is English, of which 97.7% of all publications were published (Table 1). The reason why the sum of publications in individual languages is higher than the searched 1,665 publications is that Scopus registers 11 publications in two languages.

The most productive authors

Based on the number of publications, the 10 most active authors in each V4 country were selected. Based on the number of citations, the higher the number of citations, the better the ranking will be given to authors with the same number of publications. The list of the 10 most productive authors is shown in Table 2. A specific situation occurs with Jiří J. Klemeš, who has 35 publications with 2,115 citations and is thus the most cited author. However, he spent his career both at universities in Hungary and at the Brno University of Technology in Czechia. Therefore, the affiliations of his publications were individually analyzed in order to correctly assign them to individual countries.

TABLE 2. A list of the 10 most active authors from each V4 country

Poland	Number of publications	Number of citations	Czechia	Number of publications	Number of citations
D. Burchart-Korol	38	929	V. Kočí	35	419
J. Kulczycka	28	110	J.J. Klemeš	21	528
A. Lewandowska	25	646	A. Lupíšek	18	125
K. Grzesik,	21	55	J. Furch	17	66
J. Adamczyk	19	401	P. Hájek	16	239
B. Bieda	18	157	K. Struhala	16	127
A. Tomporowski	17	261	D. Vališ	12	134
A. Żelazna	16	50	R. Černý	10	328
R. Dylewski	15	232	J. Fořt	10	282
K. Pikoń	15	167	B. Teplý	9	91
Hungary	Number of publications	Number of citations	Slovakia	Number of publications	Number of citations
L. Horváth	77	465	S. Vilčeková	20	90
I.J. Rudas	71	352	A. Eštoková	16	85
Z. Szalay	15	146	E.K. Burdová	12	31
J.J. Klemeš	14	1,587	J. Štefko	11	51
V. Mannheim	13	112	J. Mitterpach	10	86
A.J. Toth	13	212	M. Ondová	10	52
B. Kiss	12	198	M. Potkány	8	83
P. Mizsey	12	275	A. Sedláková	7	44
G.L. Kovács	10	54	R. Vaňová	7	30
D. Fozer	9	247	M. Debnár	5	76

Source: own work.

Cooperation

LCA researchers in the V4 countries collaborate with scientists from around the world, as illustrated in Figure 3. However, cooperation within the V4 countries represents only a small part of international cooperation.

Table 3 shows that the share of cooperation within the V4 is the highest in the case of Slovak authors and the lowest in the case of Polish authors. There is no publication that is authored by authors from all four V4 countries, and only one publication (Ključnikov et al. 2023) was authored by authors from three V4 countries.

Table 4 shows the five countries for each V4 country with which they most often publish LCA research. Authors from the V4 cooperate with authors from 75 other countries. Excluding other V4 countries, Polish authors cooperate with authors from 68 countries, Czech authors cooperate with authors from 52 countries, Hungarian authors cooperate with authors from 49 countries, and Slovak authors cooperate with authors from 30 countries.

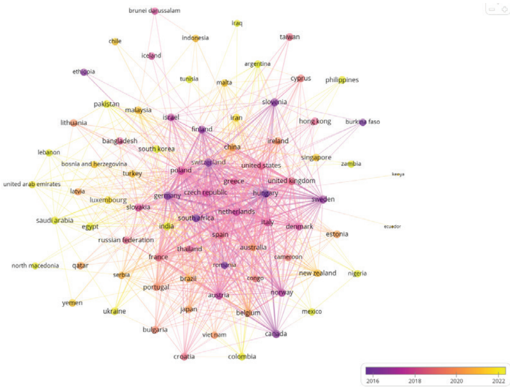

FIGURE 3. Cooperation networks between V4 countries based on co-authorship of published articles
Source: own work based on Scopus data.

TABLE 3. Share of co-authorship within V4 countries

Country	Total number of publications	Number of publications with co-authors from					Share of co-authors from the V4 [%]
		Poland	Czechia	Hungary	Slovakia	V4	
Poland	801	–	22	9	10	40	5.0
Czechia	455	22	–	6	13	40	8.8
Hungary	317	9	6	–	2	17	5.4
Slovakia	153	10	13	2	–	24	15.7

Source: own work.

TABLE 4. Top five partner countries for publishing research on LCA

Poland	Czechia	Hungary	Slovakia
Germany (40)	USA (23)	Austria (22)	Czechia (13)
Italy (39)	Poland (22)	Italy (16)	Poland (10)
Spain (26)	Germany (22)	Spain (14)	Spain (6)
USA (25)	China (18)	USA (14)	Germany (5)
UK (25)	Italy (16)	Germany (13)	the Netherlands (4)

Source: own work.

Conversely, the number of articles that were not created in collaboration with partners from other countries is shown in Table 5, which proves that the involvement of scientists from V4 countries in international research groups is still very limited. If authors from the V4 cooperate internationally, then they cooperate with authors mainly from other European countries, as well as the USA or China. Cooperation with researchers from Australia or South America is very rare.

TABLE 5. Publications written only by authors from a particular V4 country

Country	Total number of publications	Number of publications written by authors only from the given country	Share of publications written by authors only from the given country [%]
Poland	801	565	70.5
Czechia	455	289	63.5
Hungary	317	193	60.9
Slovakia	153	111	72.5

Source: own work.

Another perspective provides cooperation on the author level. Figure 4 shows cooperation between authors with 10 or more papers. The figure shows that the cooperation between the most active authors is very limited.

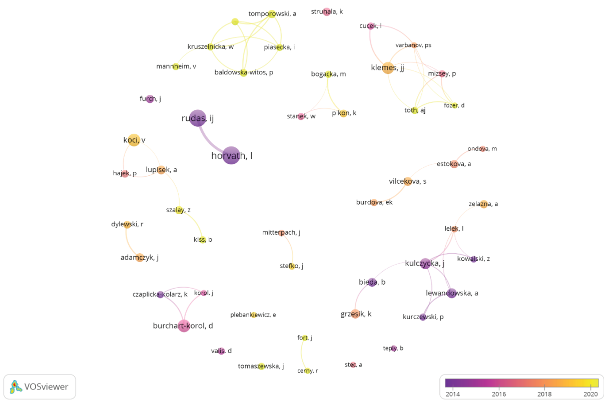

FIGURE 4. Cooperation networks between authors with 10 or more published articles from V4 countries based on co-authorship

Source: own work based on Scopus data.

Authors create clearly defined author collectives that are not interconnected through joint articles. In particular, there is practically no international cooperation within the V4 among the most active authors.

Most frequently used journals

Journals in which authors from the V4 countries most often publish research in the field of LCA were analyzed. Table 6 lists the journals in which ten or more articles were published. These journals published one-third of the total number of publications on LCA research in the V4 countries. The most often used is the journal Energies from the publishing house MDPI, which is mainly used by authors from Poland. Even in the field of LCA, the fact that the publishing house MDPI is very popular among Central European scientists (despite certain controversies) has been confirmed (Sasvari & Urbanovics, 2023). This is evidenced by the placement of several journals of the MDPI publishing house (Energies, Sustainability, Materials, Applied Science, Buildings) in Table 6. In second place is the Journal of Cleaner Production, which is the second most frequently used journal, even among authors from around the world (Gaurav et al., 2021).

TABLE 6. Journals in which authors from V4 publish research on LCA

Journal	Number of		Number of articles from			
	articles	citations	Poland	Czechia	Hungary	Slovakia
Energies	91	811	77	9	9	4
Journal of Cleaner Production	83	4,357	49	25	13	2
Sustainability	77	956	34	26	10	9
International Journal of Life Cycle Assessment	45	975	35	7	5	0
International Multidisciplinary Scientific Geoconference Surveying Geology and Mining Ecology Management SGEM	33	64	17	6	0	11
IOP Conference Series Materials Science and Engineering	23	100	12	10	0	2
Science of the Total Environment	22	701	15	8	1	0
IOP Conference Series Earth and Environmental Science	18	43	4	11	0	1
E3S Web of Conferences	18	91	17	0	0	1
Procedia Engineering	17	318	5	10	0	1
Chemical Engineering Transactions	17	107	9	5	0	1
Energy	16	914	10	3	3	0
Przemysł Chemiczny	14	32	14	0	0	0
Materials	14	245	12	1	0	1
Applied Sciences	14	152	8	3	1	3
CESB 2016 – Central Europe Towards Sustainable Building 2016: Innovations for Sustainable Future	13	19	0	12	0	1
Renewable and Sustainable Energy Reviews	12	401	5	7	0	0
Transport Means Proceedings of the International Conference	11	20	1	9	0	1
Buildings	11	85	5	6	0	0
Advanced Materials Research	11	40	2	4	2	3
MATEC Web of Conferences	10	44	6	3	0	1
Journal of Environmental Management	10	180	6	2	2	0

Source: own work.

It is worth mentioning that of the ten most frequently used journals, five are conference proceedings journals (International Multidisciplinary Scientific Geoconference Surveying Geology and Mining Ecology Management SGEM, IOP Conference Series Materials Science and Engineering, IOP Conference Series Earth and Environmental Science, E3S Web of Conferences, Procedia Engineering). The other five journals in the top 10 are highly visible journals that are in the first or second quartiles, according to SJR. On the one hand, this is an example of the fact that authors from the V4 prefer high-quality journals. On the other hand, it should also be noted that with the exception of the International Journal of Life Cycle Assessment, the other four journals (Energies, Journal of Cleaner Production, Sustainability, Science of the Total Environment) are examples of mega-journals that publish tens of thousands of articles per year.

Publications with high citations

Table 7 shows the 20 articles with the highest number of citations. The most cited articles are in the fields of energy, engineering, and environmental science.

The most cited publication (Čuček et al., 2012) is the study of authors from Hungary and Slovenia. This publication is an overview or narrative review of footprints, which are defined footprint-based indicators that can be used to measure sustainability. The publication also assesses composite footprints, which combine two or more individual footprints, and create multi-objective optimization problems. Currently, the researchers combine individual footprints into the environmental footprint family.

Polish authors co-authored the second and the third most-cited publications. The second most cited article (Kacprzak et al., 2017) is again a narrative review that compares existing sewage sludge management solutions for environmental sustainability, focusing on treatment and disposal strategies within current European and national legislation. It discusses using decision-making tools like end-of-waste criteria and LCA to evaluate environmental, economic, and technical aspects of different systems. The third most cited publication (Kargarzadeh et al., 2018) is also a narrative review that presents the recent advances made in the production of cellulose nanofibrils and cellulose nanocrystals, including conventional mechanical and chemical treatments, as well as other promising techniques and pretreatment processes aimed at designing an economically efficient and eco-friendly production route for nanocellulose. These most cited articles thus confirm the conclusions of some studies (e.g., Montori et al., 2003; Cronin et al., 2008), showing that review articles have a greater social impact than original research articles.

TABLE 7. The most cited publications – top 20 (only citations before 2024 are included)

Authors	Title	Year	Source	DOI	Number of citations
Čuček et al.	A review of footprint analysis tools for monitoring impacts on sustainability	2012	Journal of Cleaner Production	10.1016/j.jclepro.2012.02.036	692
Kacprzak et al.	Sewage sludge disposal strategies for sustainable development	2017	Environmental Research	10.1016/j.envres.2017.03.010	516
Kargarzadeh et al.	Advances in cellulose nanomaterials	2018	Cellulose	10.1007/s10570-018-1723-5	329
De Benedetto & Klemeš	The Environmental Performance Strategy Map: an integrated LCA approach to support the strategic decision-making process	2009	Journal of Cleaner Production	10.1016/j.jclepro.2009.02.012	299
Mikulčić et al.	Reducing greenhouse gasses emissions by fostering the deployment of alternative raw materials and energy sources in the cleaner cement manufacturing process	2016	Journal of Cleaner Production	10.1016/j.jclepro.2016.04.145	241
Boyano et al.	Exergoenvironmental analysis of a steam methane reforming process for hydrogen production	2011	Energy	10.1016/j.energy.2010.05.020	236
Ürge-Vorsatz et al.	Mitigating CO_2 emissions from energy use in the world's buildings	2007	Building Research and Information	10.1080/09613210701325883	203
Burchart-Korol	Life cycle assessment of steel production in Poland: A case study	2013	Journal of Cleaner Production	10.1016/j.jclepro.2013.04.031	202
Den et al.	Lignocellulosic biomass transformations via greener oxidative pretreatment processes: access to energy and value-added chemicals	2018	Frontiers in Chemistry	10.3389/fchem.2018.00141	198
Mayer et al.	Environmental and economic multi-objective optimization of a household level hybrid renewable energy system by genetic algorithm	2020	Applied Energy	10.1016/j.apenergy.2020.115058	194

Čuček et al.	Total footprints-based multi-criteria optimisation of regional biomass energy supply chains	2012	Energy	10.1016/j.energy.2012.01.040	191
Weinzettel et al.	Life cycle assessment of a floating offshore wind turbine	2009	Renewable Energy	10.1016/j.renene.2008.04.004	180
Frenger et al.	Reducing energy consumption in LTE with cell DTX	2011	IEEE Vehicular Technology Conference	10.1109/VETECS.2011.5956235	179
Weißbach et al.	Energy intensities, EROIs (energy returned on invested), and energy payback times of electricity generating power plants	2013	Energy	10.1016/j.energy.2013.01.029	173
Jędrzejczak et al.	The role of lignin and lignin-based materials in sustainable construction – A comprehensive review	2021	International Journal of Biological Macromolecules	10.1016/j.ijbiomac.2021.07.125	172
Mia et al.	Multi-objective optimization and life cycle assessment of eco-friendly cryogenic N_2 assisted turning of Ti-6Al-4V	2019	Journal of Cleaner Production	10.1016/j.jclepro.2018.10.334	165
Pfister et al.	Understanding the LCA and ISO water footprint: A response to Hoekstra (2016) "A critique on the water-scarcity weighted water footprint in LCA"	2017	Ecological Indicators	10.1016/j.ecolind.2016.07.051	155
Puppán	Environmental evaluation of biofuels	2002	Periodica Polytechnica Social and Management Sciences	–	124
Sun et al.	Uncovering energy use, carbon emissions and environmental burdens of pulp and paper industry: A systematic review and meta-analysis	2018	Renewable and Sustainable Energy Reviews	10.1016/j.rser.2018.04.036	121
Bong et al.	A review on the global warming potential of cleaner composting and mitigation strategies	2017	Journal of Cleaner Production	10.1016/j.jclepro.2016.07.066	119

Source: own work.

Czech authors contributed up to the ninth most cited publication. Slovak authors did not participate in the most cited publications.

Subject areas

The Scopus database ranks individual indexed contributions into subject areas. LCA is an interdisciplinary research field; therefore, the division into subject areas makes it easier to identify the area on which LCA research focuses. The dominant subject areas are technical fields, and the most widespread in all V4 countries is engineering. This makes the V4 countries slightly different from the rest of the world, where environmental sciences are the most widespread and engineering the second (Gaurav et al., 2021). Environmental sciences are the second most common field of researchers involved in LCA in Poland, Czechia, and Slovakia. On the other hand, in Hungary, environmental sciences are in third place and the second most widespread field is computer science. In Poland and Czechia, energy is in third place, while in Slovakia it is the field of social sciences. Table 8 lists the top ten subject areas in which V4 scientists working on LCA are active.

TABLE 8. Subject areas in which authors from V4 countries publish articles on LCA

Subject area	V4	Share [%]	Poland	Czechia	Hungary	Slovakia
Engineering	804	48	367	251	147	72
Environmental Science	582	35	337	149	75	43
Energy	424	25	267	96	58	23
Computer Science	265	16	80	50	117	22
Material Sciences	194	12	99	58	23	20
Social Science	181	11	69	63	32	28
Mathematics	169	10	98	23	42	16
Business, Management and Accounting	154	9	86	43	22	12
Chemical Engineering	127	8	62	25	33	13
Earth and Planetary Sciences	104	6	57	27	8	18

Source: own work.

The same analysis was done for 20 highly cited papers listed in Table 7. A total number of 13 papers were involved in the subject of engineering. The same number of papers were involved in the subject area of energy. The subject area of environmental science contains 12 papers. That's a similar situation to the group of all articles on LCA published by authors from the V4. Only two other subject areas (business, management and accounting) have more than two papers, with seven papers, and mathematics with four papers.

Keyword co-occurrence analysis

Keywords often reflect the aim and focus of the study. The authors used a total of 3,977 keywords. Figure 5 shows the links between 45 keywords that were used at least 10 times in the analyzed articles (Table 9). The diameter of the circle represents the occurrence of the keyword – the larger the circle is, the more often the keyword occurs. Co-occurrence relationships of two keywords are shown by a line connecting two circles. Circle colors indicate distinct clusters, and cluster structure is determined by the interaction between keywords, culminating in clusters of highly connected keywords. As can be seen, the keyword “life cycle assessment” is surrounded by many other keywords. Some of these keywords are similar; for example, for one term such as life cycle assessment, authors use other different notation variants such as LCA, life-cycle assessment, etc. Figures 6 and 7 show links between keywords that were used at least ten times in articles by Polish (Fig. 6) and Czech (Fig. 7) authors. Figures for Hungarian and Slovak authors are not presented because Hungarian authors met the limit of ten uses of only five keywords (life cycle assessment – 66×; product lifecycle management – 29×; LCA – 16×; product modeling – 16×; sustainability – 14×) and Slovak authors only four keywords (life cycle assessment – 41×; LCA – 24×; environmental impact – 16×; sustainability – 10×).

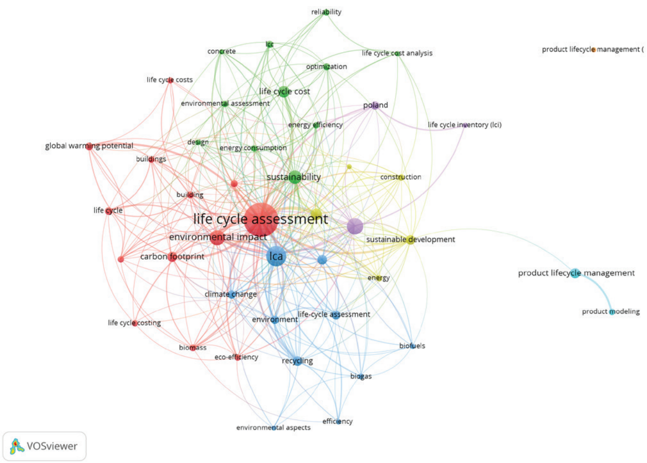

FIGURE 5. Co-occurrence analysis of LCA publication keywords published by V4 authors (keywords used at least 10 times are included)

Source: own work based on Scopus data.

TABLE 9. Most frequently used keywords

Keyword	Number of occurrences	Keyword	Number of occurrences
life cycle assessment	412	construction	16
lca	147	energy	16
life cycle assessment (lca)	94	energy efficiency	16
environmental impact	84	life cycle costing	16
sustainability	65	life cycle costs	16
life cycle cost	49	product modelling	16
circular economy	46	reliability	16
product lifecycle management	38	eco-efficiency	15
carbon footprint	37	energy consumption	15
recycling	35	environmental assessment	15
sustainable development	34	buildings	14
environmental impacts	33	greenhouse gases	14
life-cycle assessment	28	biogas	12
climate change	26	design	12
poland	25	concrete	11
environment	24	efficiency	11
global warming potential	20	biofuels	10
life cycle	20	environmental aspects	10
optimization	19	life cycle cost analysis	10
waste management	19	life cycle inventory (lci)	10
building	18	product lifecycle management (plm)	10
biomass	17	renewable energy sources	10
lcc	17		

Source: own work.

Figure 5 shows several automatically generated clusters based on the co-occurrence of keywords according to the VOS methodology (van Eck & Waltman, 2007). The first cluster (red) focuses on the LCA of buildings and its impact on global warming. The second cluster (green) focuses on the impact of energy consumption and the improvement of energy efficiency. The third cluster (blue) focuses on the sustainability of biogas and biofuels. These three clusters are the largest, and each contains at least 10 keywords. However, most keywords are interconnected with keywords in other clusters, so the above interpretation of the focus of individual clusters should be considered significantly simplistic. The fourth cluster (yellow) focuses on the circular economy, renewable energy resources, and sustainability of buildings and constructions. The fifth cluster (purple) is not sector-specific, but deals with LCA in Poland. If the first five clusters can be said to be closely interconnected, then the last two clusters (light blue and orange) are relatively independent and deal with product life cycle management.

Figure 6 shows generated clusters for publication authored by authors from Poland. The main topics for authors from Poland are sustainability, eco-efficiency, and improving energy consumption and its impact on carbon footprint and global warming. The next topics are circular economy, recycling, waste management, and sustainable use of biomass.

Figure 7 shows generated clusters for publication authored by authors from Czechia. The topics of circular economy, recycling, and climate change are similar to those in Poland. On the other hand, there are far fewer keywords meeting the selection criteria, which may be due to the significantly smaller number of publications in which Czech authors participated.

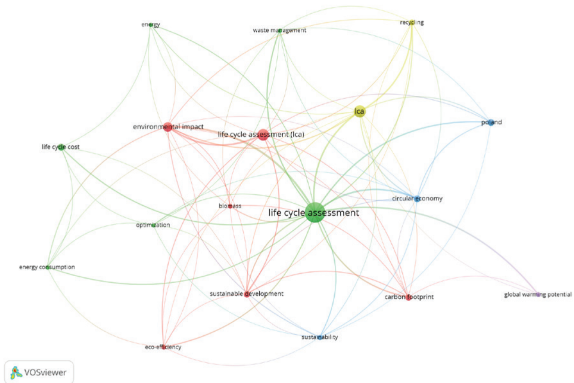

FIGURE 6. Co-occurrence analysis of LCA publication keywords published by authors from Poland (keywords used at least 10 times are included)

Source: own work based on Scopus data.

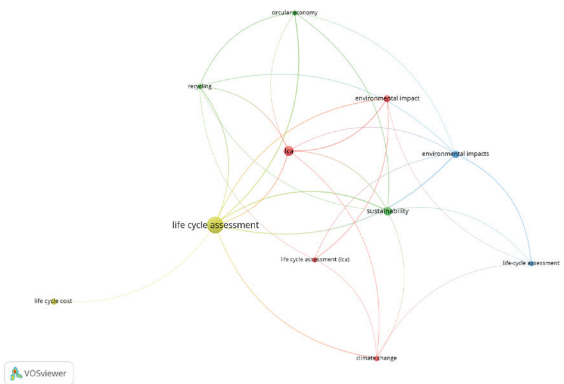

FIGURE 7. Co-occurrence analysis of LCA publication keywords published by authors from Czechia (keywords used at least 10 times are included)

Source: own work based on Scopus data.

The main funding organization

Most publications do not have the research support stated. The most important support providers are the European Union and its programs, such as Horizon. The most important supporters with 20 or more supported publications include agencies and ministries from all V4 countries (Table 10).

TABLE 10. Most important funding agencies

Funding agency	State	Number of publications
European Commission	EU	132
Horizon 2020 Framework Programme	EU	59
Narodowe Centrum Badań i Rozwoju (National Center for Research and Development)	Poland	43
Ministerstvo Školství, Mládeže a Tělovýchovy (Ministry of Education, Youth and Physical Education)	Czechia	36
European Regional Development Fund	EU	35
Ministerstwo Edukacji i Nauki (Ministry of Education and Science)	Poland	33
Grantová Agentura České Republiky (Technology Agency of the Czech Republic)	Czechia	33
Vedecká Grantová Agentúra MŠVVaŠ SR a SAV (Scientific Grant Agency of the Ministry of Education, Science and Research of the Slovak Republic and the Slovak Academy of Sciences)	Slovakia	28
Nemzeti Kutatási, Fejlesztési és Innovaciós Alap (National Research, Development and Innovation Fund)	Hungary	22
Technologická Agentur České Republiky (Technology Agency of the Czech Republic)	Czechia	21
Seventh Framework Programme	EU	21
UK Research and Innovation	UK	20

Source: own work.

Limitations and uncertainties of the study

This study has several limitations. First, the study was limited to Scopus data, so publications that are not indexed in this database but in other ones (such as Web of Science) are not included. As an example, an article by the author of this paper (Ansorge & Beránková, 2017) was published in the European Journal of Sustainable Development and is not indexed in Scopus. Authors from V4 countries will most probably also publish part of their research in national journals that are not indexed in prestigious international databases. An example is the articles by Vladimír Kočí (Kočí et al. 2019; Kráľová et al., 2020), who is the most active Czech author.

The second limitation results from the choice of search query. LCA is currently a highly widespread methodology, so many authors use only the abbreviation "LCA" as a keyword. Another article by Vladimír Kočí can be mentioned as an example (Pavlů et al., 2019). The point is that the abbreviation LCA is not only used for "life cycle assessment", but also in medicine (LCA = lithocholic acid), mathematics (LCA group = locally compact Abelian group), statistics (LCA = latent class analysis), etc. The Scopus database indexes 472 publications with "LCA" in the keywords, title, or abstract, which were written by authors from V4 countries and do not meet the criteria of the search query used. A portion of these publications will probably also be focused on life cycle assessment.

The last limitation may result from the fact that many authors may not use some form of LCA notation in the title, keywords, or abstract, but their research may still relate to LCA or use LCA techniques. It may be cases where the authors used more general terms such as "life cycle analysis", "life cycle", and "life cycle thinking" or studies that consider individual impact indicators, such as water footprint, for example, the article by Jiří J. Klemeš (Jia et al., 2019).

Conclusions

LCA is a widespread tool for environmental impact assessment and one of the main tools to promote steps leading to the achievement of sustainable development. Research in this area is worldwide, and the V4 countries are no exception. Researchers from Poland are the most active, followed by researchers from Czechia and Hungary, and the least extensive LCA research is in Slovakia. The most active researchers are László Horváth and Imre J. Rudas from Hungary, whose more than 70 publications significantly exceed the number of publications of other V4 researchers. Dorota Burchart-Korol from Poland has 38 publications, and Jiří J. Klemeš and Vladimír Kočí from Czechia have 35 publications. The most active Slovak researcher is Silvia Vilčeková, with 20 publications. Three researchers from Poland have more than 20 publications.

The most cited publications in the field of LCA are those of Jiří J. Klemeš, who worked in Hungary and subsequently in Czechia. However, such international connectivity is rather an exception, as cooperation in LCA research within the V4 countries is not high (expressed by co-authorships). Only for Slovak researchers are the main collaborators researchers from Czechia and Poland.

At the same time, international cooperation within the LCA topic is widespread and includes countries from all continents, except Antarctica.

The most widespread subject area in which LCA research is conducted is engineering, followed by environmental sciences. In Hungary, second place belongs to computer science, although the importance of computer science in Hungary is not reflected in keywords. The main areas that (according to keywords) are connected with LCA are mainly the impact on the environment, sustainability, circular economy, and sustainable development.

Due to its popularity among Polish authors, Energies is the most significant journal for the dissemination of LCA research conducted in V4 countries; in the other V4 countries, the journal was used less frequently. Other widely used journals are the Journal of Cleaner Production, Sustainability, and the International Journal of Life Cycle Assessment.

LCA research is gaining increasing attention in the V4 countries, albeit slowly compared to other parts of the world. This suggests that LCA will play a key role in fulfilling European environmental legislation and achieving the Sustainable Development Goals. The study highlights current and potential future areas of interest for LCA research. The knowledge published via this study can serve not only researchers working in the field of LCA but also research managers who are managing research in this field.

Acknowledgments

We would like to thank our colleague Lada Stejskalová for the English corrections. We would like to thank anonymous reviewers for their comments.

References

Ansorge, L., & Beránková, T. (2017). LCA water footprint AWARE characterization factor based on local specific conditions. *European Journal of Sustainable Development*, *6* (4), 13–20. https://doi.org/10.14207/ejsd.2017.v6n4p13

Aparna, K., & Baskar, K. (2024). Scientometric analysis and panoramic review on life cycle assessment in the construction industry. *Innovative Infrastructure Solutions*, *9* (4), 96. https://doi.org/10.1007/s41062-024-01402-y

Asubiaro, T., Onaolapo, S., & Mills, D. (2024). Regional disparities in Web of Science and Scopus journal coverage. *Scientometrics*, *129* (3), 1469–1491. https://doi.org/10.1007/s11192-024-04948-x

Baas, J., Schotten, M., Plume, A., Côté, G., & Karimi, R. (2020). Scopus as a curated, high-quality bibliometric data source for academic research in quantitative science studies. *Quantitative science studies*, *1* (1), 377–386. https://doi.org/10.1162/qss_a_00019

Bjørn, A., Owsianiak, M., Molin, C., & Hauschild, M. Z. (2018a). LCA History. In M. Z. Hauschild, R. K. Rosenbaum, & S. I. Olsen (Eds), *Life cycle assessment: theory and practice* (pp. 17–30). Springer International Publishing. https://doi.org/10.1007/978-3-319-56475-3_3

Bjørn, A., Owsianiak, M., Molin, C., & Laurent, A. (2018b). Main characteristics of LCA. In M. Z. Hauschild, R. K. Rosenbaum & S. I. Olsen (Eds), *Life cycle assessment: theory and practice* (pp. 9–16). Springer International Publishing. https://doi.org/10.1007/978-3-319-56475-3_2

Bodunrin, M. O., Burman, N. W., Croft, J., Engelbrecht, S., Goga, T., Ladenika, A. O., MacGregor, O. S., Maepa, M., & Harding, K. G. (2018). The availability of life-cycle assessment, water footprinting, and carbon footprinting studies in Brazil. *The International Journal of Life Cycle Assessment*, *23*, 1701–1707. https://doi.org/10.1007/s11367-018-1484-2

Brent, A. C., Rohwer, M. B., Friedrich, E., & Blottnitz, H. V. (2002). Status of life cycle assessment and engineering research in South Africa. *The International Journal of Life Cycle Assessment*, *7*, 167–172. https://doi.org/10.1007/BF02994051

Burman, N. W., Croft, J., Engelbrecht, S., Ladenika, A. O., MacGregor, O. S., Maepa, M., Bodunrin, M. O., & Harding, K. G. (2018). Life-cycle assessment, water footprinting, and carbon footprinting in Portugal. *The International Journal of Life Cycle Assessment*, *23*, 1693–1700. https://doi.org/10.1007/s11367-018-1483-3

Carrión-Mero, P., Montalván-Burbano, N., Herrera-Franco, G., Domínguez-Granda, L., Bravo-Montero, L., & Morante-Carballo, F. (2022). Research trends in groundwater and stable isotopes. *Water*, *14* (19), 3173. https://doi.org/10.3390/w14193173

Croft, J., Engelbrecht, S., Ladenika, A. O., MacGregor, O. S., Maepa, M., Bodunrin, M. O., Burman, N. W., Goga, T., & Harding, K. G. (2019). The availability of life-cycle studies in Sweden. *The International Journal of Life Cycle Assessment*, *24*, 6–11. https://doi.org/10.1007/s11367-018-1510-4

Cronin, P., Ryan, F., & Coughlan, M. (2008). Undertaking a literature review: A step-by-step approach. *British Journal of Nursing*, *17* (1), 38–43. https://doi.org/10.12968/bjon.2008.17.1.28059

Čuček, L., Klemeš, J. J., & Kravanja, Z. (2012). A review of footprint analysis tools for monitoring impacts on sustainability. *Journal of Cleaner Production*, *34*, 9–20. https://doi.org/10.1016/j.jclepro.2012.02.036

Donthu, N., Kumar, S., Mukherjee, D., Pandey, N., & Lim, W. M. (2021). How to conduct a bibliometric analysis: An overview and guidelines. *Journal of Business Research*, *133*, 285–296. https://doi.org/10.1016/j.jbusres.2021.04.070

Dunmade, I. (2019, 8–10 March). *Lifecycle assessment education in Nigeria: An exploratory evaluation of the trend.* Procedia Manufacturing, The 2nd International Conference on Sustainable Materials Processing and Manufacturing, Sun City, South Africa, 35. https://doi.org/10.1016/j.promfg.2019.05.065

Eck, N. J. van, & Waltman, L. (2007). VOS: A new method for visualizing similarities between objects. In R. Decker, & H. J. Lenz (Eds), *Advances in data analysis* (pp. 299–306). Springer. https://doi.org/10.1007/978-3-540-70981-7_34

Eck, N. van, & Waltman, L. (2010). Software survey: VOSviewer, a computer program for bibliometric mapping. *Scientometrics*, *84*(2), 523–538. https://doi.org/10.1007/s11192-009-0146-3

Eck, N. J. van, & Waltman, L. (2014). Visualizing bibliometric networks. In Y. Ding, R. Rousseau & D. Wolfram (Eds), *Measuring scholarly impact: methods and practice* (pp. 285–320). Springer International Publishing. https://doi.org/10.1007/978-3-319-10377-8_13

Engelbrecht, S., Ladenika, A. O., MacGregor, O. S., Maepa, M., Bodunrin, M. O., Burman, N. W., Croft, J., Goga, T., & Harding, K. G. (2018). A discussion on the availability of life-cycle assessment studies in New Zealand. *The International Journal of Life Cycle Assessment*, *23*, 1708–1713. https://doi.org/10.1007/s11367-018-1485-1

Fava, J. A., Smerek, A., Heinrich, A. B., Morrison, L. (2014). The role of the Society of Environmental Toxicology and Chemistry (SETAC) in Life Cycle Assessment (LCA) Development and Application. In W. Klöpffer (Ed.), *Background and future prospects in Life Cycle Assessment* (pp. 39–83). Springer. https://doi.org/10.1007/978-94-017-8697-3_2

Gaurav, G., Singh, A. B., Mistry, S., Gupta, S., Dangayach, G. S., & Meena, M. L. (2021). Recent progress of scientific research on life cycle assessment. *Materials Today: Proceedings*, *47*, 3161–3170. https://doi.org/10.1016/j.matpr.2021.06.208

Gaurav, G., Singh, A. B., Khandelwal, C., Gupta, S., Kumar, S., Meena, M. L., & Dangayach, G. S. (2023). Global development on LCA research: a bibliometric analysis from 2010 to 2021. *International Journal of Social Ecology and Sustainable Development (IJSESD)*, *14* (1), 1–19. https://doi.org/10.4018/IJSESD.327791

Ghosh, S. (2023). A bibliometric analysis of social Life Cycle Assessment (2008–2022). In R. Al Khaddar, S.K. Singh, N. D. Kaushika, R. K. Tomar & S. K. Jain (Eds), *Recent developments in energy and environmental engineering* (pp. 75–86). Springer Nature. https://doi.org/10.1007/978-981-99-1388-6_6

Güereca, L. P., Sosa, R. O., Gilbert, H. E., & Reynaga, N. S. (2015). Life cycle assessment in Mexico: overview of development and implementation. *The International Journal of Life Cycle Assessment*, *20*, 311–317. https://doi.org/10.1007/s11367-014-0844-9

Harding, K. G., Friedrich, E., Jordaan, H., Roux, B. le, Notten, P., Russo, V., Suppen-Reynaga, N., Laan, M. van der, & Goga, T. (2021). Status and prospects of life cycle assessments and carbon and water footprinting studies in South Africa. *The International Journal of Life Cycle Assessment*, *26*, 26–49. https://doi.org/10.1007/s11367-020-01839-0

Hauschild, M. Z., Rosenbaum, R. K., Olsen, S. I. (2018). *Life Cycle Assessment theory and practice.* Springer International Publishing. https://doi.org/10.1007/978-3-319-56475-3

He, X., & Yu, D. (2020). Research trends in life cycle assessment research: A 20-year bibliometric analysis (1999–2018). *Environmental Impact Assessment Review*, *85*, 106461. https://doi.org/10.1016/j.eiar.2020.106461

Hellweg, S., & Milà i Canals, L. (2014). Emerging approaches, challenges and opportunities in life cycle assessment. *Science*, *344* (6188), 1109–1113. https://doi.org/10.1126/science.1248361

Herrera-Franco, G., Carrión-Mero, P., Montalván-Burbano, N., Mora-Frank, C., & Berrezueta, E. (2022). Bibliometric analysis of groundwater's life cycle assessment research. *Water*, *14* (7), 1082. https://doi.org/10.3390/w14071082

Hodgkinson, G. P., & Ford, J. K. (2014). Narrative, meta-analytic, and systematic reviews: what are the differences and why do they matter? *Journal of Organizational Behavior*, *35* (S1), S1–S5. https://doi.org/10.1002/job.1918

Hou, Q., Mao, G., Zhao, L., Du, H., & Zuo, J. (2015). Mapping the scientific research on life cycle assessment: a bibliometric analysis. *The International Journal of Life Cycle Assessment*, *20*, 541–555. https://doi.org/10.1007/s11367-015-0846-2

International Organization for Standardization [ISO]. (2015). *Environmental management systems. Requirements with guidance for use* (ISO 14001).

Isah, M. E., Zhang, Z., Matsubae, K., & Itsubo, N. (2024). Bibliometric analysis and visualisation of research on life cycle assessment in Africa (1992–2022). *The International Journal of Life Cycle Assessment*, *29* (7), 1339–1351. https://doi.org/10.1007/s11367-024-02313-x

Jia, X., Varbanov, P. S., Klemeš, J. J., & Wan Alwi, S. R. (2019). Water availability footprint addressing water quality. *Journal of Sustainable Development of Energy, Water and Environment Systems*, *7* (1), 72–86. https://doi.org/10.13044/j.sdewes.d6.0223

Kacprzak, M., Neczaj, E., Fijałkowski, K., Grobelak, A., Grosser, A., Worwag, M., Rorat, A., Brattebo, H., Almås, Å., & Singh, B. R. (2017). Sewage sludge disposal strategies for sustainable development. *Environmental Research*, *156*, 39–46. https://doi.org/10.1016/j.envres.2017.03.010

Kargarzadeh, H., Mariano, M., Gopakumar, D., Ahmad, I., Thomas, S., Dufresne, A., Huang, J., & Lin, N. (2018). Advances in cellulose nanomaterials. *Cellulose*, *25* (4), 2151–2189. https://doi.org/10.1007/s10570-018-1723-5

Karuppiah, K., Sankaranarayanan, B., & Ali, S. M. (2023). Evaluating the challenges to life cycle assessment using best-worst method and decision-making trial and evaluation laboratory. *Environmental Progress & Sustainable Energy*, *42* (1), e13991. https://doi.org/10.1002/ep.13991

Ključnikov, A., Siwiec, D., Pacana, A., & Lacko, J. (2023). Life cycle assessment (LCA) of heavy vehicles used in the mining industry. *Acta Montanistica Slovaca*, *28* (3), 553–565. https://doi.org/10.46544/AMS.v28i3.03

Klöpffer, W., & Grahl, B. (2014). *Life Cycle Assessment (LCA): A guide to best practice*. John Wiley & Sons. https://doi.org/10.1002/9783527655625

Koblianska, I., Kalachevska, L., & Schlauderer, R. (2024). Agricultural life cycle assessment: a system-wide bibliometric research. *Agricultural and Resource Economics: International Scientific E-Journal*, *10* (1), 46–72. https://doi.org/10.51599/are.2024.10.01.03

Kočí, V., Benešová, E., & Rajchl, A. (2019). Porovnání environmentálních dopadů skladování a dopravy jablek do ČR [Comparison of environmental impacts of importing and storing apples in the Czech Republic]. *ENTECHO*, *1*, 13–19. https://doi.org/10.35933/ENTECHO.2019.06.002

Kráľová, N., Šerešová, M., & Kočí, V. (2020). Porovnání environmentálních dopadů různých typů jogurtových kelímků [Comparison of environmental impacts of different types of yoghurt cups]. *ENTECHO*, *1*, 6–9. https://doi.org/10.35933/ENTECHO.2020.02

Maepa, M., Bodunrin, M. O., Burman, N. W., Croft, J., Engelbrecht, S., Ladenika, A. O., MacGregor, O. S., & Harding, K. G. (2017). Life cycle assessments in Nigeria, Ghana, and Ivory Coast. *The International Journal of Life Cycle Assessment*, *22*, 1159–1164. https://doi.org/10.1007/s11367-017-1292-0

Martinho, V. J. P. D. (2023). Life-cycle cost analysis (LCCA): comparing outputs for bibliographic coupling and citation links. *Heliyon*, *9* (11), e21182. https://doi.org/10.1016/j.heliyon.2023.e21182

Matos, C., Junkes, V. H., Lermen, F. H., Magalhães, R. F. D., Matias, G. D. S., Ribeiro, J. L. D., Lenzi, G. G., & Siqueira, H. V. (2024). Life cycle sustainability assessment of the agri-food chain: empirical review and bibliometrics. *Production*, *34*, e20230043. https://doi.org/10.1590/0103-6513.20230043

Moed, H. F. (2005). *Citation analysis in research evaluation* (Vol. 9). Springer-Verlag. https://doi.org/10.1007/1-4020-3714-7

Montori, V. M., Wilczynski, N. L., Morgan, D., Haynes, R. B., & the Hedges Team. (2003). Systematic reviews: A cross-sectional study of location and citation counts. *BMC Medicine*, *1*, 1–7. https://doi.org/10.1186/1741-7015-1-2

Moutik, B., Summerscales, J., Graham-Jones, J., & Pemberton, R. (2023). Life cycle assessment research trends and implications: a bibliometric analysis. *Sustainability*, *15* (18), 13408. https://doi.org/10.3390/su151813408

Nie, Z. (2013). Development and application of life cycle assessment in China over the last decade. *The International Journal of Life Cycle Assessment*, *18*, 1435–1439. https://doi.org/10.1007/s11367-013-0591-3

Odey, G., Adelodun, B., Kim, S. H., & Choi, K. S. (2021). Status of environmental life cycle assessment (LCA): A case study of South Korea. *Sustainability*, *13* (11), 6234. https://doi.org/10.3390/su13116234

Pavlů, T., Kočí, V., & Hájek, P. (2019). Environmental assessment of two use cycles of recycled aggregate concrete. *Sustainability*, *11* (21), 6185. https://doi.org/10.3390/su11216185

Pryshlakivsky, J., & Searcy, C. (2013). Fifteen years of ISO 14040: a review. *Journal of Cleaner Production*, *57*, 115–123. https://doi.org/10.1016/j.jclepro.2013.05.038

Reap, J., Roman, F., Duncan, S., & Bras, B. (2008). A survey of unresolved problems in life cycle assessment: Part 2: impact assessment and interpretation. *The International Journal of Life Cycle Assessment*, *13*, 374–388. https://doi.org/10.1007/s11367-008-0009-9

Sasvari, P., & Urbanovics, A. (2023). The current situation of MDPI publications? Findings from the EU-27 Member States. In *Proceedings of the Central and Eastern European eDem and eGov Days 2023, CEEeGov'23* (pp. 191–197). Association for Computing Machinery. https://doi.org/10.1145/3603304.3604071

Tranfield, D., Denyer, D., & Smart, P. (2003). Towards a methodology for developing evidence-informed management knowledge by means of systematic review. *British Journal of Management*, *14* (3), 207–222. https://doi.org/10.1111/1467-8551.00375

Villagrán, E., Romero-Perdomo, F., Numa-Vergel, S., Galindo-Pacheco, J. R., & Salinas-Velandia, D. A. (2023). Life Cycle Assessment in protected agriculture: Where are we now, and where should we go next? *Horticulturae*, *10* (1), 15. https://doi.org/10.3390/horticulturae10010015

Yılmaz, Y., & Seyis, S. (2021). Mapping the scientific research of the life cycle assessment in the construction industry: A scientometric analysis. *Building and Environment*, *204*, 108086. https://doi.org/10.1016/j.buildenv.2021.108086

Zupic, I., & Čater, T. (2015). Bibliometric methods in management and organization. *Organizational Research Methods*, *18* (3), 429–472. https://doi.org/10.1177/1094428114562629

Summary

Life cycle assessment in the Visegrad Group: a bibliometric analysis. Purpose: Life cycle assessment (LCA) research has been going on for several decades. However, it is not obvious how the post-communist countries of Central Europe participate in LCA research. The aim of this paper is to gather knowledge on the recent progress of scientific research related to LCA in the Visegrad Group (Visegrad Four, V4). Methods: A bibliometric analysis was chosen for the evaluation. Studies published by authors with affiliations in the V4 countries were extracted from the Scopus database. Descriptive analyses were performed, such as analyzing the distribution of types of scientific papers, language, journals used, keywords, and research fields. Using the VOSviewer application, bibliometric mapping was performed to express the links between individual works. The most active authors from the V4 countries and the most influential articles were identified using citation analysis. Results and discussion: A total of 1,665 studies have been found. Almost all studies originate from engineering or environmental sciences. Poland is the most active in LCA research within the V4. However, the most active scientists are affiliated with Hungarian universities. Likewise, the most cited scientist carried out most of his research in LCA at universities in Hungary. Slovakia has the least developed LCA research. It has also been noted that there is a low level of collaboration among authors from V4 countries. Conclusions: The analysis demonstrated differences in LCA research within the V4. Nevertheless, LCA research is gaining popularity in all V4 countries, albeit slowly. At the same time, LCA is of fundamental importance, especially in the implementation of European environmental legislation in practice and in achieving the goals of sustainable development. The findings obtained through this analysis can serve not only researchers working in LCA research but also scientific managers in the management of research in this area.

Scientific Review Engineering and Environmental Sciences (2025), 34 (2), 170–182

Sci. Rev. Eng. Env. Sci. (2025), 34 (2) https://srees.sggw.edu.pl

ISSN 1732-9353 (suspended) eISSN 2543-7496 DOI 10.22630/srees.10047

Received: 22.10.2024
Accepted: 23.05.2025

Youssef IDRISSI[1] ✉
Nisrine BOUGHOU[2]
Essediya CHERKAOUI[1]
Mohamed KHAMAR[1]
Abderrahman NOUNAH[1]

[1] Mohammed V University in Rabat, Higher School of Technology of Sale, Materials, Water and Environment Team, Civil Engineering and Environment Laboratory (LGCE), Morocco
[2] Higher Institute of Nursing Professions and Health Techniques of Rabat Ministry of Health and Social Protection, Morocco

The impact of the depollution project on the environmental condition of the Salé coastline

Keywords: coastline, wastewater treatment plant, wastewater, littoral

Introduction

The Moroccan coastline, particularly the Salé region, faces significant environmental challenges due to rapid urbanization and insufficient wastewater management (Duncan, 2024). Every day, approximately 200,000 m³ of untreated domestic and industrial wastewater is discharged into the coastline and the Bouregreg River (Snoussi, 2020), leading to pollution and associated health risks. Urban development projects, such as the Bouregreg Valley initiative, have further exacerbated environmental degradation through increased coastal erosion and ecosystem disruption (Conseil, Ingénierie et Développement [CID], 2017; Oualalou, 2019).

✉ idrissi.job1@gmail.com

This study focuses on assessing the impact of the depollution project in Salé by analyzing the quality of the coastal waters. Through this evaluation, we aim to determine the effectiveness of the project in improving water quality, providing insights into the current environmental state of the coastal ecosystem.

Material and methods

Study area

Salé, a coastal Moroccan city, is situated on the right bank of the Bouregreg River, at an altitude of approximately 60 m above sea level. It is geographically bordered to the north by the city of Kénitra, to the south by the city of Rabat, to the east by the province of Khémisset, and to the west by the Atlantic Ocean. The city spans a vast area of 672 km² and is home to a population nearing one million inhabitants (Ministère de l'intérieur, Royaume du Maroc [MI], 2015). Salé has an extensive coastline along the northern Atlantic Ocean, measuring approximately 15,500 m, as depicted in Figure 1.

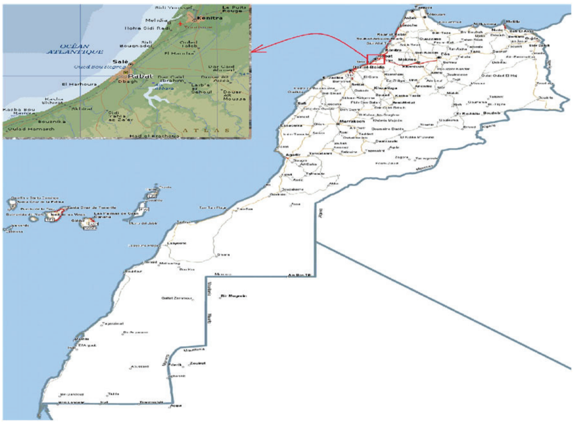

FIGURE 1. Geographical location of the city of Salé
Source: own work.

Part of the Rabat–Salé–Kénitra region, Salé is characterized by a dense urban population, representing 39.5% of the region's urban population, according to the 2014 census. With 982,163 inhabitants, a population density exceeding

500 inhabitants per square kilometer, and an annual growth rate of 1.78%, the city has undergone rapid urban expansion. This growth includes the construction of approximately 3,700 houses per year (Haut Commissariat au Plan du Maroc [HCP], 2014).

The climate of Salé is Mediterranean, characterized by a dry season from May to October with high temperatures and irregular precipitation during the rainy season. These climatic conditions, combined with regular marine winds, contribute to the environmental challenges facing the city.

This study aims to compare the environmental status of Salé's coastal area before and after the implementation of the depollution project and the wastewater treatment plant (WWTP). The WWTP, managed by REDAL, became operational in 2020 and has a treatment capacity of 10,000 m³ per day. The plant utilizes the activated sludge process, a biological treatment method effective in removing organic matter and pollutants from wastewater (ATNER, n.d.)

The state of Salé's coastline before the Salé coastal depollution project

Before the project, the direct discharge of large volumes of untreated liquids into these receiving environments caused significant biological and chemical pollution. This form of pollution, resulting from numerous discharges of untreated effluents, inevitably had a detrimental impact on the quality of aquatic ecosystems (MI, 2015).

The coastline of the city of Salé includes 12 beaches with diverse characteristics, ranging from rocky to sandy shores. However, this natural richness faced environmental challenges, including multiple points of direct or indirect discharge of domestic and/ /or industrial wastewater into coastal environments. The mouth of the Bouregreg River also significantly influenced the quality of the coastline, particularly at Salé Beach (Établissement public de coopération intercommunale [EPCI], 2015; Fig. 2).

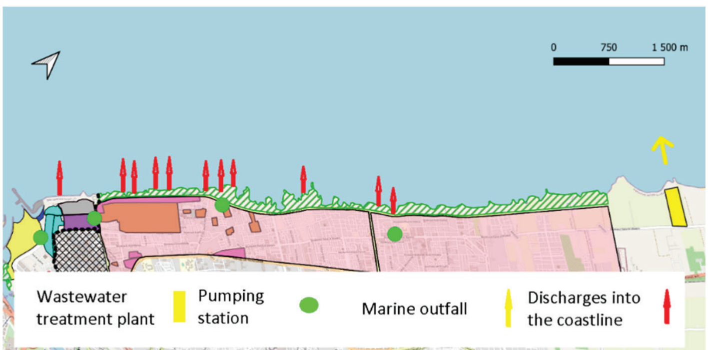

FIGURE 2. Coastal discharges in Salé before and after the implementation of the depollution project
Source: own work.

Biological pollution from pathogens present in untreated wastewater led to detrimental consequences for local fauna and flora. Pathogenic microorganisms such as bacteria, viruses, and protozoa proliferated, endangering the health of aquatic ecosystems (Smahi, 2021).

Simultaneously, chemical pollution, resulting from the presence of toxic substances in wastewater, altered the chemical composition of receiving environments. Harmful compounds such as heavy metals, industrial chemicals, and excessive nutrients contaminated surrounding waters, impacting water quality and compromising ecological balance (Fisson, 2014).

The influence of this extensive pollution on the quality of aquatic ecosystems was considerable, with potential repercussions on biodiversity, the health of marine organisms, and the natural cycles of the coastal ecosystem (Landos et al., 2021). It was imperative to take appropriate measures to mitigate these undesirable effects, emphasizing more effective wastewater treatment practices and initiatives for the preservation of the marine ecosystem (Intergovernmental Oceanographic Commission of UNESCO [UNESCO-IOC] & United Nations Environment Programme [UNEP], 2016).

This analysis underscored the urgent need for sustainable management of wastewater discharge to protect the health and viability of the coastal ecosystem. Toxic substances in wastewater, such as heavy metals, industrial chemicals, and excessive nutrients, contaminated surrounding waters, affecting water quality and ecological balance. This pollution significantly impacted aquatic ecosystems, compromising biodiversity, the health of marine organisms, and natural cycles (Cherkaoui et al., 2010).

The state of Salé's coastline after the coastal depollution project

To preserve the health and viability of the coastal ecosystem, it is crucial to mitigate the impacts of human activities by adopting more effective wastewater treatment practices and adhering to Moroccan discharge standards and coastal protection laws.

As part of the Bouregreg Valley development project, a coastal and Bouregreg River depollution initiative was launched to mitigate the effects of human activities. This project involves redirecting all discharges to a pre-treatment station through nine pumping stations, and extending sewers over more than 20 km, including extending the network more than 2.2 km offshore along the Atlantic coast. With significant environmental mechanisms in place, this project aims to meet environmental standards and enhance the value of the Atlantic coastline and the Bouregreg estuary while improving the quality of bathing water (CID, 2017; Fig. 2).

The positive impacts of this depollution system on the city of Salé are numerous:
- Improved living conditions for citizens;
- Preservation of public hygiene;
- Elimination of unpleasant odors along the coastline and Bouregreg River;
- Development of tourism through the revitalization of the coastal front and Bouregreg Valley;
- Support for development projects along Salé's waterfront and Bouregreg Valley;
- Preservation of the environment and coastal and riverine ecosystems;
- Reuse of treated wastewater for the irrigation of green spaces in the city of Salé.

Sampling

To evaluate the impact of the Salé depollution project, three sampling sites (S1, S2, S3) were designated based on accessibility, ease of sampling, and proximity to previously identified pollution sources (Fig. 3).

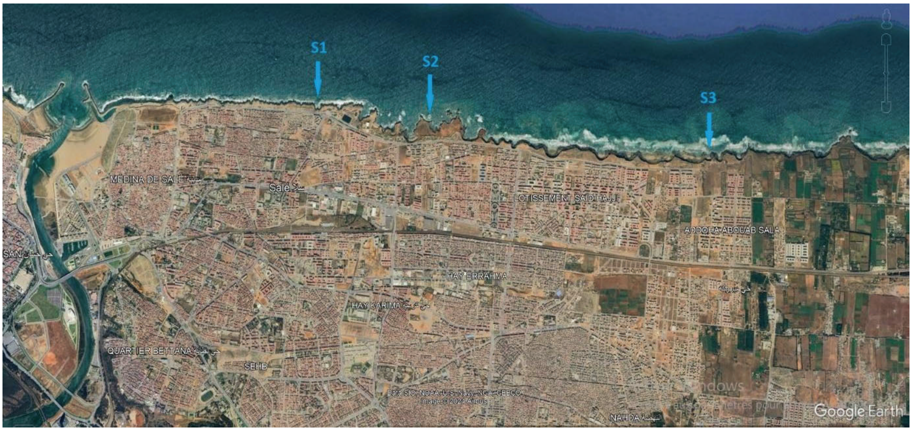

FIGURE 3. Location of sampling stations (S1, S2, S3)
Source: own work.

Sampling was conducted during four distinct seasons (summer, autumn, winter, and spring), with one sample collected per season at each station. Samples were taken a few meters from the shoreline and at a depth of 10 to 20 cm below the water surface. The selection of stations included sites near wastewater discharge points to capture direct pollution effects, as well as station S3 further away, which served as a reference point for comparison. These criteria ensured a comprehensive assessment of spatial and seasonal variations in water quality.

Analytical methods

The physicochemical parameters measured included total material, organic material, inorganic material, suspended solids (SS), pH, chemical oxygen demand (COD), turbidity, conductivity, content of orthophosphates (PO_4^{3-}), and content of nitrates (NO_3^-). In certain cases, sample dilution was applied prior to analysis to ensure accurate measurements, following the guidelines in the work by Rodier et al. (2009). Water samples were collected in pre-cleaned mineral water bottles to avoid contamination and were transported to the laboratory under controlled conditions (4°C) to preserve sample integrity.

In situ parameters were measured as follows: pH was determined using a Lutron 206 pH meter equipped with a temperature probe, turbidity was quantified with a HACH 21009 turbidity meter, and conductivity was assessed via a WTW LF90 conductivity meter.

Laboratory parameters were analyzed using standardized methodologies: trace metals (ZN, Pb) were quantified via inductively coupled plasma mass spectrometry (ICP-MS) following acid digestion of the samples in a microwave digestion system. Chemical oxygen demand was determined by oxidizing organic matter in the sample with potassium dichromate ($K_2Cr_2O_7$) in an acidic medium and measuring the residual unreacted dichromate through titration with a reducing solution. Orthophosphates (PO_4^{3-}) were measured using the colorimetric phosphomolybdic complex method, while nitrates (NO_3^-) were analyzed with the sodium salicylate spectrophotometric method.

Total material was determined by gravimetric analysis after oven-drying samples at 105°C to constant weight. Organic and inorganic fractions were differentiated using loss-on-ignition at 550°C (organic material) and residual ash (inorganic material). For suspended solids, coastal water samples were pre-treated by filtration through 0.45-micron cellulose filters to isolate particulate matter, followed by gravimetric quantification.

The bacteriological analysis focused on the presence of fecal coliforms (FC) and fecal streptococci (FS) in water, as they are widely recognized indicators of fecal contamination and help determine pollution sources. Water samples were subjected to the most probable number (MPN) method. For this, serial dilutions of the samples were prepared, and aliquots were inoculated into a series of tubes containing selective media for FC and FS. Incubation was carried out under conditions optimized for each bacterial group, and enumeration was based on the statistical distribution of positive results (Chahouri et al., 2021).

Statistical analysis

To assess spatial variations along the coastline, statistical analyses were performed using SPSS (Statistical Package for the Social Sciences). Principal component analysis (PCA) was employed to reduce data dimensionality and identify patterns among variables. One-way analysis of variance (ANOVA) was conducted at a 5% significance level to determine statistically significant differences among sampling sites, followed by Tukey's HSD post-hoc test for pairwise comparisons of means.

Normality assumptions were evaluated using the Shapiro–Wilk test ($\alpha = 0.05$) for all 30 datasets (10 parameters × three sites). Three parameters (total materials at S1, conductivity at S1 and S2) exhibited significant deviations from normality ($p < 0.05$). To assess the severity of non-normality, skewness and kurtosis were calculated for these datasets. Skewness values ranged from −1.587 to +1.88, and kurtosis values fell within −1.727 to +4.236, both within acceptable thresholds for parametric analyses (skewness: ±2; kurtosis: ±7). Given the minor deviations and robustness of ANOVA to moderate non-normality, parametric tests were retained for all parameters. The remaining 27 datasets adhered to normality assumptions ($p > 0.05$).

Results and discussion

Spatial evolution of physicochemical parameters

The average differences between the various stations were not statistically significant, with p-values significantly greater than 0.05 and F-factors ranging between 0.82 and 1.048, indicating homogeneity in the concentrations of physicochemical parameters along the city's coastline. Despite this, the data reveal some noticeable tendencies. For example, turbidity and COD exhibit slight increases from S1 to S3, which may reflect the cumulative impacts of diffuse pollution sources. Conversely, parameters like nitrates and orthophosphates show decreasing trends, potentially indicating the self-purification capacity of the coastal environment or dilution effects due to mixing with seawater. These patterns, though not statistically validated, suggest localized influences that may require further investigation (Fig. 4).

The observed homogeneity across stations can be attributed to the effective operation of the WWTP, which likely ensures consistent treatment and discharge quality. Additionally, hydrodynamic processes, such as tidal mixing and ocean currents, play a significant role in dispersing pollutants, further minimizing spatial

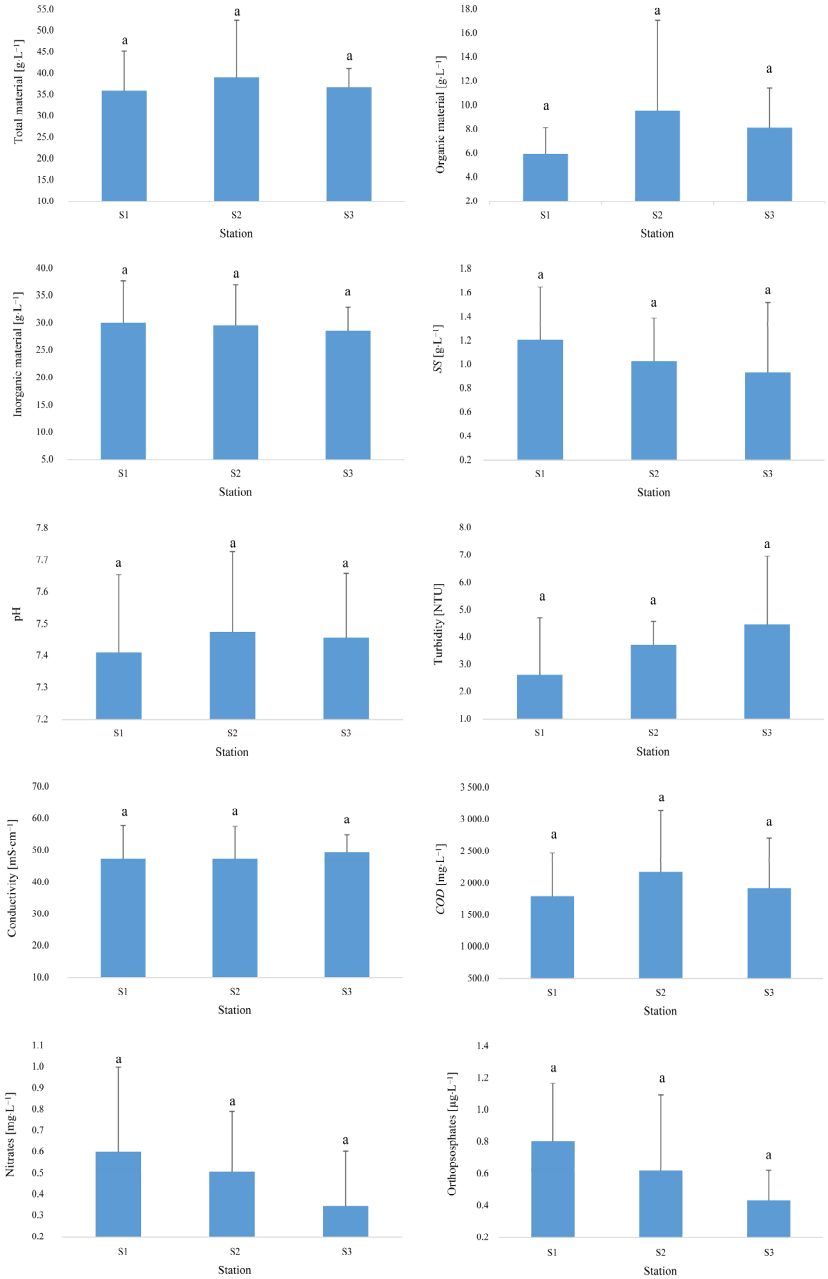

FIGURE 4. Spatial evolution (across stations) of physicochemical parameters. Bars represent averages, and vertical lines show standard deviation

Source: own work.

Idrissi, Y., Boughou, N., Cherkaoui, E., Khamar, M., Nounah, A. (2025). The impact of the depollution project on the environmental condition of the Salé coastline. *Sci. Rev. Eng. Env. Sci.*, *34* (2), 170–182. DOI 10.22630/srees.10047

variability. Other pollution sources, such as agricultural runoff or untreated sewage from smaller settlements, may also contribute to masking the WWTP's influence, creating a baseline level of contamination.

Fecal pollution indicators and water quality assessment in Salé beaches

Due to the wide range of bacterial counts observed, values were log--transformed and expressed as $\log_{10}(\text{MPN}\cdot\text{mL}^{-1})$ to facilitate statistical analysis and interpretation. It is observed that the evolution of concentrations of fecal coliforms and fecal streptococci, indicators of fecal pollution, shows statistical significance depending on the seasons (Fig. 5). However, this difference is not statistically significant across sites (Fig. 5). Measurements of fecal pollution indicators at the examined stations reveal a trend that lacks statistical significance. For fecal coliforms, the maximum average concentration is recorded at S3 with 7.03 $\log_{10}(\text{MPN}\cdot\text{mL}^{-1})$, while the minimum average concentration is at S2 with 5.55 $\log_{10}(\text{MPN}\cdot\text{mL}^{-1})$. For fecal streptococci, the maximum average concentration is at S3 with 4.39 $\log_{10}(\text{MPN}\cdot\text{mL}^{-1})$, and the minimum average concentration is at S1 with 2.80 $\log_{10}(\text{MPN}\cdot\text{mL}^{-1})$. According to the CF/SF ratio, which is greater than 4, the source of fecal pollution is strictly human (Cherkaoui et al., 2013).

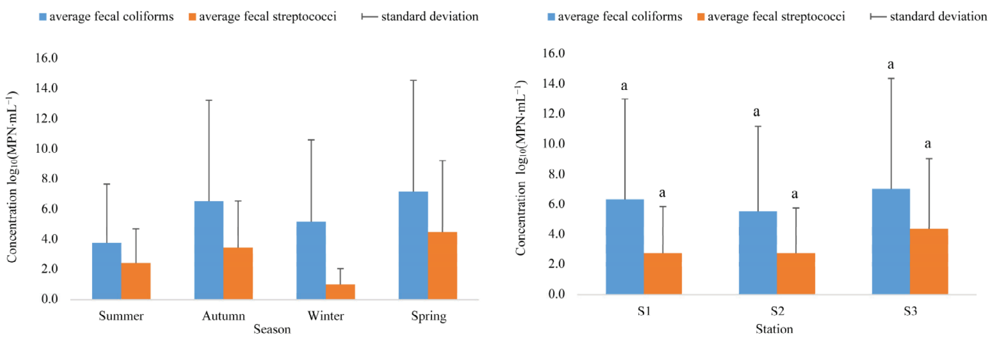

FIGURE 5. Seasonal averages of fecal pollution indicators from stations S1–S3: pre- and post-WWTP installation

Source: own work.

The seasonal evolution of fecal pollution indicators in our study shows a highly significant difference. Fecal coliforms exhibit a maximum concentration in spring with 7.16 $\log_{10}(\text{MPN}\cdot\text{mL}^{-1})$ and a minimum concentration in summer with 3.76 $\log_{10}(\text{MPN}\cdot\text{mL}^{-1})$. For fecal streptococci, the maximum concentration is 4.49 $\log_{10}(\text{MPN}\cdot\text{mL}^{-1})$, while the minimum concentration is 0.98 $\log_{10}(\text{MPN}\cdot\text{mL}^{-1})$.

According to standard NM 03.7.199 (Institut Marocain de Normalisation [IMANOR], 2014) concerning the management of bathing water quality, it has been established that beaches located in the city of Salé are categorized as having insufficient quality. Therefore, they do not meet the required standards for bathing (Ministere de la transition energetique et du developpement durable, Royaume du Maroc [MTEDD], 2023).

Heavy metal concentrations in coastal waters: a preliminary assessment of zinc and lead levels

The coastal waters exhibit relatively modest concentrations of certain heavy metal elements, with values ranging from 0.1 $\mu g \cdot L^{-1}$ to 83 $\mu g \cdot L^{-1}$ for Zinc (Zn) and 0.1 $\mu g \cdot L^{-1}$ for lead (Pb). These concentrations indicate a low presence of heavy metals in the studied coastal aquatic environment (Table 1).

TABLE 1. Heavy metal concentrations [$\mu g \cdot L^{-1}$] in the city of Salé

Metal	Mean	Min	Max
Zinc (Zn)	42.0	0.1	83.9
Lead (Pb)	0.1	0.1	0.1

Source: own work.

Moreover, statistical analysis revealed no significant differences in heavy metal concentrations between the sampling sites ($p > 0.05$), suggesting a relatively uniform distribution along the coastline.

The impact of the WWTP on fecal coliforms and physicochemical parameters: pre- and post-WWTP comparison

To assess the impact of the WWTP, we chose to compare the averages with studies conducted before the WWTP's operation (2020) by the Civil Engineering and Environment Laboratory (LGCE), which utilized the same sampling stations (S1, S2, and S3) and employed the same methods. These methods included identical seasonal sampling (four measurements per year) and analytical techniques to ensure consistency and comparability between the pre- and post-WWTP data (Table 2, Fig. 6).

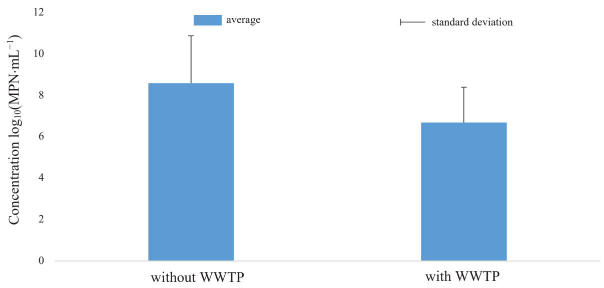

FIGURE 6. Log-transformed average fecal coliform concentrations from stations S1–S3 (seasonal data, pre- and post-WWTP)

Source: own work.

TABLE 2. Seasonal average of selected physicochemical parameters from stations S1–S3: pre- and post-WWTP installation

Water quality parameter	Unit	Without WWTP	With WWTP	Percentage reduction
Turbidity	NTU	7.99	3.81	52.25
Solid material	$mg \cdot L^{-1}$	52.34	37.82	27.74
Inorganic material	$mg \cdot L^{-1}$	34.12	28.84	15.48
Organic material	$mg \cdot L^{-1}$	18.22	8.98	50.68

Source: own work.

The average concentration of fecal coliforms shows a decrease after the installation of the WWTP, with an efficiency of approximately 24% in the city of Salé (Fig. 6). Similarly, in the city of Rabat, the WWTP led to a reduction in fecal coliform concentrations, achieving an efficiency rate of about 5.16% (Idrissi et al., 2023).

Similarly, a decrease was observed in certain physicochemical parameters, with efficiency ranging from 7% for pH to 50% for organic matter (Table 2).

Conclusions

This study evaluated the effectiveness of the coastal depollution project in Salé to improve water quality and offers insights into the current environmental state of its coastal waters. Prior to the project's implementation, untreated wastewater discharges severely degraded water quality, posing risks to marine biodiversity and limiting recreational use of the beaches. The installation of the WWTP, as part of the Bouregreg Valley development project, has led to notable improvements in the physicochemical quality of the coastal waters.

However, persistent bacterial contamination, evidenced by high levels of fecal coliforms and fecal streptococci, indicates ongoing pollution linked to human activities. While the WWTP has promoted spatial consistency in physicochemical parameters across sampling sites, seasonal variations remain significant, driven by climatic factors. Salé's beaches, currently classified as insufficient quality under NM 03.7.199 standards, require continuous monitoring and targeted interventions to improve water quality further, protect marine ecosystems, and ensure safe recreational conditions. This research provides a crucial foundation for shaping future environmental management strategies in the region.

References

ATNER [n.d.]. *STEP Salé*. https://www.atner.ma/index.php/project/step-sale

Chahouri, A., El Ouahmani, N., El Azzaoui, A., Yacoubi, B., Banaoui, A., & Moukrim, A. (2021). Combined assessment of bacteriological and environmental indicators of fecal contamination in Agadir bay ecosystems (South-West Morocco). *International Journal of Environmental Science and Technology*, *19*, 1–14. https://doi.org/10.1007/s13762-021-03380-5

Cherkaoui, E., Nounah, A. & Khamar, M. (2010). *Impact de la contamination métallique de l'eau sur la qualité des moules*. Paper presented at the 3rd International Conference on Recent Advances in Composite Materials (ICRACM-2010), Limoges.

Cherkaoui, E., Nounah, A., & Khamar, M. (2013). The impact of pollution on the Bouregreg estuary (Morocco, Atlantic Ocean): the molluscs as an indicator of metal contamination. *Journal of Environmental Science and Engineering*, *B2*, 432–435.

Conseil, Ingénierie et Développement [CID]. (2017). *Programme wessal Bouregreg. Etude d'impact sur l'environnement* (Version définitive). https://www.eib.org/attachments/registers/84479898.pdf

Duncan, D. (2021). L'Extraction du sable au Maroc, de la ressource au produit. *The Journal of Architectural, Urban, and Landscape Research*, *11*, 1–14. https://doi.org/10.4000/craup.7464

Établissement public de coopération intercommunale, Royaume du Maroc [EPCI]. (2015). *Gestion deleguee des services d'assainissement liquide et de distribution d'eau potable et d'electricite de Rabat-Sale: Cahier des charges du service de l'assainissement liquide* (Avenant 2).

Fisson, C. (2014). *Qualité des eaux de l'estuaire de la Seine*. GIP Seine-Aval Public Interest Group.

Haut Commissariat au Plan du Maroc [HCP]. (2014). *Caractéristiques Démographiques et Socio--Economiques de la Population – Rapport National*.

Idrissi, Y., El Hamdouni, S., Cherkaoui, E., Khamar, M., & Nounah, A. (2023). Effect of the depollution project on the physico-chemical and bacteriological quality of Rabat's coastal waters. *Ecological Engineering & Environmental Technology*, *24*(8), 321–328. https://doi.org/10.12912/27197050/172671

Intergovernmental Oceanographic Commission of UNESCO [UNESCO-IOC] & United Nations Environment Programme [UNEP]. (2016). *Large marine ecosystems. Status and trends. Summary for policymakers* (Vol. 4).

Institut Marocain de Normalisation [IMANOR]. *La gestion de la qualité des eaux de baignade* (NM 03.7.199).

Landos, M., Llyod-Smith, M., & Immig J. (2021). *Aquatic pollutants in oceans and fisheries. International Pollutant Elimination Network (IPEN)*. https://ipen.org/sites/default/files/documents/ipen-fisheries-v1_6cw-en.pdf

Ministère de l'intérieur, Royaume du Maroc [MI] (2015). *Monographie générale de la région de Rabat-Salé-Kénitra*.

Ministere de la transition energetique et du developpement durable, Royaume du Maroc [MTEDD]. (2023). *Surveillance de la qualité des eaux de baignade*.

Oualalou, F. (2019). *Rabat: transformation of a territory – urban development and future prospects*. Policy Centre for the New South. Morocco. https://coilink.org/20.500.12592/rjw7b7

Rodier, J., Legube, B., & Merlet, N. (2009). *L'analyse de l'eau, eaux naturelles, eaux résiduaires, eau de mer, chimie, physico-chimie, microbiologie, biologie, interprétation des résultats* (ed. 9). Dunod.

Smahi, K. (2021). *Étude de l'efficacité d'épuration des eaux usées domestiques de l'oued de Bechar par l'utilisation du sable et les graines de* Moringa oleifera *Lam* [Doctoral thesis]. Université abou Bekr Belkaid Tlemcen. http://dspace.univ-tlemcen.dz/handle/112/17418

Snoussi, M. (2020). *EFH-MO-5: Contribution à l'élaboration d'un Plan de gestion intégrée pour les zones côtières de la Région de Rabat-Salé-Kenitra. Tâche 1, Diagnostic des zones côtières de la Région de Rabat-Salé-Kenitra* (EFH-MO-5). https://www.swim-h2020.eu/wp-content/uploads/2019/05/EFH-MO-5-Task-1-Diagnostic-Analysis-fr.pdf

Summary

The impact of the depollution project on the environmental condition of the Salé coastline. The city of Salé, situated along Morocco's Atlantic coast, faces severe pollution due to human activities. Significant discharges of solid and liquid waste have resulted in contamination along its coastline, affecting water used for swimming, fishing, and irrigation. This has raised concerns about the quality of life for residents and the sustainability of local natural resources. This study evaluates the impact of the depollution project, part of the Bouregreg Valley development, on the physicochemical and bacteriological quality of Salé's coastal waters. Monitoring was conducted at three stations to assess the spatiotemporal evolution of water quality, focusing on indicators of fecal contamination (fecal coliforms – FC, fecal streptococci – FS). The results show a notable improvement in the physicochemical quality of the waters. However, bacteriologically, the waters remain highly polluted and unsafe for swimming, with pollution primarily of human origin (CF/SF > 4).

Scientific Review Engineering and Environmental Sciences (2025), 34 (2), 183–197

Sci. Rev. Eng. Env. Sci. (2025), 34 (2) https://srees.sggw.edu.pl

ISSN 1732-9353 (suspended) eISSN 2543-7496 DOI 10.22630/srees.10405

Received: 10.04.2025
Accepted: 20.06.2025

Ethar Wahab RASHEED✉
Yahya K. ATEMIMI
University of Babylon, Department of Civil Engineering, Babylon, Iraq

Effect of pH value on contaminated clay soil

Keywords: liquid acid, pH, soil contamination, geotechnical properties, clayey soil

Introduction

Rapid industrial growth and economic expansion have led to the construction of numerous industrial facilities, resulting in increased environmental pollution. Acid infiltration into soil is a prominent environmental and engineering issue in geotechnical engineering, resulting in significant changes in soil properties. This infiltration occurs due to several factors, including industrial waste discharge, chemical accidents, or the indiscriminate use of acidic substances on construction sites. Acids affect soil structure by dissolving certain minerals, leading to modifications in cohesion and permeability properties, thereby lowering its ability to withstand structural loads. The chemical response between acids and soil additives also results in a change in pH, negatively impacting the organic and chemical health of the soil. Therefore, analyzing the impact of acid seepage on soil from an engineering perspective is necessary to enhance the use of effective techniques to protect facilities and soil from environmental and structural degradation.

Sunil et al. (2006) investigated the location behavior of soil underneath the influence of pH on the engineering and chemical properties of laterite soils soaked in solutions of various pH levels (pH 5.0), neutral (pH 7.0), and alkaline

✉eng376.aythar.whab@student.uobabylon.edu.iq

(pH 8.0) for about 90 days. It was found that the solution's pH strongly influences the chemical properties of laterite soils. The engineering properties of the soil change when compared to the initial soil properties. Umesh et al. (2011) studied how acid pollutants influence soil by changing its physical and chemical properties, including its fluidity. This decreases the soil's water-preserving ability, increases frictional resistance, and reduces cohesion. These modifications negatively affect soil compressive strength and overall stability. Umesha et al. (2012) focused on the engineering properties of black cotton soils, which are extensively altered through acid infection. Hydrochloric, phosphoric, and sulfuric acids impact the compressive strength and the ultimate compressive strength. Understanding these modifications is crucial for effective soil management and reclamation in contaminated sites. Jain and Jain (2015) explored the differences in engineering characteristics between virgin soil and acid-contaminated soil. The findings showed that acidification of black cotton soil reduces its engineering qualities. As the acid concentration rises, the soil's strength decreases. However, the extent of the damage is determined by the acid's concentration and type.

Prasad and Reddy (2016) showed that acid contamination has a significant impact on soil morphology and mineral composition. Prolonged exposure to acids like phosphoric and sulfuric acid causes severe morphological changes, such as clay structure disintegration, as well as mineral transformations, including the production of new minerals such as berilinite, stilbite, gypsum, anhydrite, and albite. These changes impact soil qualities such as compressibility, strength, and fluid conductivity, which in turn impair the serviceability of foundations and superstructures constructed on contaminated soil.

Prasad et al. (2018) examined how acid pollution, notably sulfuric and phosphoric acids, affected the swelling properties of three soil types: natural black cotton soil, bentonite, and kaolin clay. The study investigated soil swelling under various acidity conditions and found that interaction with sulfuric acid produced the most significant swelling ratio, followed by interaction with phosphoric acid. Acidity (pH) is important in establishing the nature of the interaction between soil and acid because a drop in pH causes greater ion exchange effects and mineral changes, which impact soil stability and the ability to sustain engineering pressures. Wang et al. (2020) investigated how acid contamination influences evaporation rates and the formation of drought cracks in soils. As acid concentrations rise, pore structure and bulk density alter, reducing the soil's mechanical strength. When acid reacts with clay minerals, soil cohesion and tensile strength are lowered, resulting in increased deformation and instability.

Liu et al. (2021) presented results on loess soils and showed that exposure to acidic solutions can alter the particle size distribution of loess. In contrast, acidic solutions can reduce the Atterberg limits, loess strength, and permeability, although the Atterberg limits and loess strength increase significantly in a high-sulfuric acid environment. Subsequently, there is an important change in the influence of different types of acidic solutions on soil particle gradation. The permeability of contaminated loess is negatively correlated with the acid solution concentration. Shan et al. (2023) explore how contamination with acidic materials can affect the geotechnical characteristics of soil. The interaction of soil, water, and acid can lead to significant variations in the compressibility of soil specimens. The effect of the acidic solution increases the pore volume of the soil and changes its structure. Therefore, soil specimens in acidic solutions exhibit higher compressibility. The quality of soil specimens contaminated with acidic solutions is poor. The reason is that some of the materials in the particles react with the acid and dissolve in the liquid. Conversely, the quality of soil specimens in alkaline solutions increases. The study by Chen et al. (2023) indicates that acid-alkali contamination leads to changes in mineralogy, chemistry, and microstructure, affecting properties such as limit moisture content, shear strength, and internal friction angle. Chemical interactions between water and soil are also affected.

The current work focuses on measuring the effects of liquid industrial waste on the geotechnical characteristics of intact clayey soil due to increased industrial activities at the Al-Musiab chemical factory.

Experimental work

Soil sampling and classification

The soil samples utilized in this research were obtained from clayey soils from an open excavation at Al-Furat General Company for Chemical Industries in Al-Musaib, south of Babylon Governorate. The excavation was carried out using an eight-meter-long and four-meter-wide Pocline machine, and the specimens were extracted from a depth of 2 m below ground level to study the effect of industrial pollutants on their geotechnical characteristics.

The soil underwent an initial visual classification, where it was identified as high plasticity (ML) clay soil according to the Unified Soil Classification System (USCS). Table 1 presents features of the natural soil.

TABLE 1. The physical features of normal soil

Characters	Color	*LL* [%]	*PL* [%]	*PI* [%]	*MDD* [g·cm^{-3}]	*OMC* [%]	*UCS* [kPa]	*Gs* [g·cm^{-3}]	USCS category	pH [-]
Value	light brown	49	36	13	1.66	18.5	25	2.67	ML	7.7

LL – liquid limit, *PL* – plastic limit, *PI* – plasticity index, *MDD* – maximum dry density, *OMC* – optimum moisture content, *UCS* – unconfined compression strength, *Gs* – specific gravity

Source: own work.

Materials used

After visual classification and soil sampling, disturbed specimens were air--dried and divided into portions for experiments. In this study, sulfuric acid (H_2SO_4) at a concentration of 97% was used. This hazardous chemical is known to be a strong inorganic acid characterized by its severe corrosiveness and dangerous effects. The acid is usually colorless or yellowish and produces dense vapors at high concentrations with a pungent odor. When diluted, an exothermic reaction occurs with gaseous emissions. Soil samples were immersed in the acid, which was used as a contaminant to simulate the effect of pollution on soil properties. The contaminant was added at different percentages (0%, 10%, 20%, 30%, and 50%) by the weight of the dry soil sample. Table 2 shows the classification and symbols of the soil specimens tested in this study.

TABLE 2. Designation keys of samples

Soil sample	Description
S0	natural soil sample
S1	soil samples contaminated with 10% by weight of acid
S2	soil samples contaminated with 20% by weight of acid
S3	soil samples contaminated with 30% by weight of acid
S4	soil samples contaminated with 50% by weight of acid

Source: own work.

Curing process

The contaminant was added to the soil specimens at changing concentrations (10%, 20%, 30%, and 50%) by the weight of the dry sample. The contaminated samples were then placed in sealed plastic containers for 24 hours, a period sufficient to ensure complete penetration of the contaminant into the soil. The soil specimens used in this research were classified according to contamination levels

(Table 1). After the mixing process was completed, the contaminated samples were transferred to polyethylene bags and stored in a desiccator before testing. Table 3 shows the changes in contaminant concentrations in the sulfate liquid.

TABLE 3. The design mixture of the study

Soil sample	Content of sulfate in soil by volume [%]	Concentration of sulfate contaminant [%]	pH [-]
S0	0	0.32	7.7
S1	10	1.74	6.7
S2	20	2.67	1.4
S3	30	3.87	0.3
S4	50	6.43	0

Source: own work.

PH testing

Acidity (pH) was measured using a Hanna instrument, model HI 98107, according to ASTM D4972-13 (ASTM International [ASTM], 2013). The test was performed on natural and contaminated soil samples with varying concentrations of sulfuric acid (H_2SO_4).

Scanning electron microscope (SEM)

Scanning electron microscope (SEM) tests were conducted at the Scientific Research Center of the Commission of Science and Technology, using soil samples contaminated with different concentrations of the pollutant (10%, 20%, 30%, and 50%). These tests aimed to analyze the morphological changes that occurred in the soil structure and study the influence of acid pollution on its behavior. The images used in the analysis were carefully selected from a large collection of images taken of selected samples, using multiple magnification levels, allowing for accurate and detailed visualization of the changes that occurred in the soil surface structure due to exposure to acid pollutants.

Unconfined compression strength test (UCS)

Specimens were prepared with mixing ratios corresponding to the optimum moisture content and maximum dry density derived from the standard Proctor test, with predetermined contaminant concentrations applied. The vertical displacement rate of the device was set at 1 mm·min^{-1} according to ASTM D2166 (ASTM, 2010).

During the test, the stress–strain relationship was recorded at 10–15 measurement points, with the load adjusted so that the failure time did not exceed 15 min or 20% of the specimen height, to ensure accurate and comparable results. The face structure is affected by exposure to acid pollutants.

Sulfuric ion test

The sulfuric ion test was conducted at the Scientific Research Center of the Commission of Science and Technology, according to ASTM D516 (ASTM, 2023). The test was performed on normal and contaminated soil specimens with varying concentrations of sulfuric acid (H_2SO_4).

Results and discussion

Atterberg limits

The findings of the Atterberg limit tests, which include the liquid limit, plastic limit, and plasticity index, show that increasing the contamination concentration of sulfuric acid (H_2SO_4) in the soil results in a significant reduction in both the liquid limit and plasticity index. This reduction is attributed to the chemical and physical variations that occur in the soil structure due to the acid's action and can be explained by the following reasons:

– Disintegration of clay structure and degradation of clay minerals, which is consistent with the study by Aubaid (2004).
– Sulfuric acid decomposes clay minerals – for example, montmorillonite and kaolinite, altering their water-holding capacity according to Panda et al. (2010).
– Decomposition weakens the soil's water absorption and increases swelling, leading to a decrease in liquid limit, which is consistent with previous studies, such as Sivapullaiah et al. (2008), AlShammari et al. (2019), and Min et al. (2023).
– Reduced soil water-holding capacity, according to Umesh et al. (2011).
– Sulfuric acid reacts with clay particles and water, causing the soil to lose its plastic properties (Chari et al., 2023).
– The water required to initiate flow decreases, thus reducing the liquid limit (Sivapullaiah et al., 2009).
– The effect of chemical reactions on intermolecular bonds (Caselles et al., 2023). Sulfuric acid weakens the chemical bonds within the activated clay network, resulting in a loss of cohesion and plasticity.

The pH value is critical in defining soil geotechnical features, particularly those related to Atterberg limits, including the liquid limit, plastic limit, and plasticity index. When the pH drops due to exposure to acidic pollutants, such as sulfuric acid, clay minerals undergo chemical changes that cause the lamellar structure to disintegrate. According to Gratchev and Towhata (2013) and Momeni et al. (2020), as a result of this action, the soil's water-holding capacity decreases significantly, as does its plastic behavior. Acid reactions contribute to the formation of hardening and cracking. Experimental findings demonstrate that the plastic limit steadily decreases with the early phases of acid pollution and continues to diminish with increasing sulfuric acid concentration, with a maximum plastic limit value reported at 50% of the pollution concentration. Figure 1 reflects this pattern of changes, showing a direct relationship between increasing acid pollution rates and decreasing Atterberg limits, highlighting the profound structural impact of changes in pH on the plastic behavior of soils.

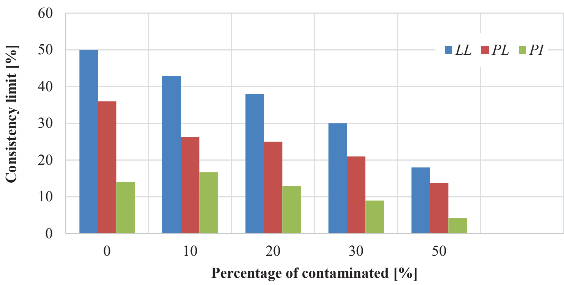

FIGURE 1. Impact of contamination on Atterberg limits
Source: own work.

Unconfined compression test (UCS)

Unconfined compression tests were conducted on disturbed soil samples to determine the strength of clayey soil. Figure 2 shows that when the soil was contaminated with sulfuric acid at different concentrations (10%, 20%, 30%, and 50%), the highest strength was recorded at 20% at pH 1.4; then the strength began to decrease with increasing contamination. This trend reflects the effect of the chemical interaction between the acid and soil components. Moderate acid (10% and 20%) at pH 6.7 and 1.4, respectively, led to the hardening of some minerals and enhanced cohesion, while higher percentages (30% and 50%) at pH 0.3 and 0.0, respectively, led to the dissolution of the mineral structure and weakening of the soil's mechanical properties, resulting in a reduction in its strength. The findings also showed that the strength increased for all contamination levels after 28 days of treatment, indicating an initial reaction that temporarily improved the soil properties. However, after 56 days and 90 days, a decrease in strength was observed as a result of the continued chemical reactions between the acid and the soil minerals, leading to the dissolution of the soil structure and the weakening of its cohesion over time. The rate of decrease in soil strength increased with increasing contamination, confirming the impact of acid pollution on its mechanical characteristics (Abdulhussein Saeed et al., 2014). The results of the unconfined compression tests are shown in Figure 2.

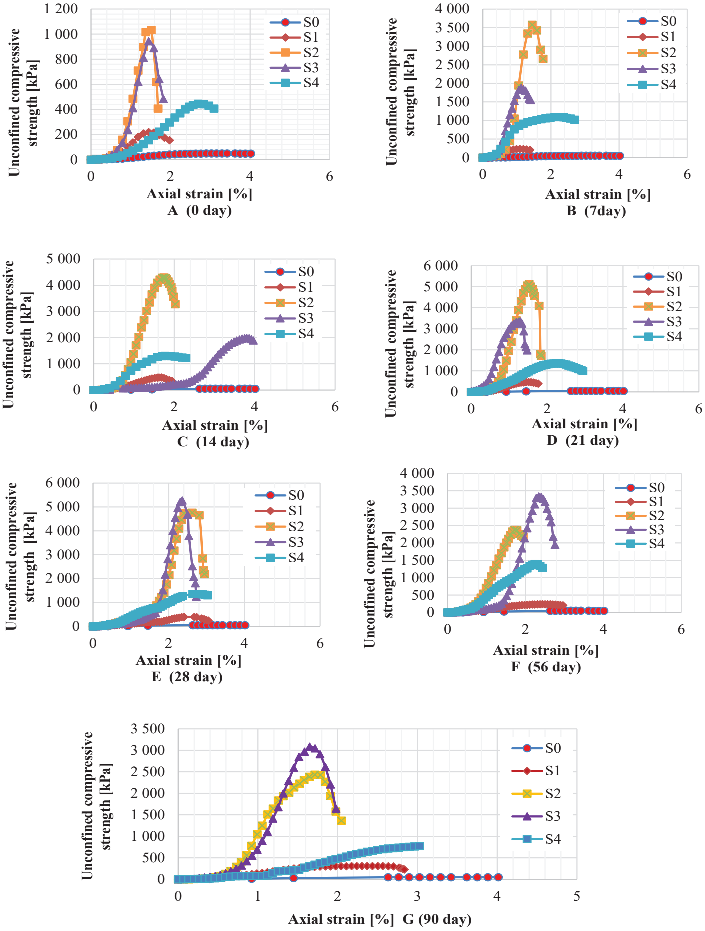

FIGURE 2. The uncompressed strength for natural and contaminated soil for different curing time (A to G)

Source: own work.

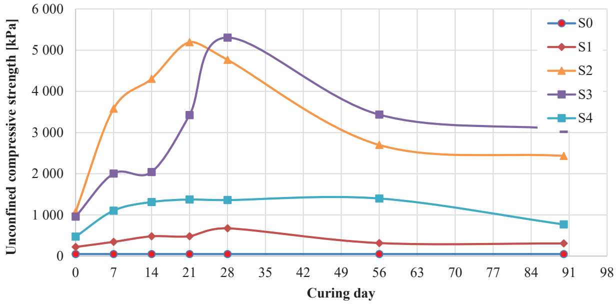

FIGURE 3. The average unconfined compressed strength for natural and contaminated soil with curing time
Source: own work.

From Figure 3, it can be concluded that the influence of time on the strength of soil is significant. At the beginning, the S2 (20% sulfate) sample had a maximum strength of around 1,000 kPa, with a maximum increase in strength of 1,900%. After a curing period of 7 days, the strength continued to increase for the same soil sample (S2) until it reached 3,600 kPa. The strength further increased to 5,100 kPa after 21 days for the same soil sample (S2). After that, the soil with 30% chemical (S3) began to surpass the S2 samples, reaching 5,200 kPa at 28 days, and at 56 days, the S3 samples had more strength than the other soil samples. From these results, it can be concluded that the effect of the chemical over time depends on the percentage of the chemical, as some percentages do not react at the beginning but need time to start. On the other hand, all samples showed a decrease in strength after 56 days and 90 days, indicating a found relationship between the chemical (sulfate) and time during the chemical reaction in the soil media. From Figure 3, these results can be confirmed. While S0 and S1 had high pH values, it can be noted that S2 and S3 had lower pH values, which, in acidic media, increases the shear strength for this soil type (ML).

Results of chemical tests

pH test

The pH value of a given solution reflects its hydrogen ion concentration, making it an important indicator for understanding chemical reactions in soil. The pH value provides vital information about changes that may occur in soil properties, as it significantly affects the charge distribution in the clay network, making it a key factor in controlling the solubility of clay minerals. A study conducted on soil contaminated with sulfuric acid showed that low pH not only affects chemical reactions but also extends to the geotechnical characteristics of the soil, such as its cohesion and water-holding capacity. It may be that the soil's cation exchange capacity decreases with increasing acid concentration, leading to reduced stability (SD) (Venkataraja Mohan & Ramesh, 2014; Venkataraja & Ramesh, 2014). Figure 4 illustrates the relationship between pH and contamination level. Three different contamination levels (10%, 20%, and 30%) were used to study their effect over time. The results showed that pH values gradually increased over time and then stabilized after 21 days; this is likely the result of ion exchange processes, where clay minerals and soil organic matter absorb or release ions to achieve chemical balance. In addition, sulfuric acid reacts with basic minerals and calcium carbonate ($CaCO_3$), consuming hydrogen ions and contributing to a gradual decrease in pH until it reaches stability.

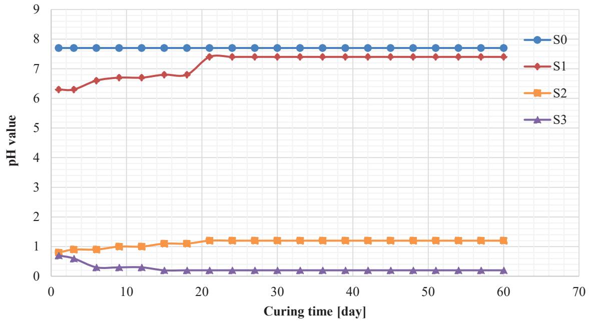

FIGURE 4. Variation of pH for the contaminated acidic percentages with time
Source: own work.

Scanning electron microscopy (SEM)

When fine clay particles are exposed to sulfuric acid contamination, carbonate bonds are formed, leading to the formation of loose structures with extensive voids, causing significant swelling and compression, as noted by Mohan et al. (2018) and Khodabandeh et al. (2020). The dissolution of calcite, ankerite, and aluminum minerals, along with the formation of sulfates, contributes to the disintegration of the clay structure. As the microscopic images in Figure 5 illustrate, natural clay appears as agglomerated particles with interconnected crystal structures and hexagonal clusters with voids. Upon interaction with a 10% contaminated concentrate, these structures transform into sintered, irregular crystal plates with an increased void ratio. When the H_2SO_4 concentration increases to 20%, the clay microstructure changes to irregular, agglomerated structures covered with fine, needle-like crystal plates, exhibiting a higher void content. Upon interaction with a 30% contaminated concentrate, cohesive, agglomerated crystal structures with greater void content are formed. As the concentration increases to 50%, the microstructure of the clay becomes composed of thin crystalline plates and needle-shaped crystals, with a marked increase in void content. These changes highlight the microscopic effects of acid contamination on the clay after 28 days of exposure. The results of the SEM test confirm that the 30% chemical (S3) becomes coarser and stronger than the other soil samples. In contrast, the S4 (50% acid) becomes weaker due to an increase in chemical content and a decrease in pH, resulting in a thin and sharp layer, marking the change from an agglomerated structure to a layered structure.

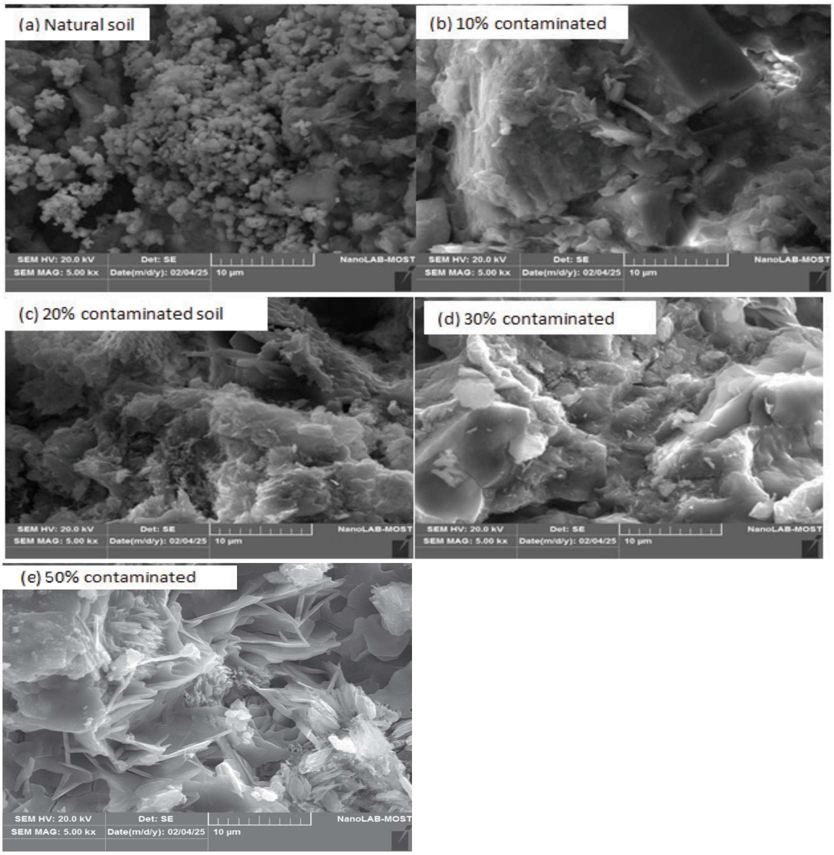

FIGURE 5. SEM images of lay interacting with (a) natural soil, (b) 10% H_2SO_4, (c) 20% H_2SO_4, (d) 30% H_2SO_4, and (e) 50% H_2SO_4

Source: own work.

Conclusions

The liquid industrial waste resulting from leakage obtained from the Furat State Company for Chemical Industries in Al-Musaib City has diverse effects on the geotechnical characteristics of clayey soil. This diversity ranged from slight in some characteristics to significant in others. Additionally, increasing the ratio of contaminants enhanced the diverse effects on the geotechnical properties of the soil. The conclusion can be summarized in the following points:

– The contaminant causes a significant decrease in pH value, which decreases by 96% at a concentration of 30%.
– The pH values increase over time and then stabilize after three weeks.
– The contaminant causes a reduction in liquid limit, plastic limit, the plasticity index, which decreased by 63%, 61.6%, and 67.7% at a concentration of 50%.
– The findings of the unconfined compressive strength displayed a significant increase of 10,921% at a contaminant concentration of 20%, followed by a further 2,851% increase at 50% concentration compared to uncontaminated soil.
– The unconfined compressive strength decreased by 51% to a 20% contaminant concentration, and this decrease continued with increasing contaminant levels, reaching a 5.24% decrease at a 50% concentration after 56 days compared to 28 days. This change in the mechanical behavior of soil is attributed to the gradual decrease in pH over time, as the acidic environment resulting from pollution contributes to the disintegration of the soil structure, weakening the cohesion of particles and leading to a significant deterioration in its mechanical resistance.

Microstructure images taken from the SEM show the agglomeration of soil particles, which increases the percentage of voids and causes a change in soil density, leading to increased dispersion and resulting in decreased resistivity. This decrease in resistivity is attributed to the reduction in pH resulting from increased contamination levels. Soil contamination with sulfuric acid leads to an increase in sulfate ion content in the soil.

References

Abdulhussein Saeed, K., Kassim, K. A., & Nur, H. (2014). Physicochemical characterization of cement treated kaolin clay. *Gradevinar*, *66*, 513–521. https://doi.org/10.14256/JCE.976.2013

Al-Amoudi, O. S., Alshammari, A. M., Aiban, S. A., & Saleh, T. A. (2018). Volume change and microstructure of calcareous soils contaminated with sulfuric acid. *Process Safety and Environmental Protection*, *120*, 227–236. https://doi.org/10.1016/j.psep.2018.08.035

Alshammari, A. M., Al-Amoudi, O. S. B., Aiban, S. A., & Saleh, T. A. (2019). Phosphoric acid contaminated calcareous soils: Volume change and morphological properties. *Powder Technology*, *352*, 340–349. https://doi.org/10.1016/j.powtec.2019.04.039

ASTM International [ASTM]. (2010). *Standard test method for unconfined compressive strength of cohesive soil* (ASTM D2166). ASTM.

ASTM International [ASTM]. (2013). *Standard test method for pH of soils* (ASTM D4972-13). ASTM.

ASTM International [ASTM]. (2023). *Sulfate ion in water* (ASTM D516). ASTM.

Aubaid, K. S. (2004). *Effect of sulphuric acid on the geotechnical properties of clayey silt soil containing calcite* (MSc. thesis). Civil Engineering Department, Baghdad University.

Caselles, L., Balsamo, B., Benavent, V., Trincal, V., Lahalle, H., Patapy, C., Montouillout, V., & Cyr, M. (2023). Behavior of calcined clay based geopolymers under sulfuric acid attack: Meta-illite and metakaolin. *Construction and Building Materials*, *363*, 129889. https://doi.org/10.1016/j.conbuildmat.2022.129889

Chari, C. T. S., Heimann, J. E., Rosenzweig, Z., Bennett, J. W., & Faber, K. T. (2023). Chemical transformations of 2D kaolinic clay mineral surfaces from sulfuric acid exposure. *Langmuir*, *39*(20), 6964–6974. https://doi.org/10.1021/acs.langmuir.3c00113

Chen, Y., Tang, L., Sun, Y., Cheng, Z., & Gong, W. (2023). Physical–mechanical properties and microstructure degradation of acid–alkali contaminated granite residual soil. *Geomechanics for Energy and the Environment*, *36*, 100501. https://doi.org/10.1016/j.gete.2023.100501

Gratchev, I., & Towhata, I. (2013). Stress–strain characteristics of two natural soils subjected to long--term acidic contamination. *Soils and Foundations*, *53*(3), 469–476. https://doi.org/10.1016/j.sandf.2013.04.008

Jain, S., & Jain, R. (2015). Change in engineering properties of black cotton soil due to acid contamination. *International Journal of Engineering Research & Technology*, *4*(11), 256–259.

Khodabandeh, M. A., Nokande, S., Besharatinezhad, A., Sadeghi, B., & Hosseini, S. M. (2020). The effect of acidic and alkaline chemical solutions on the behavior of collapsible soils. *Periodica Polytechnica Civil Engineering*, *64*(3), 939–950. https://doi.org/10.3311/PPci.15643

Liu, H., He, J. T., Zhao, Q., & Wang, T. H. (2021). An experimental investigation on engineering properties of undisturbed loess under acid contamination. *Environmental Science and Pollution Research*, *28*, 29845–29858. https://doi.org/10.1007/s11356-021-12749-5

Min, Y., Wu, J., Li, B., Zhang, M., & Zhang, J. (2023). Physicochemical and mechanical behavior of the one-part geopolymer paste exposed to hydrochloric and sulfuric acids. *Journal of Materials in Civil Engineering*, *35*(3), 04022456. https://doi.org/10.1061/(ASCE)MT.1943-5533.0004621

Mohan, S. D., & Ramesh, H. N. (2014). Effect of pH on the geotechnical properties of soil. *International Journal of Engineering Research and Applications*, *4*(3), 1–6.

Momeni, M., Bayat, M., & Ajalloeian, R. (2020). Laboratory investigation on the effects of pH-induced changes on geotechnical characteristics of clay soil. *Geomechanics and Geoengineering*, *17*(1), 188–196. https://doi.org/10.1080/17486025.2020.1716084

Panda, A. K., Mishra, B. G., Mishra, D. K., & Singh, R. N. (2010). Effect of sulphuric acid treatment on the physico-chemical characteristics of kaolin clay. *Colloids and Surfaces A: Physicochemical and Engineering Aspects*, *363*(1), 98–104. https://doi.org/10.1016/j.colsurfa.2010.04.022

Prasad, C. R. V., & Reddy, P. H. P. (2016). Influence of acid contamination on morphology and mineralogy of black cotton soil. *Indian Journal of Science and Technology*, *9*(30), 1–5. https://doi.org/10.17485/ijst/2016/v9i30/99190

Prasad, C. R. V., Reddy, P. H. P., Murthy, V. R., & Sivapullaiah, P. V. (2018). Swelling characteristics of soils subjected to acid contamination. *Soils and Foundations*, *58*(1), 110–121. https://doi.org/10.1016/j.sandf.2017.11.005

Shan, Y., Cai, G., Zhang, C., Wang, X., Shi, Y., & Li, J. (2023). Effects of acidic/alkaline contamination on the physical and mechanical properties of silty clay. *Sustainability*, *15*(2), 1317. https://doi.org/10.3390/su15021317

Sivapullaiah, P. V., Prasad, G. B., & Allam, M. (2008, October 1–6). *Volume change behaviour of soil influenced with sulfuric acid.* The 12th International Conference of International Association for Computer Methods and Advances in Geomechanics (IACMAG), Goa, India.

Sivapullaiah, P. V., Prasad, B. G., & Allam, M. M. (2009). Effect of sulfuric acid on swelling behavior of an expansive soil. *Soil & Sediment Contamination*, *18*(2), 121–135. https://doi.org/10.1080/15320380802660289

Sunil, B. M., Nayak, S., & Shrihari, S. S. N. A. (2006). Effect of pH on the geotechnical properties of laterite. *Engineering Geology*, *85*(1–2), 197–203. https://doi.org/10.1016/j.enggeo.2005.09.039

Umesh, T. S., Sharma, H. D., Dinesh, S. V., Sivapullaiah, P. V., & Basim, S. C. (2011). Physico-chemical changes in soil due to sulphuric acid contamination. *Proceedings of Indian Geotechnical Conference*, *2011*, 765–768.

Umesha, T. S., Dinesh, S. V., & Sivapullaiah, P. V. (2012). Effects of acids on geotechnical properties of black cotton soil. *International Journal of Geology*, *6*(3), 69–76.

Venkataraja Mohan, S. D. & Ramesh, H. N. (2014). Effects on pH behaviour of expansive and non expansive soils contaminated with acids and alkalis. *International Research of Research in Engineering and Technology*, *3*(6), 61–66.

Wang, X., Yang, B., Jin, L., Zhang, Z., & Xu, X. (2020). Management and fractal analysis of desiccation cracks of soils with acid contamination. *Advances in Civil Engineering*, *2020*(1), 6678620. https://doi.org/10.1155/2020/6678620

Summary

Effect of pH value on contaminated clay soil. Clay soil is one of the most unusual and widely used soil types in geotechnical engineering and construction due to its various physical and chemical properties that make it a key material in many engineering applications. This research focuses on studying the effect of changes in pH resulting from acidic contaminants, an important indicator of chemical reactions inside the soil, and their effect on the geotechnical characteristics of clayey soil. These contaminants simultaneously alter pH values, making the study of these changes essential for understanding the extent of deterioration in soil mechanical and chemical properties and assessing the damage caused by contamination. The study covered fundamental geotechnical checks, such as the Atterberg limits, Proctor check, unconfined compression check, SEM, and pH check. Clayey soil samples were artificially contaminated using four different contaminant ratios

(10%, 20%, 30%, and 50%) relative to the weight of water used for soaking for 24 hours. The results showed that the variations in chemical and physical characteristics were slight, as pH values gradually increased and stabilized after three weeks. From a mechanical perspective, resistance showed a significant increase, recording a ratio of 10,921% increase at 20% concentration after four weeks, followed by a further ratio of 2,851% increase at 50% concentration compared to uncontaminated soil. However, after 56 days, this significant increase began to decline, with resistance decreasing to a ratio of 51% at 20% concentration and a ratio of 5.15% at 50% concentration, compared to values recorded four weeks after the test. Scanning electron microscope (SEM) images also showed an increase in the ratio of voids with increasing contaminant concentration, indicating a negative impact of contamination on the soil microstructure.

Scientific Review Engineering and Environmental Sciences (2025), 34 (2), 198–217

Sci. Rev. Eng. Env. Sci. (2025), 34 (2) https://srees.sggw.edu.pl

ISSN 1732-9353 (suspended) eISSN 2543-7496 DOI 10.22630/srees.10391

Received: 14.04.2025
Accepted: 09.06.2025

Bariza BOUKNI[1]
Sara BENSALEM[1]
Mohamed Lyes Kamel KHOUADJIA[1]
Oussama TEMAMI[1]
Salim HAMLAOUI[1]
Cherif BELEBCHOUCHE[1, 2]✉

[1] University Frères Mentouri Constantine 1, Department of Civil Engineering, Laboratory of Materials and Durability of Constructions, Algeria
[2] Setif 1 University – Ferhat Abbas, Faculty of Technology, Department of Civil Engineering, Algeria

The influence of iron powder content on the fresh and hardened properties of mortar

Keywords: iron powder, waste, mortars, physical properties, mechanical properties

Introduction

Concrete, a cornerstone of construction, typically combines cement, sand, gravel, and water. Researchers have explored incorporating waste materials to enhance their properties or eco-friendliness (Krikar et al., 2018; Largeau et al., 2018). Waste materials, often discarded as useless or obsolete (Harrison, Ed., 2023), can provide multiple advantages when incorporated into concrete. Utilizing

✉cherif.belebchouche@univ-setif.dz

these materials can reduce waste disposal, decrease the demand for traditional raw materials, and create more sustainable building solutions (Miah et al., 2021). Recent research has highlighted the potential benefits of integrating waste materials into mortar and concrete mixtures. Recycled construction and demolition waste, such as bricks and road debris, has been examined as a viable and economical alternative to traditional aggregates and cement, thereby reducing environmental impact (Belebchouche et al., 2024). Moreover, waste paper and plastic waste have been successfully utilized to improve the mechanical properties of mortars, particularly in applications like wall plastering (Harabi et al., 2024). Incorporating steel and aluminum fibers has been shown to enhance the strength and durability of concrete, mitigating the propagation of cracks and microcracks (Khouadjia et al., 2023). Finally, the addition of glass waste has been observed to positively influence mortars' compressive and flexural strength (Małek et al., 2021).

The global metal powder industry generates over 700,000 tons of iron-based waste annually, presenting a substantial opportunity for valorization in sustainable construction materials (Khouadjia et al., 2025). Among these underutilized industrial by-products, waste iron powder (IP) resembles fine cement in particle size and characteristics, making it a promising candidate for partial replacement in mortars and concrete (Giovanni et al., 2024). Instead of discarding this waste, which contributes to metal loss and environmental pollution, its inherent mechanical properties can be leveraged for construction applications, promoting ecological sustainability (Thakur et al., 2019; Fahad & Jassim, 2020).

Numerous studies have explored the potential of incorporating IP waste as a substitute for either cement or aggregates. For instance, research has shown that including waste materials can lead to significant benefits. In a relevant study, incorporating 20% waste industrial tire powder (WITP) into mortar mixtures resulted in a 20% reduction in cement consumption and a corresponding 19.98% decrease in overall economic cost (Cui et al., 2022). This demonstrates the broader economic and environmental advantages of using industrial construction by-products.

Other studies have investigated the use of recycled IP as a partial replacement for sand and cement. These studies have yielded mixed results. While some research (Largeau et al., 2018; Cui et al., 2022) observed a decrease in flowability and an increase in dry density with increasing IP content. Researchers Fahad and Jassim (2019), Lu et al. (2020), Miah et al. (2020), and Miah et al. (2021) reported improvements in dry density, porosity, and water absorption. Research conducted by Largeau et al. (2018) revealed that partial substitution of portland cement with industrial by-products (IP) at varying levels (1.5%, 2.5%, 3.5%, and 5% by weight) resulted in a decline in workability and a substantial decrease in porosity. Notably, 21.88% and 26.77% porosity reductions were observed at replacement levels of 1.5% and 2.5%, respectively. Furthermore, Dias et al. (2020) observed a more homogeneous behavior in mixtures incorporating IP and concerning the effect of IP on mechanical properties. Largeau et al. (2018) reported improved compressive and tensile strengths of concrete with up to 5% iron powder replacement, with optimal values observed at 2.5% and 1.5%, respectively. Similarly, Lu et al. (2020) found that the incorporation of iron powder led to an increase in tensile bond strength, compressive strength, and flexural strength. Furthermore, Miah et al. (2021) investigated the use of waste iron powder (WIP) as a partial replacement for fine aggregates, observing significant enhancements in the compressive, tensile, and flexural strengths of mortar up to a 7.5% replacement level. These findings align with Dias et al. (2020) and Kong et al. (2023), who reported increases in 28-day compressive strength of up to 13.2% and improvements in both axial compression and tensile strength of 13.83% and 14.34%, respectively, when IP was incorporated into concrete. However, other research has found that recycling iron powder (IP) decreased compressive strength significantly with increasing IP percentage, particularly at higher curing ages (Tayeh & Al Saffar, 2018; Giovanni et al., 2024). The results indicated a general trend of reduced compressive strength with increasing iron powder content compared to control concrete (Belebchouche et al., 2024). The optimal replacement percentage was determined to be 12%, which yielded the highest compressive and flexural strength in the shortest curing time. Increasing the iron waste content beyond 12% led to a decrease in concrete strength (Krikar et al., 2018). Studies have shown that the addition of IP can enhance certain aspects of concrete performance. For instance, the nucleation and pozzolanic effects of waste iron powder (WIP) have been observed. It has been observed that WIP promotes cement hydration, leading to improved durability (Cui et al., 2022). However, concerns have also been raised regarding dimensional stability, with shrinkage and expansion observed in mortars containing IP, particularly at higher replacement percentages (exceeding 5%) (Miah et al., 2020). Furthermore, research suggests that IP can act as a barrier, hindering the access of chloride ions to steel reinforcement, thereby mitigating the risk of corrosion (Largeau, 2018; Largeau et al., 2018). This research investigates the potential of IP as a viable alternative to cement in mortar formulations. The study primarily focuses on evaluating the influence of IP incorporation on both the fresh and hardened state properties of mortar. In the fresh state, this encompasses an assessment of flow time, consistency, setting time, air content, and density, while hardened state properties under investigation include compressive and flexural strengths. This research offers significant practical implications by providing a viable and sustainable pathway for utilizing industrial waste, reducing landfill burden, conserving natural resources, and developing greener, high-performance construction materials, thereby contributing valuable insights into the feasibility and substantial benefits of incorporating iron powder as a sustainable construction material.

Materials

Cement components

Cement. This study employed commercial portland cement (CEM I) with a 42.5 MPa strength class, sourced from the SPA Biskra cement factory. The cement's quality adheres to the requirements of standard NF EN 197-1 (AFNOR, 2012a). The chemical and mineralogical compositions of the cement are presented in Table 1. The potential mineralogical composition was subsequently calculated using the empirical formula of Bogue (1947).

TABLE 1. Chemical and physical characteristics of portland cement CEM I/42.5R

Specification	Chemical composition							
Content [%]	SiO_2	Al_2O_3	Fe_2O_3	CaO	MgO	K_2O	TiO_2	Na_2O
	20.14	5.53	3.54	61.60	0.19	0.03	0.008	0.06
	Mineralogical composition							
Content [%]	C_3S		C_2S		C_3A		C_4AF	
	55.43		15.53		8.67		10.76	
	Physical properties							
Specific density [$kg \cdot m^{-3}$]	3 100.0							
Fineness [$cm^2 \cdot g^{-1}$]	3 500.0							
Initial setting time [min]	170.0							
Final setting time [min]	255.0							

Source: own work.

Water. The tap water used in this study was obtained from the Genie Civil Laboratory at the University of Constantine 1. The water temperature was maintained at 20 ±2°C. Water quality met the requirements of the NF EN 206+A2/CN standard (Association Française de Normalisation [AFNOR], 2022a).

Sand. Crushed sand (0/5 mm) obtained from the National Company of Aggregates in Constantine was used in this study. Table 2 presents the chemical and physical properties of the crushed sand. All physical property measurements adhered to the following standards: NF EN 933-1 (AFNOR, 2012c), NF EN 933-8+A1 (AFNOR, 2015), and NF EN 1097-7 (AFNOR, 2022b). Figure 1 illustrates the grading curves of the different sands.

TABLE 2. Chemical properties of crushed sands

Specification	Chemical composition							
Content [%]	SiO_2	Al_2O_3	Fe_2O_3	CaO	MgO	K_2O	TiO_2	Na_2O
	0.05	0.03	0.02	56.03	0.19	0.03	0.008	0.06
	Physical properties							
Specific density [$kg \cdot m^{-3}$]	2,750.0							
Apparent density [$kg \cdot m^{-3}$]	1,460.0							
Fineness [$cm^2 \cdot g^{-1}$]	3,700.0							
Sand equivalent [%]	69.0							
Absorption coefficient [%]	1.1							

Source: own work.

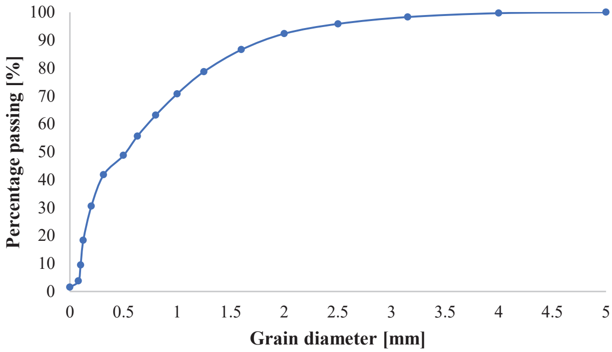

FIGURE 1. Grading curves of crushed sand

Source: own work.

Iron powder. This material was procured from Algerian Qatari Steel (AQS). This IP largely originates from industrial by-products, notably fine dust from iron and steel machining and fabrication, as well as sludges from furnaces and air pollution control systems. We employed scanning electron microscopy (SEM) for morphological analysis, energy dispersive X-ray spectroscopy (EDS) for elemental composition, and X-ray diffraction (XRD) for phase identification and crystallinity. As previously documented in NF EN 1097-7 (AFNOR, 2022b), EDS analysis (Fig. 2) of the IP confirmed a high iron content, along with trace elements such as O, Ca, Si, Mg, Na, Al, K, and S. On the other hand, the XRD pattern (Fig. 3) identified iron oxides, specifically Fe_2O_3 and FeO. Although some iron-rich materials can exhibit pozzolanic activity, the absence of crystalline silica or alumina phases in the pattern suggests limited pozzolanic reactivity in this material. The iron particles, observed in Figure 4, display irregular shapes and some agglomeration. This structure can impact air entrainment, water absorption, and compressive strength.

TABLE 3. Chemical and physical properties of iron powder

Specification	Chemical properties							
Content [%]	SiO_2	Al_2O_3	Fe_2O_3	CaO	MgO	K_2O	FeO	P_2O_5
	4.80	1.13	64.75	0.85	0.07	–	1.00	0.05
	Physical properties							
Specific density [$kg \cdot m^{-3}$]	2,250.0							
Apparent density [$kg \cdot m^{-3}$]	1,220.0							

Source: own work.

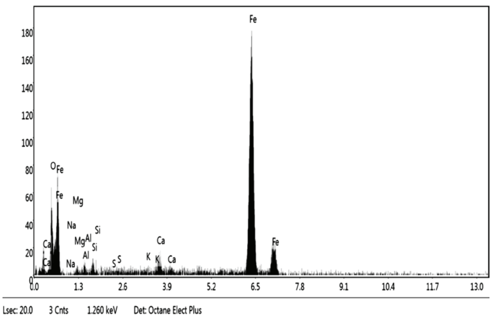

FIGURE 2. EDS spectrum of iron powder

Source: own work.

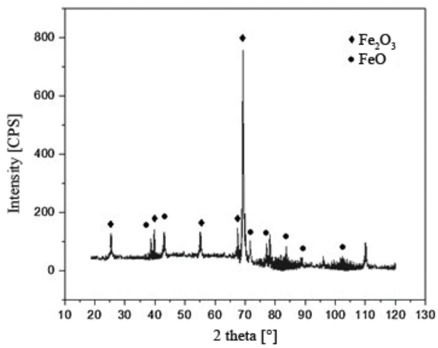

FIGURE 3. XRD patterns of iron powder

Source: own work.

Boukni, B., Bensalem, S., Khouadjia, M. L. K., Temami, O., Hamlaoui, S., Belebchouche, C. (2025). The influence of iron powder content on the fresh and hardened properties of mortar. *Sci. Rev. Eng. Env. Sci.*, *34* (2), 198–217. DOI 10.22630/srees.10391

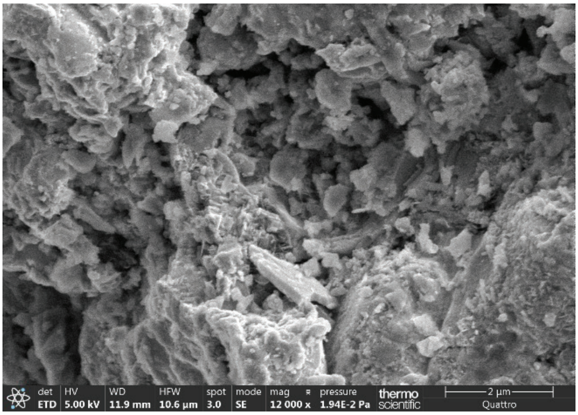

FIGURE 4. SEM image of iron powder
Source: own work.

Mix proportions

A reference mortar mixture was prepared, comprising 75% sand and 25% cement with a water-to-cement (W/C) ratio of 0.5. To systematically assess the effects of iron powder on mortar properties, the sand content of the reference mixture was progressively replaced with varying percentages of iron powder. Six distinct iron powder replacement levels were investigated: 1%, 2%, 3%, 4%, 10%, and 20%. This systematic replacement resulted in eight distinct mortar mixtures in total, including the control mixture. The detailed quantitative compositions of all eight mixtures, including the exact proportions of cement, sand, water, and iron powder for each mix, are presented in Table 4.

TABLE 4. Compositions of mortars

Designation	Crushed sand content [g]	Cement content [g]	Iron powder content [g]	Water content [g]
MC0	1 350.0	450.0	0	225.0
MIP1	1 350.0	445.5	4.5	225.0
MIP2	1 350.0	441.0	9.0	225.0
MIP3	1 350.0	436.5	13.5	225.0
MIP4	1 350.0	432.0	18.0	225.0
MIP5	1 350.0	427.5	22.5	225.0
MIP10	1 350.0	405.0	45.0	225.0
MIP20	1 350.0	360.0	90.0	225.0

Source: own work.

All mortar mixtures were prepared in accordance with the specifications outlined in EN206+A2/CN (AFNOR, 2022a). This involved using a standard laboratory planetary mixer and following a specific mixing sequence: dry components were mixed for 2 mins, water was added over 30 s, followed by 2 mins of mixing at high speed. To ensure statistical robustness and reproducibility of results, all experimental tests for each mortar mixture were repeated a minimum of three times. The reported results represent the average of these replicates, with standard deviations provided where appropriate.

After preparation, the fresh mortar mixtures were cast into prismatic molds with dimensions of 4 × 4 × 16 cm for subsequent evaluation of flexural strength and compressive strength. The molds were filled in two layers, with each layer compacted using a vibratory table for 60 s. Following casting, the samples were cured in their molds at 20 ±2°C and over 95% relative humidity for a period of 24 h. After this initial curing period, the samples were carefully demolded and subsequently left to cure in ambient air conditioning at 20 ±2°C for 28 days until testing.

Results and discussion

Setting time and consistency

The setting time and consistency of the mortar were determined using a Vicat apparatus following EN 196-3 (European Committee for Standardization [CEN] 2016). For consistency, the mortar was placed in a conical mold, and the 10 mm plunger penetration depth was measured, aiming for a standard value. For setting times, a specific needle was used to track penetration; initial setting was when the needle no longer reached the bottom, and final setting was when only a surface impression remained. These tests were conducted at regular intervals until both points were identified. Figures 5 and 6 present the results.

Figure 5 presents the setting times of mortars with varying iron powder content. The control mortar (MC) without iron powder exhibits a setting time of approximately 2 h. The mortars with 1% (MIP1) and 2% (MIP2) iron powder show a slight increase in setting time compared to the control. However, a substantial increase in setting time was observed for MIP3, MIP4, and MIP5, reaching a maximum of 3 h. Interestingly, as the iron powder content increases to 10% (MIP10) and 20% (MIP20), the setting time decreases, falling back to approximately 2 h. The initial addition of small amounts of iron powder (MIP1, MIP2) to the cement paste resulted in a slight increase in setting time. This can be attributed to the nucleation effect of the iron particles, which act as nucleation sites for the formation of hydration products, initially accelerating the setting process. However, as the iron powder content increased further (MIP3, MIP4, MIP5), the setting time began to delay significantly. The mixture likely required more water to achieve the desired workability. This is probably because numerous nucleation sites cause rapid water consumption. This observation aligns with previous research (Thakur et al., 2019).

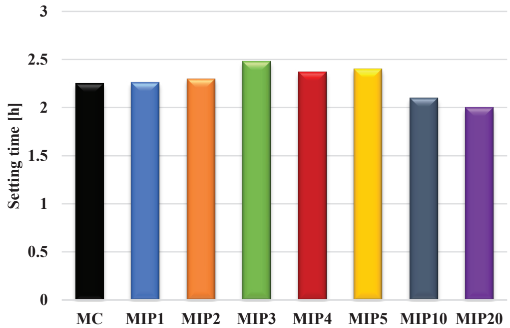

FIGURE 5. Evolution of setting time according to the substitution rate of iron powder
Source: own work.

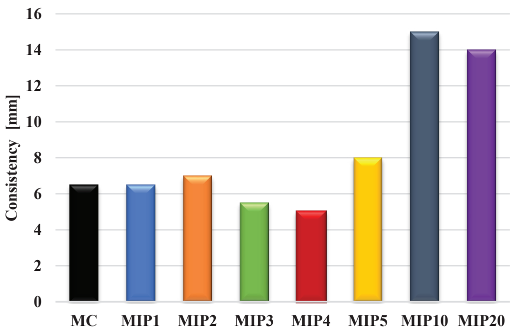

FIGURE 6. Evolution of consistency according to the substitution rate of iron powder
Source: own work.

Conversely, at higher iron powder concentrations (MIP10, MIP20), the setting time decreased. This could be attributed to several factors. Firstly, the excessive amount of iron powder may have interfered with the hydration process, potentially hindering the proper packing of cement particles and reducing the overall reaction rate. Secondly, the presence of a large number of iron particles may have disrupted the formation of the hydration product network, leading to a faster setting time.

Concerning the evolution of consistency as a function of the iron powder substitution rate, as shown in Figure 6, the results indicate that the MC exhibits a consistency of 6 mm. Upon introducing 1–5% iron powder (MIP1 to MIP5), the consistency shows minor fluctuations, suggesting a limited impact at these low concentrations. These results agree with those of Largeau et al. (2018).

However, a significant increase in consistency is observed in higher iron powder contents (MIP10 and MIP20), reaching 15 mm and 14 mm, respectively. This trend likely arises from the increased particle size and surface area of the iron powder, leading to greater interparticle friction and a stiffer mortar mix.

Air content and bulk density

To characterize the fresh mortar properties, air content was determined using a mortar aerometer in accordance with EN 1015-7 (AFNOR, 1999). This involved filling a standardized vessel with fresh mortar, striking off the excess, and then using the aerometer to measure the entrapped air volume based on the pressure method. Furthermore, the bulk density of the fresh mortar was measured following NF EN 1015-6/A1 (AFNOR, 2007). For this, a known volume of fresh mortar was carefully placed into a tared container of specified dimensions, and its mass was determined. The bulk density was then calculated by dividing the mass of the mortar by the volume of the container. The resulting air content and bulk density values for each mortar mixture are presented in Figures 7 and 8, respectively.

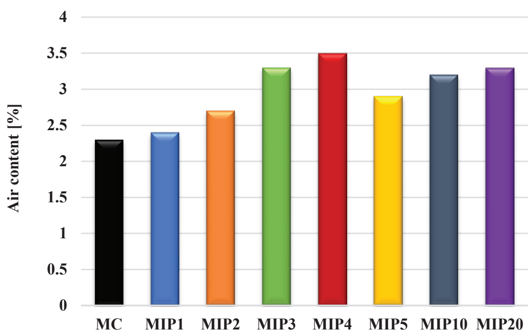

FIGURE 7. Evolution of air content according to the substitution rate of iron powder
Source: own work.

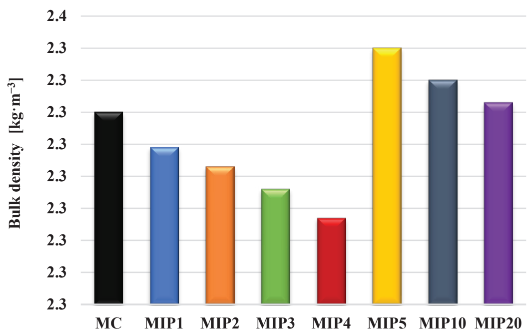

FIGURE 8. Evolution of bulk density according to the substitution rate of iron powder
Source: own work.

Figure 7 depicts the air content of mortars expressed as a percentage. The MC, devoid of iron powder, displays an air content of approximately 2%. The inclusion of 1% (MIP1) and 2% (MIP2) iron powder results in a modest increase in air content. However, a slight rise in air content is observed for MIP3 (3% iron powder), MIP4 (4% iron powder), and MIP5 (5% iron powder), with air content increasing up to 3.5%. The observed initial increase in air content with the addition of small amounts of iron powder (MIP1, MIP2) can be attributed to the increased surface roughness and irregular shapes of the iron particles, as shown in Figure 4. These characteristics contribute to enhanced air entrainment within the mortar matrix. The iron particles, acting as nucleation sites, likely trap air bubbles during mixing. This effect becomes more pronounced for MIP3 and MIP4, leading to substantial increases in the measured air content. Specifically, MIP3 demonstrated a 43.47% increase, while MIP4 exhibited a 52.17% increase. An intriguing observation was the decreased air content in mortars with higher iron powder concentrations (MIP10, MIP20) compared to MIP4. This phenomenon may be attributed to several factors. Firstly, at elevated iron powder concentrations, particle agglomeration might occur, reducing the overall surface area available for air bubble nucleation. Secondly, the increased viscosity of the mortar mix at higher iron powder contents, as previously observed in consistency tests, could impede the movement and dispersion of air bubbles within the matrix, consequently limiting air entrainment. These results are concordant with the findings of work by Khouadjia et al. (2025). The results shown in Figure 8 concerning the evolution of bulk density as a function of the substitution rate of iron powder indicate that the addition of iron powder from 1% to 4% leads to a decrease in bulk density (up to 1.42%

for MIP4). However, as the iron powder content increases to 5% (MIP5), 10% (MIP10), and 20% (MIP20), the bulk density significantly increases, reaching values of 2.34 kg·m^{-3}, 2.33 kg·m^{-3}, and 2.323 kg·m^{-3}, respectively, compared to the control concrete, which has a density of 2.32 kg·m^{-3}. The initial reduction in bulk density observed with the addition of small amounts of iron powder (MIP1, MIP2, MIP3, MIP4) can be attributed to increased porosity within the mortar matrix. Iron particles possessing a higher density than the constituent cement and sand can disrupt the natural particle packing arrangement. This disruption results in the formation of voids and consequently a decrease in the overall bulk density of the mortar mixture.

On the other hand, the increase in bulk density observed at higher iron powder concentrations (MIP5, MIP10, MIP20) strongly suggests a modification of the mortar's microstructure. This enhancement is likely due to a combination of factors. Firstly, the increased presence of iron particles likely improves particle packing within the mortar matrix, reducing voids and leading to a more compact structure. Secondly, the intrinsic high density of iron significantly contributes to the overall mass of the mortar, directly resulting in an increase in bulk density. These results are similar to those obtained by Khouadjia et al. (2025) concerning the use of iron powder.

Workability (flow time)

The flow time of all mortar mixtures was determined using the LCPC workability meter (French test), in accordance with the standard NF P 18-452 (AFNOR, 2017a). The results of the flow time test are presented in Figure 9.

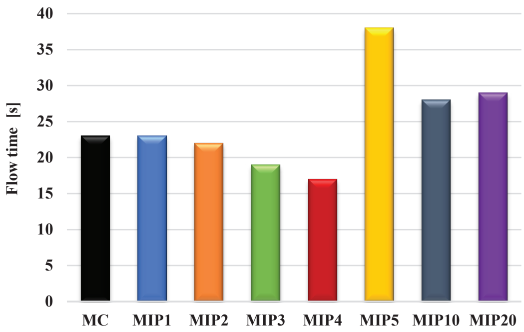

FIGURE 9. Evolution of flow time according to the substitution rate of iron powder
Source: own work.

Figure 9 shows that the MC exhibited a flow time of 23 s. The incorporation of 1–2% iron powder (MIP1 to MIP2) had a minimal impact on flow time, with values remaining largely consistent with the MC. However, a notable decrease in flow time is observed for MIP3 and MIP4, suggesting a reduction in viscosity and an increase in workability at these intermediate concentrations. This enhanced flowability can be attributed to several factors. Firstly, the incorporation of iron powder likely improved particle dispersion within the mortar matrix. Acting as fillers, the iron particles may have facilitated denser packing of cement particles, minimized voids, and promoted smoother flow. Secondly, interactions between the iron powder and cement particles may have altered the surface properties of the cement, potentially reducing particle agglomeration. This surface modification could have contributed to a more fluid and workable mortar. These results are consistent with previous findings (Ruidong et al., 2021).

However, at higher iron powder contents (MIP5, MIP10, and MIP20), a significant increase in flow time is observed, reaching 38 s, 28 s, and 29 s, respectively. This increase in flow time indicates that higher concentrations of iron powder can adversely affect the workability of the mortar. Several factors contribute to these results. A higher concentration of iron powder concentration likely leads to particle agglomeration, forming larger clusters within the mortar that impede flow and increase viscosity. Additionally, the iron powder may absorb some of the mixing water, reducing the available water and making the mortar stiffer and less workable. Consequently, this results in longer flow times, negatively impacting workability and application. These observations are consistent with findings by Bogue (1947) and Han et al. (2022).

Furthermore, the increased density of the mortar (Fig. 8), due to the addition of high concentrations of iron powder, can also contribute to the observed decrease in workability. A denser mortar may exhibit greater resistance to flow and deformation, leading to increased difficulty in shaping and placing the material.

Compressive strength

Compressive strength tests were performed on mortar specimens at 28 days of curing. We followed the NF EN 12390-3 standard (AFNOR, 2012b) precisely, using a universal testing machine to apply a controlled compressive load until failure. For each mix, six replicate specimens were tested to ensure reliability. The reported values in Figure 10 represent the average compressive strength obtained from these three measurements, providing a robust and representative data point.

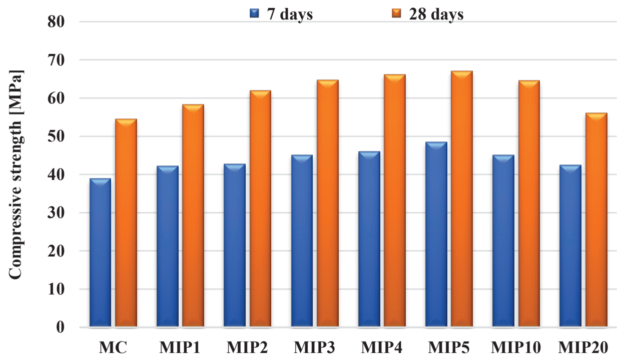

FIGURE 10. Evolution of compressive strength according to the substitution rate of iron powder
Source: own work.

Figure 10 illustrates the compressive strength of mortars at 7 days and 28 days, comparing a MC with mortars containing varying amounts of iron powder (MIP1 to MIP20). Overall, the presence of iron powder generally enhances the compressive strength, particularly at 28 days. While the 7-day strength shows a slight increase of approximately 10–12.5% compared to the control, the 28-day strength demonstrates a more substantial improvement (8–18%), suggesting that iron powder promotes strength development over time. The highest compressive strength was achieved for mortars containing 5% iron powder, exceeding 67.11 MPa. These results align with the observed trends in air content and bulk density. Specifically, the air content of the 5% iron powder mixture (MIP 5) increased slightly, while the bulk density remained relatively high. This improvement in strength can be attributed to several mechanisms: the iron powder acts as a filler material, enhances particle packing density, and facilitates better mechanical interlocking within the mortar matrix. As a result, this denser matrix leads to a more compact and robust structure. The presence of iron powder may influence the formation of ettringite, a sulfate-bearing compound that contributes to strength development over time (Tao & Dang, 2016; Largeau et al., 2018; Cui et al., 2024). Incorporating iron powder into concrete at levels of 10% and 20% resulted in reduced compressive strength at both 7 days and 28 days. This weakening effect is likely due to the iron powder replacing cement, which consequently impedes the formation of calcium silicate hydrate (C-S-H) – a key component for concrete strength, particularly in the initial stages (Giovanni et al., 2024).

Three-point flexural strength

The three-point flexural strength of the specimens was determined according to the European standard NF EN 12390-1 (AFNOR, 2017b). Each specimen was centrally loaded at a controlled rate while being supported at two points. The maximum load at failure was recorded, and the flexural strength was calculated using the specified formula, considering the specimen's dimensions. These tests provided crucial data on the material's resistance to bending. The results are presented in Figure 11.

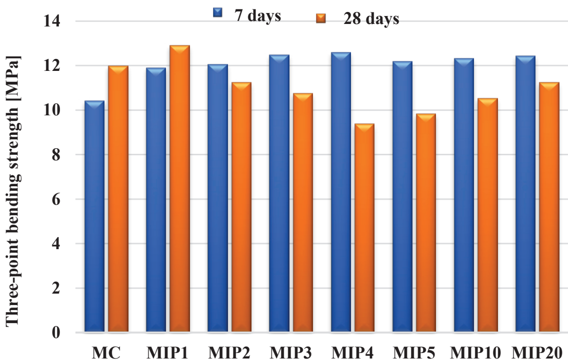

FIGURE 11. Evolution of three-point bending strength according to substitution rate of tuff with iron powder
Source: own work.

Figure 11 illustrates the three-point bending strength of mortars containing varying amounts of iron powder at 7 days and 28 days. The MC exhibits a bending strength of approximately 10 MPa at 7 days and 12 MPa at 28 days. The addition of iron powder initially leads to an increase in strength at 7 days, with MIP2 showing the highest increase of 30% compared to the control. This early strength gain can be attributed to the nucleation and refinement of cement hydration products due to the presence of iron powder.

However, in 28 days, the situation changes. While some mortars with iron powder (MIP5, MIP10) show a slight increase in strength (8.33% and 4.17%, respectively), others (MIP2, MIP3, MIP4, and MIP20) exhibit a significant decrease in strength compared to the MC, with MIP4 showing the largest decrease of 25%. This suggests that at higher iron powder concentrations, mechanisms such as iron powder aggregation or interference with the normal hydration process of cement might be detrimental to the long-term strength development of the mortar (Largeau et al., 2018; Giovanni et al., 2024).

These findings highlight the complex influence of iron powder on the mechanical behavior of mortars. While it can enhance early strength, its effect on long-term strength is more nuanced and requires careful optimization of the iron powder content to prevent negative impacts on three-point bending.

Conclusions

This study investigates the feasibility of using waste iron powder (IP) as a partial replacement for cement in mortar, with the goal of developing sustainable construction materials from industrial by-products. Our research specifically evaluates the effects of different IP percentages (1–20% by weight of cement) on the fresh and hardened properties of mortar. This work offers a viable pathway for utilizing industrial waste and contributes to reducing environmental impact.

The incorporation of iron powder significantly influenced various mortar properties. A complex relationship was observed between IP content and setting time, where small additions (1–2%) slightly delayed setting, while higher concentrations (beyond 5%) progressively accelerated it. Consistency remained relatively stable at low IP concentrations (1–5%) but significantly decreased at higher levels (10–20%), likely due to the increased surface area of IP leading to a higher water demand.

Air entrainment varied with IP content; small additions (1–2%) modestly increased air content, higher concentrations (3–4%) significantly increased it, and even higher concentrations (10–20%) led to a decrease. Mortar flow time was minimally affected at low IP concentrations (1–4%) but significantly increased at higher levels (5%, 10%, 20%), attributed to factors such as particle agglomeration, increased interparticle friction, and potentially higher water absorption by the IP.

Crucially, incorporating iron powder significantly improved compressive strength, particularly at 28 days. Mortar, with 5% IP (MIP5), achieved the highest 28-day compressive strength of 67.11 MPa, representing a notable enhancement attributed to improved particle packing and increased density. While initial flexural strength showed promise (30% increase for MIP2 at 7 days), this benefit diminished over time, with higher IP concentrations leading to significant reductions in 28-day flexural strength (MIP4 showing a 25% decrease compared to the control).

Based on these comprehensive findings, a 5% waste iron powder replacement (WIP5) stands out as the optimal percentage, consistently demonstrating superior performance in terms of compressive strength and overall balanced properties – a conclusion directly supported by our results.

These findings collectively emphasize the importance of carefully optimizing iron powder content to achieve the desired mechanical properties while balancing various characteristics of the mortar. This research offers specific insights into how iron powder affects mortar performance, guiding future applications and material design. Future research should focus on exploring hybrid binder systems with other materials that could mitigate issues like reduced flexural strength. Crucially, durability studies (e.g., sulfate and chloride resistance) and life cycle assessments are vital to confirm the long-term viability and environmental benefits of these sustainable mortars in practical applications.

References

Association Française de Normalisation [AFNOR] (1999). *Méthodes d'essai des mortiers pour maçonnerie. Partie 7: détermination de la teneur en air du mortier frais* (NF EN 1015-7) [*Methods of test for mortar for masonry. Part 7: determination of air content of fresh mortar*]. AFNOR.

Association Française de Normalisation [AFNOR] (2007). *Méthodes d'essai des mortiers pour maçonnerie. Partie 6: détermination de la masse volumique apparente du mortier frais* (NF EN 1015-6/A1) [*Methods of test for mortar for masonry. Part 6: determination of bulk density of fresh mortar*]. AFNOR.

Association Française de Normalisation [AFNOR] (2012a). *Ciment. Partie 1: Compostition, spécifications et critères de conformité des ciments courants* (NF EN 197-1) [*Cement. Part 1: composition, specifications and conformity criteria for common cements*]. AFNOR.

Association Française de Normalisation [AFNOR] (2012b). *Essais pour béton durci. Partie 3: résistance à la compression des éprouvettes* (NF EN 12390-3) [*Tests for hardened concrete. Part 3: compressive strength of the specimens*]. AFNOR.

Association Française de Normalisation [AFNOR] (2012c). *Essais pour déterminer les caractéristiques géométriques des granulats. Partie 1: détermination de la granularité. Analyse granulométrique par tamisage* (NF EN 933-1) [*Tests for geometrical properties of aggregates. Part 1: determination of particle size distribution. Sieving method*]. AFNOR.

Association Française de Normalisation [AFNOR] (2015). *Essais pour déterminer les caractéristiques géométriques des granulats. Partie 8: évaluation des fines. Équivalent de sable* (NF EN 933-8+A1) [*Tests for geometrical properties of aggregates. Part 8: assessment of fines. Sand equivalent test*]. AFNOR.

Association Française de Normalisation [AFNOR] (2017a). *Bétons. Mesure du temps d'écoulement des bétons et des mortiers au maniabilimètre* (NF P 18-452) [*Concretes. Measuring the flow time of concretes and mortars using a workabilitymeter*]. AFNOR.

Association Française de Normalisation [AFNOR] (2017b). *Essais pour béton durci. Partie 1: Forme, dimensions et autres exigences aux éprouvettes et aux moules* (NF EN 12390-1)

[*Testing hardened concrete. Part 1: shape, dimensions and other requirements for specimens and moulds*]. AFNOR.

Association Française de Normalisation [AFNOR] (2022a). *Béton. Spécification, performance, production et conformité. Complément national à la norme* (NF EN 206+A2) [*Concrete. Specification, performance, production and conformity. National addition to the standard*]. AFNOR.

Association Française de Normalisation [AFNOR] (2022b). *Essais pour déterminer les caractéristiques mécaniques et physiques des granulats. Partie 7: détermination de la masse volumique réelle du filler. Méthode au picnomètre* (NF EN 1097-7) [*Tests for mechanical and physical properties of aggregates. Part 7: determination of the particle density of filler. Pyknometer method*]. AFNOR.

Belebchouche, C., Temami, O., Khouadjia, M. L. K., Hamlaoui, S., Berkouche, A., & Chouadra, T. (2024). Recycling of brick and road demolition waste in the production of concrete. *Science, Engineering and Technology*, *4*(2), 14–23. https://doi.org/10.54327/set2024/v4.i2.154

Bogue, R. H. (1947). *Chemistry of Portland cement*. Reinhold.

Cui, L., Chen, P., Wang, L., Xu, Y., & Wang, H. (2022). Reutilizing waste iron tailing powders as filler in mortar to realize cement reduction and strength enhancement. *Materials*, *15*(2), 541. https://doi.org/10.3390/ma15020541

Cui, L., Xu, Y., Wang, L., Ying, P., & Wang, H. (2024). Investigating the hydration characteristics of iron tailings powder cement mortar produced by the mortar substitution method. *Journal of Building Engineering*, *81*, 108100. https://doi.org/10.1016/j.jobe.2023.108100

Dias, R., Bigotto, S., Benjamim, D. U., Chotolli, D. L., & de Souza, M. V. (2020). Concrete mixture with the use of iron powder waste for coarse aggregate doping. *International Journal of Multidisciplinary Sciences and Engineering*, *11*(2), 18–24. https://www.ijmse.org/Volume11/Issue2/paper3_11_2.pdf

European Committee for Standardization [CEN] (2016). *Methods of testing cement. Part 3: Determination of setting times and soundness* (EN 196-3).

Fahad, B. M., & Jassim, K. S. (2020). Behaviour of cement mortar containing iron waste powder as a substitute for sand. *IOP Conference Series: Materials Science and Engineering*, *737*(1), 012064. https://doi.org/10.1088/1757-899X/737/1/012064

Giovanni, D., Rumbyarso, Y. P. A., & Siagian, B. (2024). Analysis of concrete compressive strength with partial substitution of iron powder waste as fine aggregate. *International Journal of Multi Science*, *4*(02), 122–129.

Han, F., Zhang, H., Liu, J., & Song, S. (2022). Influence of iron tailing powder on properties of concrete with fly ash. *Powder Technology*, *398*, 117132. https://doi.org/10.1016/j.powtec.2022.117132

Harabi, H., Khouadjia, M. L. K., Bensalem, S., Isleem, H. F., & Khishe, M. (2024). Effect of waste paper aggregate and polyethylene terephthalate on mortar performance. *Scientific Reports*, *14*(1), 29588. https://doi.org/10.1038/s41598-024-80914-0

Harrison, R. M. (Ed.). (2023). *Pollution: causes, effects, and control*. Royal Society of Chemistry.

Khouadjia, M. L. K., Bensalem, S., Belebchouche, C., Boumaza, A., Hamlaoui, S., & Czarnecki, S. (2025). Sustainable geopolymer tuff composites utilizing iron powder waste: rheological and mechanical performance evaluation. *Sustainability*, *17*(3), 1240. https://doi.org/10.3390/su17031240

Khouadjia, M. L. K., Bensalem, S., Belkadi, A. A., Kessal, O., & Sebti, M. A. (2023). Influence of the shape and content of steel and aluminum fibers from industrial lathe wastes on the physico-mechanical and rheological behavior of concrete. *Journal of Applied Engineering Sciences*, *13*(26), 207–214. https://doi.org/10.2478/jaes-2023-0026

Kong, L., Xie, S., Wang, C., & Wang, L. (2023). Effect of iron tailings as fine aggregate and mineral admixture on strength and microstructure of cement mortar. *International Journal of Concrete Structures and Materials*, *17*(1), 24. https://doi.org/10.1186/s40069-023-00584-6

Krikar, M., Noori, G., & Ibrahim, H. H. (2018). Mechanical properties of concrete using iron waste as a partial replacement of sand. *Eurasian Journal of Science and Engineering*, *3*(3), 75–82. https://doi.org/10.23918/eajse.v3i3p75

Largeau, M. A. (2018). *Effect of iron powder partially used as Portland cement replacement on the structural properties of concrete* (doctoral dissertation). Jomo Kenyatta University of Agriculture and Technology.

Largeau, M. A., Mutuku, R., & Thuo, J. (2018). Effect of iron powder (Fe_2O_3) on strength, workability, and porosity of the binary blended concrete. *Open Journal of Civil Engineering*, *8*(04), 411. https://doi.org/10.4236/ojce.2018.84029

Lu, Y., Huang, J., & Gao, Y. (2020). Study on the preparation and properties of modified functional mortar mixed with reduced iron powder. *IOP Conference Series: Materials Science and Engineering*, *735*(1), 012018. https://doi.org/10.1088/1757-899X/735/1/012018

Małek, M., Jackowski, M., Łasica, W., Kadela, M., & Wachowski, M. (2021). Mechanical and material properties of mortar reinforced with glass fiber: An experimental study. *Materials*, *14*(3), 698. https://doi.org/10.3390/ma14030698

Miah, M. J., Ali, M. K., Paul, S. C., John Babafemi, A., Kong, S. Y., & Šavija, B. (2020). Effect of recycled iron powder as fine aggregate on the mechanical, durability, and high temperature behavior of mortars. *Materials*, *13*(5), 1168. https://doi.org/10.3390/ma13051168

Miah, M. J., Miah, M. S., Paul, S. C., Kong, S. Y., Babafemi, A. J., Ali, M. K., & Patoary, M. M. H. (2021). Waste iron powder is used as aggregate and as a binder in mortar production. *Magazine of Civil Engineering*, *108*(8), 10810. https://doi.org/10.34910/MCE.108.10

Ruidong, W., Yu, S., Juanhong, L., Linian, C., Guangtian, Z., & Yueyue, Z. (2021). Effect of iron tailings and slag powders on workability and mechanical properties of concrete. *Frontiers in Materials*, *8*, 723119. https://doi.org/10.3389/fmats.2021.723119

Tao, L. I., & Dang, B. (2016). Experimental study on the compressive strength of iron tailings concrete with different replacement types. *Hebei Journal of Industrial Science and Technology*, *33*, 240–245.

Tayeh, B. A., & Al Saffar, D. M. (2018). Utilization of waste iron powder as fine aggregate in cement mortar. *Journal of Engineering Research and Technology*, *5*(2), 22–27.

Thakur, A., Singh, D., & Singh, A. (2019). Enhancement in properties of cement mortar by using iron-based material: a critical review. *International Journal for Research in Applied Science & Engineering Technology*, *7*(12), 689–691.

Summary

The influence of iron powder content on the fresh and hardened properties of mortar. The growing global waste problem, combined with the environmental impact of concrete production, necessitates innovative solutions to mitigate pollution, conserve resources, and enhance concrete performance. This research explores the potential of iron powder (IP) as a partial cement replacement in mortar. The study investigates the influence of iron powder on the fresh and hardened properties of mortar at seven replacement percentages: 1%, 2%, 3%, 4%, 5%, 10%, and 20% by weight. A comprehensive range of tests, including setting times, air content, density, flow time, compressive strength, and flexural strength, were conducted to assess the performance of the IP-modified mortars. The incorporation of iron powder into mortar mixtures significantly affected its properties. For replacement percentages greater than 3%, a slight enhancement in workability (3%) was observed. In terms of compressive strength, optimal performance was achieved with a 5% iron powder replacement (MIP5), surpassing that of the control mortar despite an increase in air content. Further increasing the iron powder content beyond 5% resulted in a modest decrease in compressive and flexural strengths, confirming that 5% is the optimal replacement percentage. This research provides significant practical implications, offering a viable and sustainable pathway for utilizing industrial waste, reducing landfill burden, conserving natural resources, and developing greener, high-performance construction materials.

Instruction for Authors

The journal publishes in English languages, peer-reviewed original research, critical reviews and short communications, which have not been and will not be published elsewhere in substantially the same form. Author of an article is required to transfer the copyright to the journal publisher, however authors retain significant rights to use and share their own published papers. The published papers are available under the terms of the principles of Open Access Creative Commons CC BY-NC license. The submitting author must agree to pay the publication charge (see Charges).

The author of submitted materials (e.g. text, figures, tables etc.) is obligated to restricts the publishing rights. All contributors who do not meet the criteria for authorship should be listed in an Acknowledgements section of the manuscript. Authors should, therefore, add a statement on the type of assistance, if any, received from the sponsor or the sponsor's representative and include the names of any person who provided technical help, writing assistance, editorial support or any type of participation in writing the manuscript.

Uniform requirements for manuscripts

The manuscript should be submitted by the Open Journal System (OJS) at https://srees.sggw.edu.pl/about/submissions. All figures and tables should be placed near their reference in the main text and additionally sent in a form of data files (e.g. Excel, Visio, Adobe Illustrator, Adobe Photoshop, CorelDRAW). Figures are printed in black and white on paper version of the journal (color printing is combined with an additional fee calculated on a case-by-case basis), while on the website are published in color.

The size of the manuscript should be limited up to 10 pages including overview, summary, references and figures (the manuscript more than 13 pages is unacceptable); Please set the text format in single column with paragraphs (A4 paper format), all margins to 25 mm, use the font Times New Roman, typeface 12 points and line spacing one and half.

The submitted manuscript should include the following parts:

- name and SURNAME of the author(s) – up to 5 authors
- affiliation of the author(s), ORCID Id (optional)
- title of the work
- key words
- abstract (about 500 characters)
- text of the paper divided into: Introduction, Material and Methods, Results and Discussion, Conclusions, References and Summary
- references in APA style are listed fully in alphabetical order according to the last name of the first author and not numbered; please find the details below
- post and mailing address of the corresponding author:

  Author's address:
  Name, SURNAME
  Affiliation
  Street, number, postal code, City
  Country
  e-mail: adress@domain

- Plagiarism statement (https://srees.sggw.edu.pl/copyright)

Reference formatting

In the Scientific Review Engineering and Environmental Sciences the APA 7th edition style is used.

Detailed information

More information can be found: https://srees.sggw.edu.pl